

**Delivery of Phyto-Ceramides into the *Stratum Corneum* of the
Skin using Nanocarriers: Structural Characterization,
Formulation and Skin Permeation Studies**



Dissertation

zur Erlangung des akademischen Grades
Doctor rerum naturalium (Dr. rer. nat.)

vorgelegt der

Naturwissenschaftlichen Fakultät I-Biowissenschaften
der Martin-Luther-Universität Halle-Wittenberg

von

MSc. Pharm. Efreem Nigussu Tessema
geboren am 16. Oktober 1983 in Arsi Asasa, Äthiopien

Gutachter:

1. Prof. Dr. Dr. h.c. Reinhard Neubert
2. Prof. Dr. Tsige Gebre-Mariam
3. Prof. Dr. Kerstin Andrea-Marobela

Halle (Saale) 22.02.18

*Printed with the support of the German Academic Exchange
Service (DAAD)*

Dedicated to my Mother

Table of contents

Abbreviations.....	vi
List of Tables	ix
List of Figures.....	xi
1. Introduction.....	1
1.1. Epidermal Ceramides.....	1
1.1.1. Skin.....	1
1.1.2. Epidermis.....	1
1.1.3. Ceramides.....	2
1.1.4. Lipid Organization in the SC Lipid Lamellae.....	5
1.2. Skin Disorders Associated with Perturbed or Altered SC Lipids.....	5
1.3. Phyto-derived Ceramides (PhytoCERs).....	7
1.3.1. Plant Sphingolipids (SLs).....	7
1.3.2. Structural Comparison of Plant and Epidermal CERs.....	8
1.3.3. Commercial PhytoCER-based Preparations.....	10
1.4. Delivery of PhytoCERs for Skin Barrier Reinforcement.....	13
1.4.1. Oral Delivery of PhytoCERs.....	13
1.4.1.1. Effects of Oral PhytoCERs on Skin Barrier.....	14
1.4.1.2. Mechanisms Underlying Skin Barrier Improvement.....	15
1.4.2. Topical Delivery of PhytoCERs	15
1.4.2.1. Controlled Delivery of PhytoCERs into the SC	16
1.4.2.2. Delivery of PhytoCER Precursors into the Viable Epidermis	16
1.5. LC-MS-based Structural Characterization and Quantification of SLs.....	18
1.5.1. Liquid Chromatography.....	18
1.5.2. Ionization Techniques	19
1.5.3. Mass Analyzers	20
1.6. Nano-sized Carriers in Dermal and Transdermal Drug Delivery	21
1.6.1. Microemulsions.....	21
1.6.1.1. Formulation of MEs.....	21
1.6.1.2. Characterization of MEs.....	24
1.6.1.3. MEs in Dermal and Transdermal Drug Delivery	24
1.6.2. Polymeric Nanoparticles.....	25

1.6.2.1.	Preparation of Polymeric NPs	25
1.6.2.2.	Characterization of NPs	27
1.6.2.3.	Starch-based NPs	28
1.6.2.3.1.	Starch	28
1.6.2.3.2.	Starch Modifications	28
1.6.2.3.3.	Starch NPs	29
1.6.2.4.	NPs in Dermal and Transdermal Drug Delivery	29
1.7.	Rationale of the Study	30
1.8.	Research Questions	31
1.9.	Objectives of the Study	31
2.	Isolation, Structural Characterization and Quantification of Plant GlcCERs	32
2.1.	Introduction	32
2.2.	Materials and Methods	33
2.2.1.	Materials	33
2.2.2.	Methods	34
2.2.2.1.	Extraction and Purification of GlcCER-enriched Lipid Fractions (GELFs)	34
2.2.2.2.	Isolation of GlcCERs by Preparative LC/APCI-MS	34
2.2.2.3.	LC/APCI-MS/MS-based Structural Characterization of Plant GlcCERs	35
2.2.2.4.	AMD-HPTLC-based Quantification of Plant GlcCERs	35
2.2.2.4.1.	Instrumentation and Chromatographic Conditions	35
2.2.2.4.2.	Method Validation	36
2.2.2.4.3.	Quantification of GlcCERs	36
2.3.	Results and Discussion	37
2.3.1.	Extraction and Purification of GlcCERs	37
2.3.2.	Structural Characterization of GlcCERs	38
2.3.3.	Quantification of GlcCERs	45
2.4.	Conclusions	47
3.	Isolation and Structural Characterization of Oat CERs for SC Delivery	48
3.1.	Introduction	48
3.2.	Materials and Methods	49
3.2.1.	Materials	49
3.2.2.	Methods	49

3.2.2.1.	Extraction and Purification of Oat GlcCERs	49
3.2.2.2.	Structural Identification of GlcCERs by LC/APCI-MS/MS Analyses	50
3.2.2.3.	Quantification of Oat GlcCERs.....	50
3.2.2.4.	Cleavage of Glycosidic Linkage (Deglycosylation)	50
3.2.2.5.	Purification of Oat CERs.....	50
3.2.2.6.	Preparative LC/APCI-MS.....	51
3.2.2.7.	Structural Characterization of Oat CERs.....	51
3.2.2.8.	HPLC-Evaporative Light Scattering Detector (ELSD)	52
3.3.	Results and Discussion	52
3.3.1.	LC/APCI-MS/MS-based Structural Identification of GlcCERs	52
3.3.2.	Quantification of Oat GlcCERs.....	57
3.3.3.	Deglycosylation of Oat GlcCERs.....	57
3.3.4.	Further Structural Characterization of Oat CERs.....	61
3.4.	Conclusions	63
4.	Development and Validation of LC/APCI-MS Method for the Quantification of Oat CERs in Skin Permeation Studies	64
4.1.	Introduction	64
4.2.	Materials and Methods	66
4.2.1.	Materials.....	66
4.2.2.	Methods.....	66
4.2.2.1.	Isolation and Structural Characterization of Oat GlcCERs	66
4.2.2.2.	Cleavage of Glycosidic Linkage of Oat GlcCERs	66
4.2.2.3.	Isolation of Predominant Oat CERs	67
4.2.2.4.	LC/APCI-MS Method Development.....	67
4.2.2.5.	Extraction of SC Lipids.....	67
4.2.2.6.	Method Validation	68
4.2.2.7.	Application of the Method for <i>ex vivo</i> Skin Permeation Studies	70
4.2.2.7.1.	Preparation of Oat CER-based Cream.....	70
4.2.2.7.2.	<i>Ex vivo</i> Skin Permeability Studies.....	70
4.3.	Results and Discussion.....	71
4.3.1.	Preparation of oat CERs Reference Standards	71
4.3.2.	Method Development	72

4.3.3.	Method Validation	73
4.3.4.	Application of LC/APCI-MS Method in <i>ex vivo</i> Permeation Studies	78
4.4.	Conclusions	81
5.	Delivery of Oat CERs into the SC of the Skin using Nanocarriers: Formulation, Characterization and <i>in vitro</i> and <i>ex-vivo</i> Penetration Studies.....	82
5.1.	Introduction	82
5.2.	Materials and Methods	84
5.2.1.	Materials	84
5.2.2.	Methods.....	84
5.2.2.1.	Preparation of CERs from Oat GlcCERs	84
5.2.2.2.	Isolation and Acetylation of Cassava Starch and Determination of DS	84
5.2.2.3.	Preparation of Oat CER-based Formulations	85
5.2.2.3.1.	Preparation of LBMEs and ME Gel	85
5.2.2.3.2.	Preparation of Starch-based NPs and NP Gel	85
5.2.2.3.3.	Preparation of oat CER-based Amphiphilic Cream	86
5.2.2.4.	Characterization of Oat CER Formulations	86
5.2.2.4.1.	Cross-Polarized Light Microscope	86
5.2.2.4.2.	Dynamic Light Scattering (DLS).....	86
5.2.2.4.3.	Viscosity	87
5.2.2.4.4.	Refractive Index	87
5.2.2.4.5.	Stability	87
5.2.2.4.6.	Environmental Scanning Electron Microscopy (SEM).....	87
5.2.2.4.7.	Encapsulation Efficacy and Loading Capacity of NPs.....	88
5.2.2.4.8.	Automated Multiple Development (AMD)-HPTLC.....	88
5.2.2.5.	<i>In vitro</i> Release and Penetration of Oat CERs.....	89
5.2.2.5.1.	Preparation of Dodecanol-Collodion Model Membrane	89
5.2.2.5.2.	<i>In vitro</i> Release and Penetration Studies	89
5.2.2.6.	<i>Ex vivo</i> Skin Permeability Studies	90
5.2.2.7.	LC/APCI-MS.....	91
5.3.	Results and Discussion.....	91
5.3.1.	Preparation and Characterization of Formulations.....	91
5.3.2.	<i>In vitro</i> Release and Penetration of Oat CERs.....	96

5.3.3. <i>Ex vivo</i> Permeability of Oat CERs	99
5.3.4. Conclusions	101
6. Summary	103
7. Zusammenfassung	105
8. Outlook	108
9. Appendices	109
Appendix A: Isolation, Structural Characterization and Quantification of GlcCERs.....	109
Appendix B: Production and Characterization of Oat CERs	118
Appendix C: Formulation of Oat CERs	124
List of Publications	125
Acknowledgements	126
Curriculum Vitae	128
References	129

Abbreviations

AD	Atopic Dermatitis
AFM	Atomic Force Microscopy
AMD	Automated Multiple Development
APCI	Atmospheric Pressure Chemical Ionization
BC	Bicontinuous
CE	Cornified Envelope
CER	Ceramide
CID	Collision Induced Dissociation
d18:0	Sphinganine (dihydrosphingosine)
d18:1 ^{Δ4}	4-Sphingenine (sphingosine)
d18:1 ^{Δ8}	8-Sphingenine
d18:2	4,8-Sphingadienine
DLS	Dynamic Light Scattering
DR	Dermis
DS	Degree of Substitution
DSC	Differential Scanning Calorimetry
EE	Encapsulation Efficiency
ELSD	Evaporative Light Scattering Detector
EP	Epidermis
ESI	Electrospray Ionization
FA	Fatty Acid
GELF	Glucosylceramide-enriched Lipid Fraction
Glc	Glucose
GlcCER	Glucosylceramide
GlyCER	Glycosylceramide
GSL	Glycosphingolipid
h16:0	α -Hydroxypalmitic Acid
h20:0	α -Hydroxyarachidic Acid
h24:1	α -Hydroxynervonic Acid
¹ H COSY	Correlation Spectroscopy
HPTLC	High Performance Thin Layer Chromatography

HRMS	High Resolution Mass Spectrometry
HMBC	Heteronuclear Multiple Bond Correlation
LBME	Lecithin-Based Microemulsion
LC	Loading Capacity
LC-MS	Liquid Chromatography Mass Spectrometry
LC-MS/MS	Liquid Chromatography Tandem Mass Spectrometry
LOD	Limit of Detection
LOQ	Limit of Quantification
LPP	Long Periodicity Phase
ME	Microemulsion
MF	Matrix Factor
MS	Mass Spectrometry
MS/MS	Tandem Mass Spectrometry
NMR	Nuclear Magnetic Resonance
NP	Nanoparticle
O/W	Oil in Water
PhytoCER	Phytoceramide
RP	Reversed Phase
RSD	Relative Standard Deviation
SA	Starch Acetate
SAA	Surface Active Agent (Surfactant)
SANP	Starch Acetate Nanoparticle
SB	Sphingoid Base
SC	<i>Stratum Corneum</i>
SD	Standard Deviation
SEM	Scanning Electron Microscopy
SG	<i>Stratum Granulosum</i>
SIM	Selected Ion Monitoring
SL	Sphingolipid
S/N	Signal to Noise Ratio
SPM	Sphingomyelin
SPP	Short Periodicity Phase
SRM	Selected Reaction Monitoring
t18:0	4-Hydroxysphinganine (phytosphingosine)

t18:1	4-Hydroxy-8-sphinganine
TEM	Transmission Electron Microscopy
TEWL	Transepidermal Water Loss
Tris	Tris (hydroxymethyl) aminomethane
VLCFA	Very Long Chain Fatty Acid

List of Tables

Table 1-1: The FA composition of common plant GlcCERs.	11
Table 1-2: The SB composition of common plant GlcCERs.	12
Table 1-3: Predominant GlcCER species of common plants GlcCERs	13
Table 2-1: Amounts of total lipid extracts, CHCl ₃ fractions, GELFs and GlcCERs in oat, grass pea, Ethiopian mustard and haricot bean (n = 3)	38
Table 2-2: Fragmentation characteristics of plant GlcCERs depending on the nature of C4 of the SBs (C4-hydroxylated, C4-desaturated and C4-saturated).	39
Table 2-3: Grass pea GlcCER species identified by LC/APCI-MS/MS analyses.	42
Table 2-4: Ethiopian mustard GlcCER species identified by LC/APCI-MS/MS analyses.	43
Table 2-5: Haricot bean GlcCER species identified by LC/APCI-MS/MS analyses.	43
Table 2-6: Precision and accuracy of HPTLC method for quantification of plant GlcCERs. ...	46
Table 3-1: Preparative LC/APCI-MS gradient system for the isolation of predominant oat CERs.....	51
Table 3-2: Identification of oat-derived GlcCER species by LC/APCI-MS/MS analyses.....	55
Table 3-3: Stability of d18:1 ^{Δ8} -based GlcCERs and d18:2 ^{Δ4,8} /t18:1 ^{Δ8} -based GlcCERs in the ion source, CID and strong acidic conditions.	60
Table 3-4: ¹ H and ¹³ C chemical shift (CDCl ₃) of oat CER (d18:1 ^{Δ8E/Z} /h16:0).	63
Table 4-1: The S/N, LOD/LOQ, Recovery and MF of the LC/APCI-MS method for quantification of oat CERs in the skin.....	76
Table 4-2: Back calculated concentrations of the calibration standards and the corresponding calculated mean accuracy values.	77
Table 4-3: Within-run and between-run precision and accuracy of LC/APCI-MS method for the quantification of oat CERs in the skin layers.	77

Table 4-4: Amount of oat CERs permeated across the skin layers and sub-layers following topical application of amphiphilic cream after 300 min incubation period.....	79
Table 4-5: Skin thickness normalized amount of oat CERs (ng/10 μm skin slice) permeated across the skin layers following topical application of amphiphilic cream (Incubation periods: 30, 100, 300 min).....	80
Table 5-1: Compositions of LBMEs.....	85
Table 5-2: Viscosity, refractive index, droplet size and stability of oat CERs O/W MEs (n = 3).....	92
Table 5-3: Particle size, PDI, oat CERs EE and LC of SA NPs (n = 3).....	93
.Table 5-4: Total oat CERs released and penetrated (%) into the four-layer membrane system at three different incubation periods (15, 30 and 60 min) (n = 3).....	99

List of Figures

Figure 1-1: Lipid organization in human SC (1). The SC consists of dead cells (corneocytes) embedded in a lipid matrix (2). The intercellular lipids are arranged in layers (lamellae) (3), with either a long or short repeat distance (d), referred to as the long periodicity phase (LPP) (~13 nm) or short periodicity phase (SPP) (~6 nm), respectively. The three possible lateral organizations of the lipids are shown: a very dense, ordered orthorhombic organization, a less dense, ordered hexagonal organization, or a disordered liquid organization (adapted from [2] with permission).....	2
Figure 1-2: Chemical structure of free epidermal CERs [25]. The ω -hydroxy (R4) FAs are mostly esterified with linoleic acid (C18:2). The C16 - C32 FAs may also refer to unsaturated FAs. The structure of CER classes containing ω -hydroxy FA (CER [OS], CER [OP], CER [OH] and CER [ODS]) are not shown.....	4
Figure 1-3: Possible mechanisms for altered CERs profiles in AD patients: a decrease in <i>de novo</i> CER synthesis; increased GlcCER and SPM deacylase activities, increased ceramidase activity; decreased sphingomyelinase activity [3].	6
Figure 1-4: Chemical structure of plant GlcCERs showing the variation of CER backbones. The FAs are predominantly α -hydroxylated and they vary in chain length (C14 - C26) and ω -9-desaturation*. The SBs are amide linked with the FA moieties and they vary with the degree of desaturation or hydroxylation on C-4 and/or C-8 desaturation*	8
Figure 1-5: Structures of common C18 higher plant and mammalian SBs showing the variation at C4 of SBs: C4-saturated, C4-desaturated, C4-hydroxylated and C4-desaturated/C6-hydroxylated. Recently skin CERs with four hydroxyl SB have been reported [20]. The C4-double bond is primarily in the trans (E) configuration, whereas the C8-double bond is either cis (Z) or trans (E) configurations.....	9

Figure 2-1: Suggested route of fragmentation of a representative plant GlcCER (d18:2/h16:0) under positive ionization mode [270]. As the SB of this GlcCER is readily dehydrated, the precursor ion (m/z 714) is detected at a very low abundance and the ion that lost water (m/z 696) is highly abundant..... 40

Figure 2-2: Base peak chromatogram (full scan: m/z 100 - 2000) and extracted ion chromatograms of GlcCERs derived from grass pea (A), Ethiopian mustard (B) and haricot bean (C) using YMC-Pack ODS-AQ column. Gradient eluent: solvent A: H₂O (+0.1% formic acid) and solvent B: MeOH (+0.1% formic acid), flow rate: 0.3 mL/min, column temperature: 30 °C and injection volume: 10 μ L. 41

Figure 2-3: Individual GlcCER species identified from grass pea (GP), Ethiopian mustard (EM) and haricot bean (HB). ^aWith mono-unsaturated α -hydroxy FA, ^bboth saturated and mono-unsaturated α -hydroxy FAs. 44

Figure 3-1: TLC chromatograms of oat GELF, isolated GlcCERs and CERs (after acid treatment)..... 52

Figure 3-2: Base peak chromatogram (full scan: m/z 100 - 2000) and extracted ion chromatograms of oat GlcCERs using YMC-Pack ODS-AQ column. Gradient eluent: solvent A: H₂O (+0.1% formic acid) and solvent B: MeOH (+0.1% formic acid), flow rate: 0.3 mL/min, column temperature: 30 °C and injection volume: 10 μ L. 54

Figure 3-3: Individual oat GlcCER species identified by LC-MS/MS. 56

Figure 3-4: Acid-induced hydrolysis of predominant oat GlcCERs..... 58

Figure 3-5: Full scan (m/z 100 - 2000) base peaks obtained before (AI) and after (AII) acid treatment of oat GlcCERs. In the acid treated samples (AII), the CERs in the reaction mixture were extracted with CHCl₃. The SIM (m/z 554 and m/z 610) chromatograms of the two predominant oat CERs after column chromatographic purification (B)..... 59

Figure 3-6: A scheme showing the two possible sources of CERs (CERs obtained from acid-induced deglycosylation (red) and CERs produced by APCI source fragmentation) while analyzing acid-treated samples by LC-APCI/MS.....	60
Figure 3-7: Chemical structure of d18:1 Δ^8 -based GlcCERs and d18:2 $\Delta^{4,8}$ /t18:1 Δ^8 -based GlcCERs.....	61
Figure 3-8: Chemical structure of predominant oat CERs.	62
Figure 4-1: Chemical structures of major oat CERs.....	72
Figure 4-2: LC-MS chromatograms of skin lipid extracts obtained in full scan mode and SC extracts spiked with oat CERs acquired in SIM mode.	74
Figure 4-3: MS/MS fragmentation of oat CERs in triple quadrupole instrument (A and B) at CID 20 V and suggested fragmentation pattern (C) [270].	75
Figure 4-4: Percentage of oat CERs permeated (\pm SD) into the various layers of the skin from an amphiphilic cream containing oat CERs: SC, viable EP (EP1 + EP2), DR (For A: DR1 + DR2 + DR3 + remaining skin tissue and for 'B' without the remaining skin tissue) and acceptor (filter gauze + acceptor fluid).....	80
Figure 5-1: Strain sweep of gel formulations at 25 °C after a week of storage (0.01 - 100 % at 10 rad/s).....	94
Figure 5-2: Frequency sweep for the gel formulations (G' and G'' as a function of angular frequency at 1% strain measured at 25 °C after a week of storage).....	95
Figure 5-3: Hysteresis loop of the gel formulations (shear stress a function of shear rate measured at 25 °C after a month of storage).	96
Figure 5-4: Viscosity versus shear rate for gel formulations (at 25 °C after a month of storage).....	96
Figure 5-5: Release and penetration of oat CERs into the artificial multilayer membranes from various formulations.....	98

Figure 5-6: Percentage of oat CERs permeated into different layers of the skin from the various formulations: SC (SC1 + SC2), viable EP (EP1 + EP2), DR (DR1 + DR2 + DR3 + remaining skin tissue) and acceptor (filter gauze + acceptor fluid). 100

Figure 5-7: Skin thickness normalized distribution of oat CERs across the various skin layers (SC: $2 \times 10 \mu\text{m}$ thick slices, viable EP: $4 \times 20 \mu\text{m}$ thick slices and DR: $15 \times 40 \mu\text{m}$ thick slices).
..... 101

1. Introduction

1.1. Epidermal Ceramides

1.1.1. Skin

Skin is the largest organ of the body forming an effective barrier protecting the body from various types of stimulation and damage as well as preventing water loss from the body [1]. It is a multilayered tissue consisting of three primary layers: epidermis (EP), dermis (DR) and hypodermis [2]. The outer epidermal layer is a cellular layer mainly consisting of keratinocytes stratified into sub-layers by their stage of differentiation and is responsible for the prevention of water loss from the skin and diffusion of xenobiotics into the skin. The DR is mainly composed of fibroblasts embedded in an acellular collagen/elastin matrix [2, 3].

1.1.2. Epidermis

From outside to inside, the EP is composed of four sub-layers: *stratum corneum* (SC), *stratum granulosum* (SG), *stratum spinosum* and *stratum basale*. The barrier function of the skin depends on the outer most layer, the SC (10-20 μm thick) which consists of several layers (18-20 layers) of keratinized corneocytes (an array of flat, polygonal, keratin-filled cells) embedded in a lipid matrix of ordered lamellar structure [4] (Fig. 1.1). The corneocytes are surrounded by densely cross-linked protein structure, the cornified envelope (CE), which reduces the penetration of substances into the cells making the intercellular tortuous route as the main penetration pathway for xenobiotics including drugs delivered dermally or transdermally [5, 6]. In addition to the corneocytes and intercellular lipid matrix, the SC also contains corneodesmosomes, which hold the corneocytes together and proteolytic enzymes which degrade the corneodesmosomes in the process of desquamation [6].

The underlying three layers of EP make up the viable EP (50-100 μm thick). The viable EP ensures the generation of the SC, i.e., the cell shedding from the SC surface (desquamation) is balanced by cell growth in the viable EP [7]. First keratinocytes proliferate in the basal layer, start to differentiate upon leaving the basal layer cells and migrate to the skin surface. The final steps in keratinocyte differentiation profoundly alter their structure and occur at the SG-SC interface. The viable epidermal cells are transformed into flat dead keratin filled cells, corneocytes, surrounded by CE proteins and covalently bound lipid envelopes [1, 7].

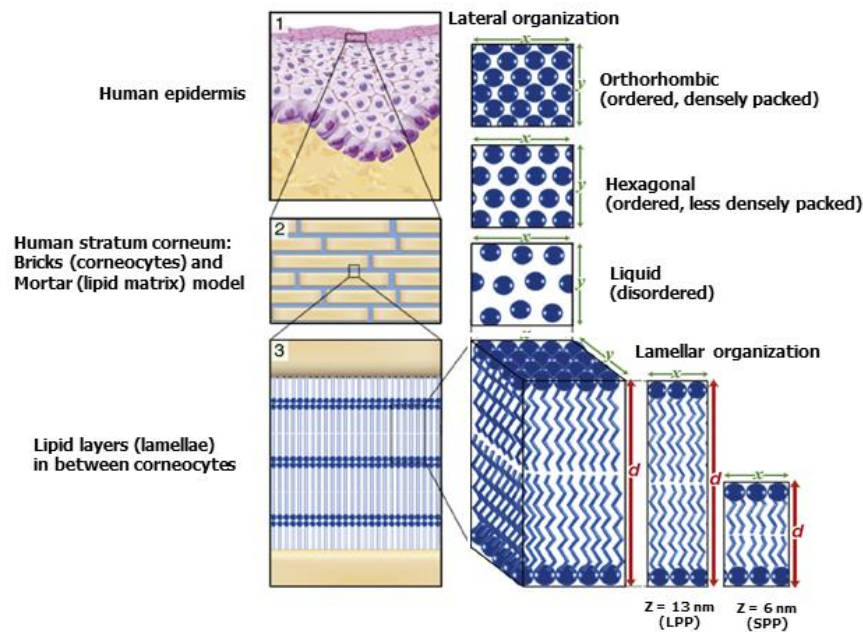


Figure 1-1: Lipid organization in human SC (1). The SC consists of dead cells (corneocytes) embedded in a lipid matrix (2). The intercellular lipids are arranged in layers (lamellae) (3), with either a long or short repeat distance (d), referred to as the long periodicity phase (LPP) ($\sim 13 \text{ nm}$) or short periodicity phase (SPP) ($\sim 6 \text{ nm}$), respectively. The three possible lateral organizations of the lipids are shown: a very dense, ordered orthorhombic organization, a less dense, ordered hexagonal organization, or a disordered liquid organization (adapted from [2] with permission).

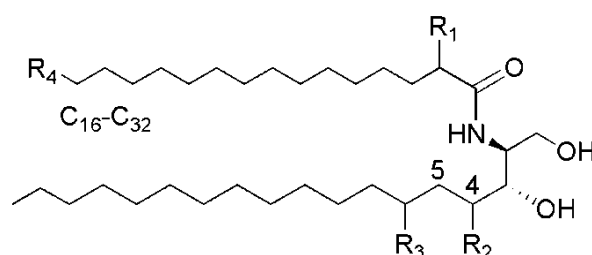
The SC is not only the main barrier against skin penetration of substances but it also regulates the release of water into the atmosphere, i.e., transepidermal water loss (TEWL)[1]. The lipid regions in the SC are very important for the barrier function as they are the only continuous structure in the SC. The lipid composition of SC is unique and different from the cell membrane of living cells. The SC has nearly equimolar quantities of ceramides (CERs), cholesterol, and long-chain free fatty acids (FAs) as major lipid components and cholesterol sulphate as well as cholesterol esters as minor components. Phospholipids are absent in the SC [1, 3, 8]. CERs are essential constituent of the lipid lamellae, representing nearly half of the total intercellular lipid content by weight, playing a critical role in skin health by providing a barrier and retaining the skin moisture [9, 10].

1.1.3. Ceramides

CERs are composed of long chain sphingoid bases (SBs) linked to long-chain FAs through amide bonding. The SBs can be dihydrosphingosine (d18:0), 4-sphingenine (sphingosine) (d18:1⁴), 4-hydroxysphinganine (phytosphingosine) (t18:0) or 6-hydroxysphingosine [11,

12]. The names and shorthand designations are according to Karlsson [13] (d: dihydroxylated, t: trihydroxylated, the following numbers indicate the number of carbon atoms (18) and double bonds (0, 1, 2)). The head groups of CERs contain hydroxyl groups capable of forming inter and intra molecular hydrogen bonds [5]. The number of the hydroxyl groups in the head group of the CERs appears to be substantial for the integrity of the barrier function of the SC [14, 15]. The acyl chain of CERs also exhibits heterogeneity in terms of chain-length (C16-C30), the degree of unsaturation (predominantly saturated) and hydroxylation pattern [11]. The FAs in the epidermal CERs can be non-hydroxy acids, α -hydroxy acids, ω -hydroxy acids or ester-linked ω -hydroxy acids [16]. While acyl chain lengths C24-C26 are the predominant FAs, chain lengths of C16-C18 are found in small amounts [7]. The EP has unique long chain FA, ω -hydroxy FA, esterified with other FA (predominantly linoleic acid (C18:2)). In addition to linoleate moiety, the ω -hydroxy FA chain can also be attached to oleate or stearate moieties [17]. The chain-length of ω -hydroxy FA varies between C28-C32. The ω -esterified acylCERs are one of the main SC lipids required for the formation of the CE as most of ω -hydroxy CERs are covalently attached to CE proteins (mainly with involucrin but also with envoplakin and periplakin) which also interdigitate with the intercellular lipid lamellae [9, 18, 19].

There are 16 free extractable CER classes in human SC, resulting from the possible combinations of the four types of the SBs with the four types of FAs, including the unique ω -acylated CERs (Fig. 1.2). Recently a new class of CERs with tetrahydroxyl SB have been reported [20]. Additionally, SC has ω -hydroxy-CERs covalently bound to CE proteins of corneocytes [21]. The nomenclature of CER [XY] is based on acyl chain and SB components of CERs. The first letter "X" indicates the acyl chain: N for non-hydroxy FA, A for α -hydroxy FA, O for ω -hydroxy FA and EO for ester-linked ω -hydroxy FA and the second letter "Y" designates the SB: S for sphingosine, P for phytosphingosine, DS for dihydrosphingosine, and H for 6-hydroxysphingosine as proposed by Motta *et al.* [22] and Robson *et al.* [21]. The newly discovered CER class with tetrahydroxy SB was annotated as CER [NT] as it contains saturated non-hydroxy FA amide linked to dihydroxy dihydrosphingosine or dihydroxy sphinganine (T for the two additional hydroxyl groups on the SB, compared to sphinganine (d18:0)) [20]. There is variation in the literature regarding the relative amount of the various CER species in the SC [20, 23, 24].



4-Sphingenine (sphingosine)-based CERs	R1	R2	R3	R4	4,5 double bond
CER [EOS]	H	H	H	OH	√
CER [NS]	H	H	H	H	√
CER [AS]	OH	H	H	H	√
4-Hydroxysphinganine (phytosphingosine)-based CERs					
CER [EOP]	H	OH	H	OH	-
CER [NP]	H	OH	H	H	-
CER [AP]	OH	OH	H	H	-
6-Hydroxy-4-sphingenine-based CERs					
CER [EOH]	H	H	OH	OH	√
CER [NH]	H	H	OH	H	√
CER [AH]	OH	H	OH	H	√
Sphinganine (dihydrosphingosine)-based CERs					
CER [EODS]	H	H	H	OH	-
CER [NDS]	H	H	H	H	-
CER [ADS]	OH	H	H	H	-

Figure 1-2: Chemical structure of free epidermal CERs [25]. The ω -hydroxy (R4) FAs are mostly esterified with linoleic acid (C18:2). The C16 - C32 FAs may also refer to unsaturated FAs. The structure of CER classes containing ω -hydroxy FA (CER [OS], CER [OP], CER [OH] and CER [ODS]) are not shown.

The precursors of the SC lipids such as glucosylceramides (GlcCERs), sphingomyelin (SPM) and phospholipids are stored in the lamellar bodies, membrane-coating granules in the SG, and they are enzymatically processed into their final constituents: CERs and free FAs [2]. Therefore, SC CERs can be generated either by serine-palmitoyl transferase catalyzed *de novo* synthesis, which converts palmitoyl CoA and L-serine into CERs [26] or by β -glucocerebrosidase [27] and acid sphingomyelinase [28] catalyzed hydrolysis of GlcCERs and SPM, respectively. The SC CER moieties are derived from epidermal GlcCERs and AcylGlcCERs, as described by Robson *et al.* [21] and Hamanaka *et al.* [29]. The total epidermal GlcCERs are composed of six distinct molecular groups, GlcCER 1-6, with non-hydroxy (C16-C24) or α -hydroxy (limited to C24, C25 and C26) FAs and C18 or C20 SBs [29, 30]. Large quantities of GlcCER and SPM precursors are produced in EP and delivered to SC extracellular lipid domains. The CER precursor metabolizing enzymes hydrolyze the GlcCER and SPM into the corresponding CER species, important process for epidermal permeability

barrier homeostasis [29, 31, 32]. It was shown that CER [NS] and CER [AS] are obtained from the hydrolysis of SPM precursors [33]. The level of epidermal CERs is, therefore, regulated by the balance between β -glucocerebrosidase, sphingomyelinase, and ceramidase (which metabolizes CERs into SBs and free FAs) [3]. The deficiency of β -glucocerebrosidase in the EP alters the distribution of CERs and GlcCERs and the epidermal permeability barrier [27, 34].

1.1.4. Lipid Organization in the SC Lipid Lamellae

The lamellar arrangement of SC lipid matrix is unique and has not yet been fully elucidated. The lipid organization showing the lipid sheets was first observed under electron microscope [35-37] and later the regular stack of lamellar sheets was characterized [38, 39]. Further understanding of the lipid organization of SC lipid lamellae was made possible by small and wide angle X-ray diffraction studies revealing the presence of 13 nm lamellar phase (LPP) unique to SC and 6 nm lamellar phase (SPP) in the SC lipid matrix (Fig. 1.1). The presence of acyl-CERs was shown to be essential for the formation of LPP [2, 40-43]. The application of neutron scattering experiments in investigating internal membrane arrangement of bilayer structures has provided a new insight into the SC lipid organization [15, 44]. From the neutron diffraction studies, the presence of CER [NP] and CER [AP] having three and four hydroxyl groups in the head group was appeared to be crucial for the formation of the SPP and for the integrity of the barrier function of the SC [14, 15, 45].

Several models describing the possible structural organization of the SC lipid matrix have been proposed. In addition to the ones recently suggested based on neutron diffraction studies, the armature reinforcement model and the asymmetry model, the other most important models like the domain mosaic model, the single gel phase model, the stacked monolayer model and the sandwich model have been reviewed elsewhere [25, 46].

1.2. Skin Disorders Associated with Perturbed or Altered SC Lipids

There are several skin diseases associated with deficiency or disturbance of SC lipids mainly CERs including epidermal protein-bound CERs. Sahle *et al.* [25] summarized the common skin diseases associated with depletion of SC lipids and the potential benefits of direct lipid replacement therapy and other approaches in treating affected, aged or diseased skin. The two common skin diseases, atopic dermatitis (AD) and psoriasis, are briefly described below.

Atopic dermatitis

AD is the most common chronic inflammatory skin condition associated with impaired permeability barrier function and increased TEWL. An altered amount and composition of SC CERs represent an etiologic factor of AD, CER [EOS] being most affected both in lesional and non-lesional skin [47]. In addition to CER [EOS], the level of CER [NP] was found to be lower in patients with AD and correlated with an increased TEWL [48]. Similarly the amounts of CER [EOS] and [NP] were found to be reduced in non-lesional skin of AD patients [49]. Another study identified CER [EOH] and CER [NP] as the most significantly reduced CERs in affected skin areas of patients with AD [50]. In contrary, elsewhere it has been demonstrated that the non-lesional skin in AD and psoriasis and healthy skin have similar free extractable CER profile [24]. The decreased levels of CERs in lesional and non-lesional skin were also associated with high expression of SMP deacylase [51, 52] and GlcCER deacylase [52, 53] (Fig. 1.3). The ceramidase-secreting bacteria colonizing the skin of patients with AD were also related to the deficiency of CERs [54]. On the other, hand the activities of β -glucocerebrosidase and ceramidase were found to be normal in atopic skin [55]. Another study showed slight increment in the amount of sphingomyelinase in the lesional skin of AD patients [56].

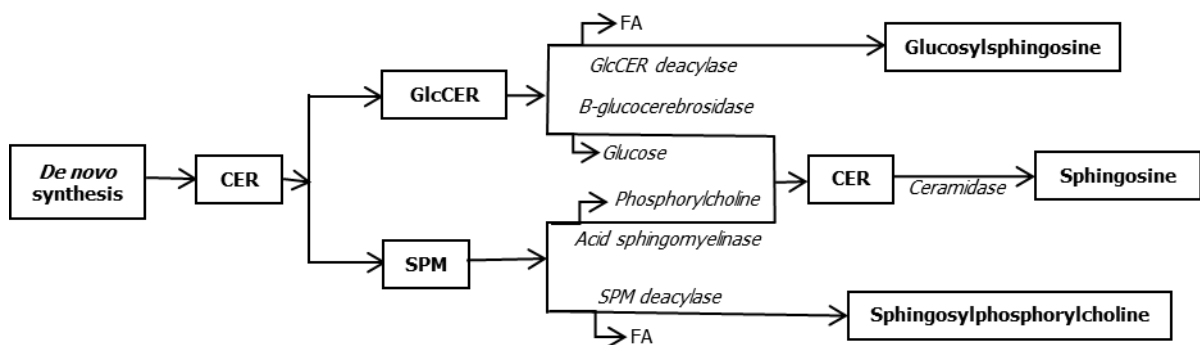


Figure 1-3: Possible mechanisms for altered CERs profiles in AD patients: a decrease in *de novo* CER synthesis; increased GlcCER and SPM deacylase activities, increased ceramidase activity; decreased sphingomyelinase activity [3].

Psoriasis

Psoriasis is a systemic chronic inflammatory disease with impaired skin barrier function. Similar to AD, the CER profile in psoriatic skin was also found to be altered. While the levels of CER [EOS], CER [NP] and CER [AP] were reduced, the amounts of d18:1^{Δ4}-based CERs

(CER [NS] and CER [AS]) were found to be higher. The defective barrier function might be attributed to the significant decrease in CER [EOS] [22, 57]. Although the TEWL increases in lesional psoriatic EP, studies have shown that there is no significant difference in terms of TEWL and water content between non-lesional psoriatic skin and normal skin [24, 58, 59]. The impaired barrier function in psoriatic skin could also be related to abnormal expression of enzymes involved in CER biosynthesis or degradation. Alessandrini *et al.* [60] indicated the possibility that disturbances in the CER generation pathways could contribute to the impairment in the psoriatic skin barrier function. Compared to non-lesional skin, the level of sphingomyelinase in lesional skin was decreased. The level of GlcCER- β -glucosidase in psoriatic non-lesional skin was found to be lower than normal skin [32].

1.3. Phyto-derived Ceramides (PhytoCERs)

1.3.1. Plant Sphingolipids (SLs)

Plant SLs are a diverse group of lipids composed of polar head groups attached to CERs. Extensive characterization of individual species in these complex and diversified class of plant lipids with powerful analytical tools led to the introduction of new research area, sphingolipidomics [61]. Plant SLs play critical roles in membrane stability and permeability, signaling and cell regulation as well as cell-to-cell interactions [62-64]. In general, plant SLs can be classified into four groups: glycosylceramides (GlyCERs), glycosyl inositol phosphor-ceramides, CERs, and free long chain bases [61]. In the first two classes, polar head groups are linked to C-1 of the N-acyl long chain bases with glycosidic linkage [63]. The polar head groups could be glycosyl residues, including the most abundant monohexoside (mainly glucose (Glc)) and other minor di, tri and tetrahexosides [65, 66] or phosphate-containing head groups [67]. Galactose-containing SL is rarely detected or reported in plants. In plants, compared to monohexoside CERs, oligo GlyCERs are not well characterized as they exist in minute amounts [62].

The most abundant class of SLs in plant tissue are mono-GlcCERs which are mostly characterized by a double bond at position 8 on the sphingoid residues and α -hydroxy FAs [68]. Fig. 1.4 shows the chemical structure of plant GlcCERs which comprises a hydrophobic CER part and a hydrophilic head group.

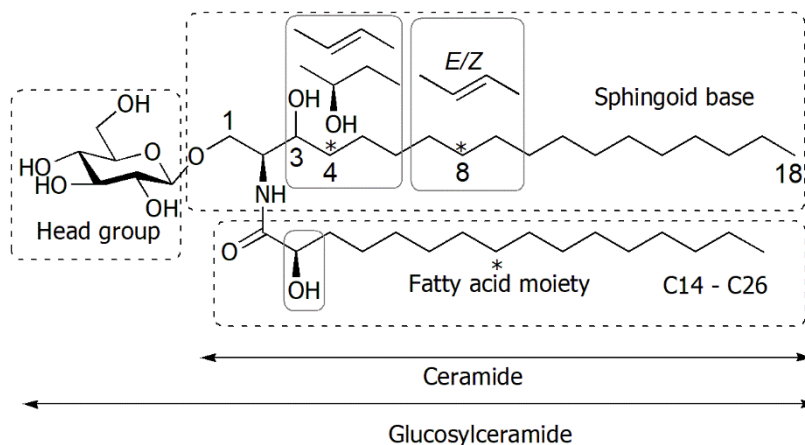


Figure 1-4: Chemical structure of plant GlcCERs showing the variation of CER backbones. The FAs are predominantly α -hydroxylated and they vary in chain length (C14 - C26) and ω -9-desaturation*. The SBs are amide linked with the FA moieties and they vary with the degree of desaturation or hydroxylation on C-4 and/or C-8 desaturation*

1.3.2. Structural Comparison of Plant and Epidermal CERs

Although the basic chemical structure of plant and skin CERs is similar, there are differences in chain length, hydroxylation pattern and degree of unsaturation of the SB and FA moieties (Fig. 1.4). In general, the SB-profile of plants is more diversified than that of mammalian SBs [69]. Previous investigations on plant SLs have identified several dihydroxy and trihydroxy SBs with one or two double bonds depending on the type of desaturase enzymes present in the plants. In addition to Δ^4 -SL desaturase, plants have Δ^8 -SL desaturase resulting in *cis* (*Z*)- and *trans* (*E*)- isomers of Δ^8 -unsaturated SBs [70]. Fig. 1.5 depicts possible modifications (hydroxylation or (*E*)-desaturation at C-4 and (*E/Z*)-desaturation at C-8) of typical C18 SBs of plant and mammalian CERs.

In plant GlcCERs, 8*E*/8*Z* isomers of 4,8-sphingadienine (d18:2 $\Delta^{4,8}$), 4-hydroxy-8-sphingene (t18:1 Δ^8) and 8-sphingene (d18:1 Δ^8) represent the dominant bases [63]. SBs with trace quantities include d18:0 and t18:0. GlcCERs containing sphingatrienine (d18:3) [71] and minor amounts of C17 and C19 SBs [72] have also been reported in some plants. While the naturally occurring dihydroxy bases have *D-erythro* configuration, trihydroxy bases have *D-ribo* configuration [63, 73]. The SBs of human epidermal CERs species differ from plant SBs in the number/position of desaturation. The skin SBs have desaturation at C-4 (d18:1 Δ^4), while plants contain C-8 desaturation in addition to C-4 in a typical plant SB [63]. The SBs which are found in relatively higher amounts in skin CERs, d18:1 Δ^4 and t18:0, have been detected in smaller amounts in plants [74-77].

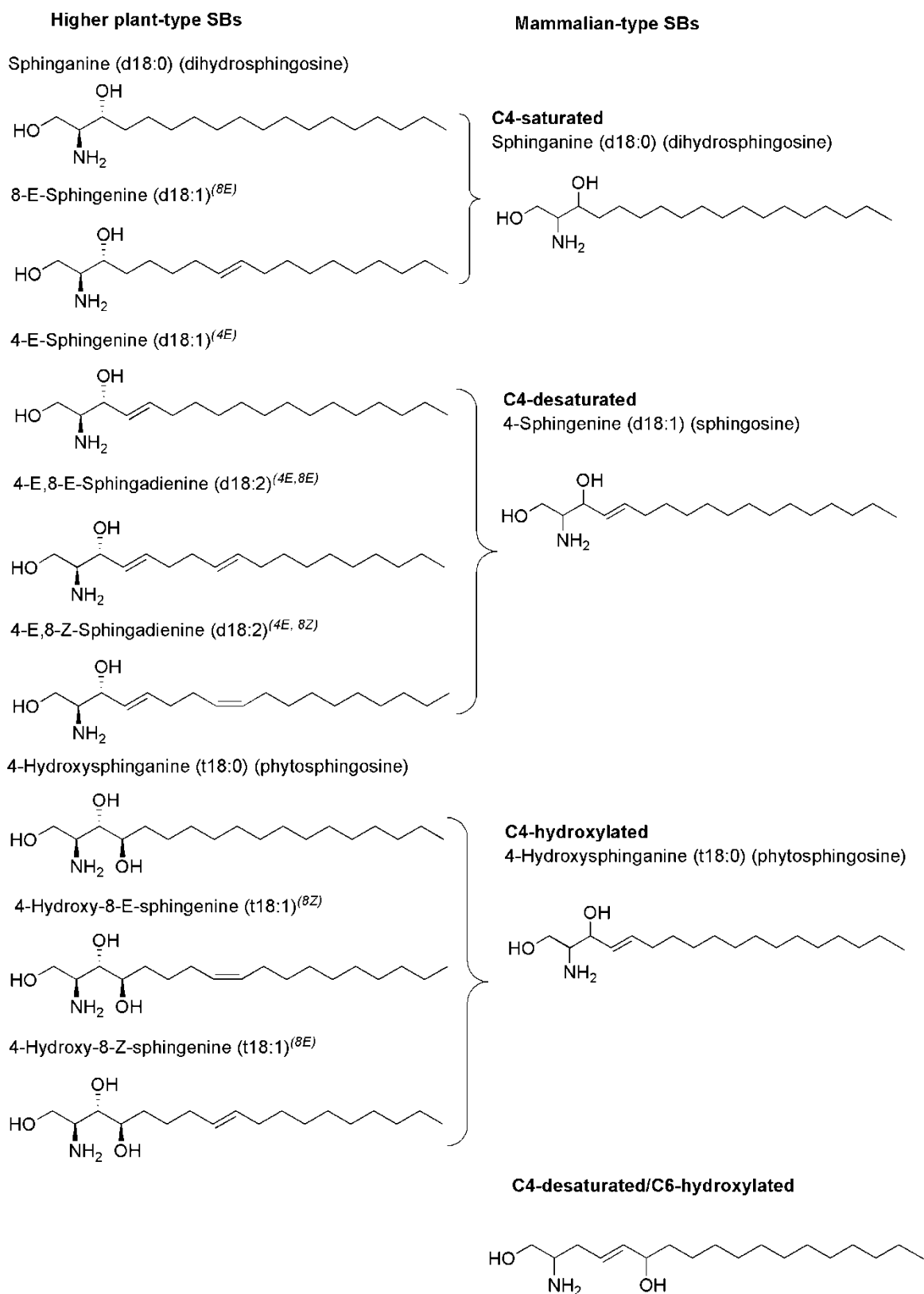


Figure 1-5: Structures of common C18 higher plant and mammalian SBs showing the variation at C4 of SBs: C4-saturated, C4-desaturated, C4-hydroxylated and C4-desaturated/C6-hydroxylated. Recently skin CERs with four hydroxyl SB have been reported [20]. The C4-double bond is primarily in the *trans* (E) configuration, whereas the C8-double bond is either *cis* (Z) or *trans* (E) configurations.

In plant GlcCERs, the FAs bound to the SBs have a chain length of C14-C26 atoms and are mostly saturated and α -hydroxylated [78]. The principal FAs are C16, C20, C22 and C24 saturated α -hydroxy FAs. Low amounts of ω -9-monounsaturated very long chain FAs (VLCFAs) (C22-C26), mostly α -hydroxynervonic acid (C24:1) in the leaf GlcCERs, are also found in plants [78-80]. On the other hand, skin CERs contain non-hydroxy, α -hydroxy or ω -hydroxy FAs, the latter having a chain length up to C32 and mostly ester-linked with unsaturated FA [81]. In plants ω -hydroxy FAs containing GlcCERs have not been yet found. The head group similarities (having 3-4 hydroxyl groups) of PhytoCERs and mammalian CERs (such as CER [NP] and CER [AP]) suggest the potential application of PhytoCERs in improving the skin barrier function of diseased and/or aged skin.

Generally, GlcCERs obtained from seed, leaf and root tissues display different SB and FA profiles. Lynch and Dunn [63] have attempted to summarize the SB and hydroxy FA profiles of soybean [82], wheat grain [76], rye leaf [83], maize leaf [74] and spinach leaf [75] GlcCERs. While dihydroxy SBs and C16-C20 saturated hydroxy FAs (the predominant being α -hydroxypalmitic acid (h16:0)) are enriched in seed tissues, trihydroxy bases and very long-chain saturated and ω -9-monounsaturated hydroxy FAs occur abundantly in leaf tissues [63, 79].

1.3.3. Commercial PhytoCER-based Preparations

PhytoCERs are naturally found in many cereal, tuber and legume dietary sources such as wheat [66, 68, 76], rice [65, 72, 84], corn [72, 85], potato and sweet potato [86], soybean [68, 87] and konjac [88, 89]. Although CERs were originally derived from soybean and bovine sources, currently there are several types of PhytoCERs available on the market. A wide variety of PhytoCER-based 'anti-aging' (which are claimed for the treatment of aging problems such as fine lines, wrinkles, and dryness) and skincare products are also widely available on the market as dietary supplements. These products are mostly formulated from two popular commercial sources of PhytoCERs: wheat and rice. There are also products containing potato and sweet potato CERs. Most of the PhytoCER-based formulations are encapsulated into veggie capsules and composed of vitamins essential for maintenance of healthy skin (including vitamin A, C, D and E). Many of the products also contain fillers, lubricants and glidants, although there are products free of these additives.

As plants contain relatively large amount of glycosphingolipids (GSLs), mainly GlcCERs, the chemical compositions (FAs and SBs) of common plant GlcCERs are described in Table 1.1 and 1.2. The predominant GlcCER species are also shown in Table 1.3. The predominant GlcCER species in most of the plants contain d18:2^{Δ4,8}/d18:1^{Δ8} and h16:0/hydroxyarachidic acid (h20:0) as the SB and FA components, respectively.

Table 1-1: The FA composition of common plant GlcCERs.

Fatty Acids	Composition (%)										
	Wheat		Rice			Sweet Potato	Potato ^a	Maize	Kidney Bean		
	Grain	Flour	Leaf	Bran	Endosperm	Leaf	Tuber	Tuber	Commercial ^b	Leaf	
16:0	-	-	-	-	-	-	6	6 - 10	-	-	4.6
16:1	-	-	-	-	-	-	1.5	0.1 - 9	-	-	0.7
h14:0	0.2	0.2		< 0.1	< 0.1		-	-	-		0.8
h16:0	39.1	40.2	8.4	0.4	0.2	0.1	78	76 - 86	6	3.9	58.2
h18:0	7.5	4.5	0.9	5.9	5.2	1.4	2	2 - 2.5	17	5.0	0.3
h20:0	43.7	44.1	7.0	30.9	42.4	42.3	1	0.1	39	29.6	0.5
h21:0	0.6	0.4	1.7	1.5	0.4	1.7	0.2	-	-	0.5	-
h22:0	3.1	3.7	17.2	14.7	12.4	31.5	4	0.2 - 1	13	31.9	5.6
h22:1			3.5								
h23:0	0.2	0.1	5.2	3.5	1.2	1.7	0.6	0.1 - 0.5	-	0.7	1.3
h24:0	2.5	5.4	23.5	30.3	29.1	20.2	3	1 - 2	22	27.3	23.3
h24:1	1.1		23.1								
h25:0	0.2	0.1	<0.1	4.2	1.4	0.2	1	0.1 - 0.3	-	0.4	0.9
h26:0	0.4	0.5	3.1	7.3	7.2	0.9	1	0.2 - 0.5	3	0.7	1.2
h26:1	-	-	2.2								
Others	1.4	0.8	-	1.3	0.5	-	4.2	0.6 - 3.9			2.6
Ref	[76]	[66]	[78]	[65]	[65]	[78]	[86]	[86]	[85]	[78]	[90]

The data reported here are expressed as % of total GlyCERs. Only the composition of mono-GlcCER has been considered. ^aThe range represents the results of the different potato species. ^bCommercial maize GlcCER-rich preparation from Nippon Flour Mills Co. Ltd. (Atsugi, Japan).

Table 1-2: The SB composition of common plant GlcCERs.

Sphingoid Bases	Composition (%)											
	Kidney Bean	Wheat Grain	Wheat Flour	Wheat Leaf	Rice Bran	Rice Endosperm	Rice Leaf	Sweet Potato	Potato ^a	Maize ^b	Maize Leaf	Konjac
d18:0	0.2	9	7.6	0.2	0.3	1.0	0.1			1	<0.1	-
d18:1 ^{Δ4E}	<0.1	1	1.2		2.5	5.9	-			3		0.6
d18:1 ^{Δ8E}	} 2.7	24	25.3	1.3	} 1.8	} 2.2	0.3			-	0.2	} 3.8
d18:1 ^{Δ8Z}		47	42.6	3.2			0.3	4.5	2.7 - 3.9	-	1.0	
d18:2 ^{Δ4E/8E}	60.1	2	8.5	5.2	16.5	34.6	11.5	} 86.0	} 91.0 - 94.0	17	17.3	} 54.0
d18:2 ^{Δ4E/8Z}	17.3	13	12.4	9.4	53.3	40.6	34.3			53	55.7	
t18:0	0.3	1	0.5	0.9	3.3	1.2	0.8			2	0.4	1.4
t18:1 ^{Δ8E}	11.0	1	0.5	6.9	6.1	2.8	3.1	} 9.5	} 3.0-5.2	2	1.6	} 40.2
t18:1 ^{Δ8Z}	8.5	2	1.4	72.9	16.2	11.9	49.6			22	23.8	
d18 base	80.2	96	97.6	19.3	74.4	84.1	46.5			74	74.2	58.4
t18 base	19.8	4	2.4	80.7	25.6	15.9	53.5			26	25.8	41.6
Ref	[90]	[76]	[66]	[74]	[65]	[65]	[74]			[85]	[74]	[88]

The data reported here are expressed as % of total GlyCERs. Only the composition of mono-GlcCERs has been considered. ^aThe range represents the results of the different potato species, ^bCommercial maize GlcCER-rich preparation from Nippon Flour Mills Co. Ltd. (Atsugi, Japan).

Table 1-3: Predominant GlcCER species of common plants GlcCERs

Plants	Scientific Name	Family	Tissue	Predominant GlcCER Species	References
Rice	<i>Oryza sativa</i>	<i>Poaceae</i>	Seed bran, Endosperm	d18:2/h20:0 and d18:2/h24:0	[65, 72]
Wheat	<i>Triticum aestivum L.</i>	<i>Poaceae</i>	Grain, flour	d18:1 ^{Δ8} /h16:0 and d18:1 ^{Δ8} /h20:0	[66, 68, 76]
Sweet Potato	<i>Ipomoea batatas (L.) Lam.</i>	<i>Convolvulaceae</i>	Tuber	d18:2-h16:0	[86]
Potato	<i>Solanum tuberosum L.</i>	<i>Solanaceae</i>	Tuber	d18:2/h16:0	[86]
Konjac	<i>Amorphophallus konjac</i>	<i>Araceae</i>	Tuber	d18:2/h18:0	[91]
Beet	<i>Beta vulgaris L.</i>	<i>Amaranthaceae</i>	Fiber	d18:2/h16:0	[92]
Maize	<i>Zea mays L.</i>	<i>Poaceae</i>	Commercial ^a	d18:2/h20:0 and d18:2/h24:0	[85]
Kidney bean	<i>Phaseolus vulgaris L.</i>	<i>Fabaceae</i>	Seed	d18:2/h16:0	[90]
Soybean	<i>Glycine max</i>	<i>Fabaceae</i>	Seed	d18:2/h16:0	[68]

^aCommercial maize GlcCER-rich preparation from Nippon Flour Mills Co. Ltd. (Atsugi, Japan).

There are PhytoCER-enriched preparations available on the market for dietary supplements intended for cosmetic applications. Most of these preparations are patented and they are available in different forms including oils and powders. The common ones include rice-derived PhytoCERs such as ORYZA CER-PCD™, wheat-derived PhytoCERs such as Lipowheat™, Cennamide™, and Ceramosides™ as well as Konjac-derived PhytoCERs. There oil extract-based formulations such as Lipowheat™ oil extract, wheat germ oil and wheat-derived Ceramosides™ oil blend are mostly encapsulated into liquid capsules/soft gelatin capsules. However, little effort has been made to deliver these PhytoCERs topically.

1.4. Delivery of PhytoCERs for Skin Barrier Reinforcement

1.4.1. Oral Delivery of PhytoCERs

In the early 1990's a large number of topical skin care products containing CERs were formulated and marketed by cosmetic companies for the treatment of skin conditions associated with ageing including fine lines, wrinkles and dryness. Most of these products were creams and lotions claimed to have skin hydration and renewal effects. Later, in 1997 Japanese nutraceutical companies started to formulate and market oral PhytoCER-based

nutritional supplements [93]. Currently both PhytoCER-based ingestible dietary supplements and CER-based topical skin moisturizing products are widely distributed on the market.

1.4.1.1. Effects of Oral PhytoCERs on Skin Barrier

The beneficial effects of oral PhytoCERs on the skin hydration and skin barrier reinforcement have been established in several studies involving animal models [94-97] as well as human subjects [93, 94, 98, 99]. These studies were mostly conducted on detergent or tape-stripped-perturbed human and/or hairless mice skin [94, 100] or on skin with diet induced AD-like symptoms in animal models [101, 102]. Tsuji *et al.* [96] examined the effect of dietary GlcCER-derived from rice and maize on the maintenance and recovery of skin barrier function in hairless mice, respectively. The mice were fed with a special skin-damaging diet which increases TEWL and reduces SC flexibility. The TEWL of GlcCER-fed hairless mouse skin was found to be significantly reduced and the SC flexibility was also improved. Feeding of maize GlcCER diet after acute barrier perturbation by tape-stripping also enhanced the recovery of skin barrier of the mice.

Recently the protective effect of orally administered beet (*Beta vulgaris*) GlcCERs against diet-induced skin barrier impairment (increased TEWL and scratching behavior, dry skin with erythema) in hairless mice was investigated [97]. The dietary supplement prevented the increase in TEWL and cumulative scratching time in mice fed with the special diet. Yeom *et al.* [95] used oxazolone-induced chronic irritant contact dermatitis in mouse model skin to investigate the beneficial effect of oral administration of soybean GlcCERs on inflammatory dry skin. The orally administered GlcCERs had anti-inflammatory action and reduced itching and the suppression of inflammation was attributed to the inhibition of cytokine production. GlcCERs also suppressed the SC dehydration and repaired the skin barrier function.

A randomized, double-blind placebo-controlled trial was conducted on women with dry skin to investigate the moisturizing effect of dietary supplement containing wheat extract enriched with GlcCERs and digalactosyldiglycerides (DGDG) [93]. According to the finding, there was a significant increase in skin hydration with improved associated clinical signs (itching, squamae, roughness and redness). Ingestion of konjac GlcCERs has also shown positive effects in AD patients as well as healthy volunteers. It has been reported that oral intake of konjac GlcCERs decreased the TEWL in AD-patients [99] and improved skin symptoms (including TEWL reduction) and reduced skin allergic responses in children with

AD [98]. In another study, oral intake of konjac GlcCERs reduced the TEWL of hairless mouse skin (rough skin induced by sodium dodecyl sulfate) and in healthy human subjects [94]. The effects of beet GlcCERs on skin elasticity in female volunteers with dry skin and fibronectin production in human dermal fibroblasts were investigated. The beet GlcCERs promoted fibronectin synthesis but had no effect on fibroblast proliferation or collagen synthesis [92]. Unlike most of the other plant GlcCERs (rice, corn and konjac), beet GlcCERs did not induce significant improvements in TEWL. The anomaly was explained by the differences in the SB and FA profiles of the plant GlcCERs as well as the existence of other unidentified lipid components in the beet CERs which might alter the skin condition.

1.4.1.2. Mechanisms Underlying Skin Barrier Improvement

Despite the structural differences between plant and skin CERs, the beneficial effects of dietary PhytoCERs have been demonstrated. The few foregoing studies suggested that the absorbed metabolites of ingested GlcCERs might have distributed to the skin to exhibit their beneficial effects. However, the underlying mechanisms by which orally administered GlcCERs improve the skin barrier remain largely unknown. Some of the proposed mechanisms include an increase in the levels of epidermal CERs [103-105], inhibition of inflammatory cytokine production [94, 95], expression of genes involved in the maintenance and formation of SC (epidermal transglutaminases, tight junction and CE related genes) [106-108], expression of genes related to CER *de novo* synthesis [88, 109] and activation of epidermal SL metabolizing enzymes [110].

1.4.2. Topical Delivery of PhytoCERs

One of the approaches to treat skin dryness and skin barrier dysfunction associated with depletion and/or disturbance of SC lipids is direct replacement of the depleted lipids [25]. Several CER [27, 111] and pseudoCER [112-114] containing topical products and CER-dominant emollients [115-119] have been shown to have beneficial effects in management of skin diseases associated with depleted SC lipids. However, many of these cosmetic products have limited published data to establish their cutaneous efficacy [120]. The CERs are mostly obtained from animal such as bovine brain or synthetic or semi-synthetic sources. Nowadays, CERs are also produced by biotechnological approach [121]. Due to unestablished safety profile of animal-based CERs and the laborious and expensive synthetic

procedure, safe and low cost alternative source of CERs are needed. The depleted native skin CERs can potentially be replaced with CERs isolated from edible plants.

1.4.2.1. Controlled Delivery of PhytoCERs into the SC

The CERs meant to replenish the depleted CERs in the SC have to be delivered deep into the SG-SC interface as the SC lipid organisation into lipid bilayers takes place at this interface [7, 25, 122]. One of the challenges in topical replenishment of depleted CERs is the poor penetration of CERs into the SC from conventional formulations. Except for a few recent studies [123, 124], most of the previous studies showing the beneficial effects of topical formulations containing CERs were unable to confirm the permeation of the CERs into the SC and deeper layers of the skin. Different formulation strategies improving the poor solubility and facilitating the permeation of CERs deep into the SC such as colloidal formulations have been designed and evaluated [123, 125-127]. PhytoCERs can also be delivered into the SC and can potentially stabilize SC lipid lamellae. So far, however, little effort has been made to directly deliver PhytoCERs into the SC. *In vitro* as well as *in vivo* studies are needed to investigate the permeation of PhytoCERs into the SC and understand their influences on the stabilization of SC lipid bilayer as well as lipid biosynthesis in the skin.

There are different possibilities once the PhytoCERs are delivered into the SC: either they directly localize in the SC, integrate with natural skin CERs and contribute to the skin barrier function or increase the production of endogenous CERs thereby improving the skin barrier. If the exogenous CERs are directly localized in the SC, further *in vitro* and *in vivo* studies are required for better understanding of the molecular arrangement of the PhytoCERs in the SC lipid matrix, their integration with endogenous skin CERs and their role in stabilizing the bilayer structure of SC. Neutron diffraction [14, 15] and x-ray diffraction [43, 128] studies are the two commonly used *in vitro* studies used to investigate the molecular organization of SC lipids. The impact of PhytoCERs on the nanostructure of SC lipid model membranes mimicking SC lipid organization has to be investigated using these instrumental methods. Furthermore, the roles of PhytoCERs in epidermal barrier function have to be studied in animal models as well as human skin (healthy and diseased).

1.4.2.2. Delivery of PhytoCER Precursors into the Viable Epidermis

An alternative strategy of increasing the CER levels in the skin and improving barrier function could be effectively delivering the CER precursors, GlcCERs and SPM, to the viable EP

assuming that the exogenous CER precursors will be metabolized by epidermal enzymes. A 3D reconstructed human EP was used to investigate the changes in CER levels in the cultured skin after the application of topical formulations containing CER precursors. The level of CER [NS] in cultured skin model was significantly increased after the application of SPM-based liposomes to the LabCyte EPI-MODEL [129]. The effect of size of liposomes in enriching the CER level in 3D model membrane was also evaluated [130]. The levels of CERs which are not derived from SPM (CER [NP] and CER [AP]) were found to increase significantly, especially when the small sized liposomes were applied. This finding suggested that the increase in the CER level in the membrane is not only attributed to the enzymatic reactions, other mechanisms might have involved as well.

Shimoda *et al.* [131] demonstrated the effects of rice GlcCERs on the changes of epidermal CERs and GlcCERs in mice, after oral dosing, as well as in human epidermal equivalent. The oral GlcCERs increased the level of CER [EOS], decreased the levels of GlcCERs (accompanied with enhanced glucocerebrosidase and GlcCER synthase expressions) and improved the TEWL. On the other hand, the rice GlcCERs increased the levels of CER [EOS], CER [NS] and GlcCERs (accompanied with enhanced expression of GlcCER synthase but not glucocerebrosidase) in the epidermal equivalent suggesting the need for further investigations to clarify the discrepancy. In another study, the level of CER [AS] in human epidermal equivalent was found to increase after application of GlcCER-based liposomes in a dose-dependent manner [132]. The other CERs (CER [NS], [NP], [AS] and [AP]) didn't show significant changes. Besides, inhibitor for β -glucocerebrosidase, conduritol B epoxide, reduced the amounts of CERs significantly.

PhytoCERs have also been incorporated into topical cosmetic products to investigate their effects on skin hydration and barrier function. Asai and Miyachi [133] evaluated the skin moisturizing effects of topically applied skin moisturizers containing rice CERs and orally administered corn CERs on human healthy volunteers. The topical moisturizers and the oral CERs have increased the water content in the SC and suppressed the TEWL. On the other hand, Shimada *et al.* [134] studied the inhibitory effect of topically applied maize GlcCERs on UVA-induced wrinkle formation and epidermal thickness in hairless mice. It was found that the topical application of maize GlcCERs reduced the formation of wrinkle and epidermal thickening suggesting its potential application in protecting photo-ageing.

1.5.LC-MS-based Structural Characterization and Quantification of SLs

Liquid chromatography tandem mass spectrometry (LC-MS/MS) is a powerful, specific and sensitive technique for qualitative as well as quantitative analyses of SLs including CERs and GlcCERs [72]. While the LC allows separation of intact molecules in a complex mixture, the tandem MS uniquely identifies the various molecular species of CERs and GlcCERs [135]. The structural identification is based on unique molecular decomposition pattern of the SLs i.e., precursor ion-product ion mass transfer at a specific retention time [71, 136-138]. The uniqueness of the precursor-product ion pair allows the MS to differentiate between many components in a complex mixture, including the co-eluting molecular species within a given class of SLs [139, 140]. Tandem MS is, therefore, useful in differentiating the interference of solvent ions and other co-eluting species with the detection of the ions of interest, particularly at lower m/z ratios where solvent ions predominate [141]. However, accurate quantification of species with identical precursor ion-product ion m/z values (such as GlcCER and galactosyl-CER) requires a baseline resolution [142]. Any possible ionization suppression or enhancement can be normalized by addition of an appropriate internal standard that co-elutes with the analytes [139, 143].

1.5.1. Liquid Chromatography

The chromatographic separation of the SLs prior to MS detection avoids the possible interferences arising from isotopes, isobars, and isomers [139]. It also allows detecting less abundant SLs and distinguishing long chain FAs with different degrees of unsaturation [143]. In addition, the ionization suppression effect of other species is greatly reduced as the separation reduces the complexity of the eluent at any given elution time. This improves also the quantitative accuracy and sensitivity of the method [142]. Both normal phase and reversed phase (RP) chromatography have been used for the analysis of SLs. While the separations in RP chromatography are based on the length and (un)saturation of the SB and/or N-acyl FA (i.e., separates molecular lipid species), normal phase chromatographic separations are mainly based on the polarity of the head group (i.e., separates lipid classes such as CERs and GlcCERs). In normal phase chromatography each class of SLs does not separate into individual components. Furthermore, it has limited reproducibility and insufficient peak shapes.[139, 140]. RP chromatography is commonly used in sphingolipidomics, the most common RP column being C18 and C8. However, in RP

chromatography, co-elution of analytes and internal standards may not be possible as the separation is chain length-dependent [140].

1.5.2. Ionization Techniques

The full scan mass spectra of SLs depend on the ionization technique and mode of ionization used. Electron ionization was used in early GC-MS-based structural characterization of SLs [144]. Electron ionization is a 'hard' ionization technique which results in extensive in-source fragmentation due to the high energy used during the ionization process [139]. Electrospray ionization (ESI) has been the most commonly utilized ionization technique for LC-MS-based qualitative and quantitative analyses of SLs [72, 86, 136, 141, 145]. Positive mode of ionization is mostly used due to the presence of polar head groups in all SLs, the dominant mass spectra being the proton adduct $[M+H]^+$, sodium adduct $[M+Na]^+$ and water molecule neutral loss $[M+H-H_2O]^+$ in all SLs. Furthermore, in-source fragmentation might result in neutral loss of sugar molecule in MS spectra of GSLs [140]. However, ESI is a 'soft' ionization technique and, if the ionization conditions are optimized, it yields primarily intact molecular ions with little or no fragmentation [139, 142]. The structural information could be obtained from tandem MS analysis and SB-FA combinations can also be determined. SLs are readily ionized and, most of them, produce abundant and distinctive product ions of the head group, SB, or FA moieties when subjected to tandem MS [143].

On the other hand, atmospheric pressure chemical ionization (APCI) often gives good results for nonpolar compounds and thus is frequently used for the analysis of many lipid classes including CERs and GlcCERs [23, 137, 146-150]. LC/APCI-MS was used for the structural characterization of neutral SLs such as CERs and GlcCERs [148]. A pronounced in-source fragmentation was observed resulting in a sequential neutral losses of the sugar moieties and water molecules. Besides, fragments of the SB and FA were also detected. The in-source fragmentation, which is normally considered to be a disadvantage for APCI, provided structural information without further MS/MS fragmentation. As compared to ESI, the ionization process in APCI is mostly independent of the nature of mobile phase used, the sample related ion suppression effect is minimal and the tendency of forming adducts is also less pronounced [137, 146, 148].

Matrix assisted laser desorption ionization (MALDI) is one of the earliest ionization techniques which has also been used for the structural characterization of SLs [151, 152]. Unlike ESI

and APCI, MALDI ionizes the analyte of interest directly from a solid phase [153]. The high background chemical noise arising from the matrix and the in-source fragmentation are the main limitations of MALDI. These limitations can be minimized by using alternative matrices to reduce fragmentation or MS/MS to filter out the background chemical noise [139, 140]. Although MALDI has been combined with TLC, it cannot be directly coupled to liquid chromatography [153].

1.5.3. Mass Analyzers

A large number of SLs have been identified and/or quantified using tandem MS techniques with different mass analyzers including triple quadrupole (tandem-in-space MS)[154] and ion trap (tandem-in-time MS) [71, 72]. This is achieved by collision induced dissociation (CID), where the analyte is dissociated into fragments due to the collision of m/z -selected molecular precursor ions with inert gas molecules such as helium or argon [153, 155]. In triple quadrupole mass analyzers, the molecular ions of the analyte are m/z -scanned, fragmented, and analyzed in three quadrupoles (Q1, Q2, Q3) aligned in a row. The fragmentation takes place in the collision cell (Q2). The various scan modes (product ion scan, parent ion scan, neutral loss scan and/or multiple reaction monitoring (MRM)) can be performed by triple quadrupole instruments [141, 155]. One disadvantage of triple quadrupole is its low resolution power. This can be overcome by using hybrid mass spectrometers such as Quadrupole-Time-of-Flight (QTOF) [153].

Unlike triple quadrupole instruments, tandem-in-time mass spectrometers such as ion trap instruments can perform multiple stage fragmentations. In ion traps, fragments are generated by collision of the analyte with an inert gas in the ion trap analyzer itself. The resulting fragments can be further fragmented n -times (with $n > 2$) [153]. There are 3D and 2D ion trap mass spectrometers. Although the 2D ion trap operates in a fashion analogous to that of the conventional 3D ion trap, the former has improved performance over the latter: greater ion trapping efficiency, greater ion capacity before observing space-charging effects (due to the linear configuration of the mass analyzer), and faster ion ejection rate [156]. Hybrid mass spectrometers such as QTOF [157, 158], linear ion trap-orbitrap [159] and MALDI-Fourier transform [160] instruments have also been used for analysis of SLs with higher mass accuracy.

1.6. Nano-sized Carriers in Dermal and Transdermal Drug Delivery

Several nanocarriers such as microemulsions (MEs), vesicular systems and nanoparticles (NPs) have been investigated to overcome the barrier of the SC, the main challenge in dermal and transdermal drug delivery. In this section, however, emphasis is given to two of these nano-sized carriers: MEs and NPs.

1.6.1. Microemulsions

MEs are optically isotropic, transparent one phase systems which are formed spontaneously by mixing appropriate amounts of lipophilic and hydrophilic components with surfactant (SAA)/co-SAA [125]. They are thermodynamically stable systems and can be characterized by Gibbs-Helmholtz equation shown below.

$$\Delta G = \gamma \Delta A - T \Delta S$$

where ΔG is the free energy of formation, γ is the oil-water interfacial tension, ΔA the change in the interfacial area upon emulsification, ΔS is the change in entropy, and T is the absolute temperature. The enormous surface area resulting from the formation of MEs tends to increase the surface free energy of the system. The thermodynamic stability and spontaneity of formation of MEs can be explained by a negative free energy of formation due to remarkable reduction of interfacial tension accompanied by a dramatic change in the entropy of the system [161].

In addition to their ease of preparation and long-term stability, MEs have the advantage of high drug solubilization capacity (both hydrophilic and lipophilic drugs) and improved drug delivery. The high drug solubilization capacity of MEs is attributed to the enormous interfacial area and existence of microenvironments of different polarity within the same single-phase system [161]. A wide range of both hydrophilic and lipophilic drugs can be solubilized in MEs as there are plenty of combinations of ME constituents which principally can form MEs [162].

1.6.1.1. Formulation of MEs

MEs are prepared by simple mixing of appropriate amounts of formulation components. In some cases a rapid microemulsification process requires a very low energy input (heat or mechanical agitation) to overcome the kinetic barriers to the formation of MEs [161]. The microemulsification process is mainly governed by the amount and nature of the oil phase,

SAA, co-SAA and aqueous phase and physicochemical properties of the drug [163]. Therefore, careful selection of oil phase, SAA, co-SAA and/or co-solvents is needed. To obtain a ME with suitable characteristics with maximal efficacy, it is necessary to find the appropriate composition and concentration of components [164].

Surfactants

Previously various SAAs, SAA blends and co-SAAs have been used for the stabilization of MEs. Zwitterionic and non-ionic SAAs are generally less toxic than ionic SAAs for topical ME formulations [162, 164]. Zwitterionic SAAs are represented by the natural, biodegradable and biocompatible SAAs, phospholipids (lecithin)[165]. Lecithin is a non-toxic SAA which showed no skin irritancy even at high concentrations in topical formulations (lecithins are normal constituents of biological membranes) [127, 166-168]. Due to their minimal toxicity profiles, the natural SAAs are generally preferred by several researchers [161]. Alternatively to lecithins, non-ionic SAAs such as polyethylene glycol alkyl ethers (Brij e.g. Brij 97) [169], sorbitan esters (Spans; e.g. Span 20 and 80) and ethoxylated sorbitan esters (polysorbates, Tweens; e.g. Tween 20, 40, 80) [161, 169-172] have been used for oral, parenteral and topical ME formulations. Polyglycerol esters such as HYDRIOL[®] PGCH.4 (polyglyceryl-4-caprate) and TEGO[®] CARE PL 4 (polyglycerol-4-laurate) [126, 173], block copolymers of polyethylene glycol and polypropylene glycol (Poloxamers such as Pluronic[®], Synperonic[®]) [174], polyoxyethylene glycerol FA esters (e.g. Tagat[®]O2) [174, 175] and sugar-based SAAs (e.g. Plantacare 1200 UP) [125, 176] have also been used for the preparation of MEs. Cationic SAAs include quaternary ammonium alkyl salts such as hexadecyltrimethylammonium bromide (CTAB) and didodecylammonium bromide (DDAB) [177]. The most widely studied anionic SAA is sodium bis(2-ethyl hexyl)sulfosuccinate (AOT).

Co-surfactants

In addition to SAAs, in most of the cases, co-SAAs are included in the formulation of MEs to sufficiently lower the oil-water interfacial tension and to fluidize the interfacial film [163]. They are amphiphilic molecules accumulating at the interfacial layer with the SAAs thereby affecting the interfacial structure, disrupting the liquid crystalline phases, promoting drug solubility and expanding the one-phase region in the phase diagram [163, 178]. They also modify the chemical composition and relative polarities of the phases by partitioning themselves between lipophilic and hydrophilic phases [163]. Different alcohols (such as

ethanol, butanol, propylene glycol, pentylene glycol (1,2-pentandiol), glycerol) [168, 179, 180], polyethylene glycols (PEG) (such as PEG 400) [161], non-ionic SAAs (such as diethylene glycol monoethyl ether (Transcutol®P)) [170, 181] have been used as co-SAAs in the formulation of MEs. Unlike the medium-chain alcohols which are potentially toxic/irritating to the skin, alkanediols and alkanetriols are nontoxic co-SAAs but, due to their extreme hydrophilic nature, they are used at high amounts to produce MEs. Generally, however, non-alcohol co-SAAs are promoted for the formulation of MEs [163, 182, 183]. As a result of the low toxicity and irritancy and biodegradability of the non-ionic SAAs, the interest in using them both as a SAA and as a co-SAA is increasing [184]. On the other hand, some twin tailed SAAs such as AOT and DDAB are capable of forming MEs by themselves and they don't need the addition of co-SAAs [161].

Oily phases

Several compounds have been used as the lipophilic components of MEs; many of them having penetration-enhancing properties [164]. The selection of a lipophilic component mostly depends on its drug solubilization capacity (to achieve maximum drug loading) and penetration-enhancing properties [125]. The ability of the oil to produce a broader ME region is also important though fulfilling both requirements (high drug loading capacity and producing a broader ME region) by a single oily component is difficult. Sometimes a mixture of lipophilic components are used to meet these requirements [163]. The oil phases used in the preparation of pharmaceutical MEs include FAs (e.g. oleic acid) [170], FA esters (e.g. isopropyl myristate, isopropyl palmitate, ethyl oleate and decyl oleate) [125, 184, 185], alcohols, medium chain triglycerides (e.g. Miglyol 812) [127, 186], terpenes (e.g. menthol and limonene) [171], vegetable oils (e.g. jojoba oil) [187]. It has been shown that, compared to high molecular volume, oils with low molecular volume such as FA esters and medium chain triglycerides improve the solubilization efficiency of SAAs possibly by penetrating the interfacial monolayer and providing optimal film curvature [184]. As a result they are easily microemulsified and give a wider homogeneous unlike oils with long hydrocarbon chains such as soybean oil [163].

Other ME constituents

MEs often contain co-solvents to increase the solubility of the drug and to stabilize the dispersed phase [178]. Besides, chemical penetration enhancers such as glycolipids, N-

methylpyrrolidone, terpenes, dimethyl sulfoxide (DMSO) and propylene glycol and solubilizer such as β -cyclodextrin may also be incorporated in the ME formulations [188, 189].

1.6.1.2. Characterization of MEs

Combinations of various techniques have been used to fully characterize MEs. The appropriate combinations of oil phase, hydrophilic phase and SAA/co-SAA resulting in the formation of MEs are determined by construction of (pseudo)-ternary phase diagram [190, 191]. The nanostructure and morphologies of MEs have been characterized by a range of different techniques. The nanostructure of MEs can be revealed by a combination of methods such as differential scanning calorimetric (DSC) [126, 170], electrical conductivity [126, 127], transmission electron microscopy (TEM) [192] and/or diffusion-ordered nuclear magnetic resonance spectroscopy [170]. Electron paramagnetic resonance method was also used to reveal the nanostructure as well as to measure micropolarity and microviscosity of MEs [126, 127, 193]. Besides, scattering techniques such as dynamic and static light scattering [123, 127, 194], small-angle neutron scattering [175, 195, 196] and small-angle X-ray scattering [197, 198] have been used to elucidate the nanostructure and to measure the droplet size and size distribution of MEs. The morphologies of MEs have been investigated by using microscopic techniques such as TEM [190, 191, 199, 200] and cryo-scanning electron microscopy (SEM) [201, 202]. Macroscopic evaluations of MEs such as viscosity and physical stability are also crucial.

1.6.1.3. MEs in Dermal and Transdermal Drug Delivery

The barrier nature of the skin, resulting in poor permeability of drugs, has limited the dermal and transdermal delivery of several drugs [171, 172]. Several chemical and physical methods such as chemical penetration enhancers, iontophoresis, electroporation and sonophoresis have been employed to overcome this barrier and improve the skin drug permeation [172]. However, these approaches have their own limitations such as skin irritation and sensitization by the chemical enhancers and the physical disruption by the other methods [203, 204]. On the other hand, the high drug-loading capacity and drug-permeation enhancing effects of MEs make them a promising colloidal carrier for dermal and transdermal delivery of drugs. The exact mechanism by which MEs enhance the cutaneous drug permeation is not yet fully elucidated. However, the high concentration gradient across the skin due to high drug solubilization capacity of MEs, the prolong absorption due to a continuous supply of drug

from internal phase (acting like a reservoir) to external phase and/or the permeation-enhancing effects of the formulation components such as SAAs, co-SAAs and oils (either by disrupting the SC lipid organization or increasing drug partitioning into the skin) might contribute to the improved dermal and transdermal drug delivery [166].

As indicated earlier, MEs are valuable vehicles for the localization (retention) of drugs within skin layers (local effects) as well as for systemic delivery [164]. The localization of drugs in the skin layer was used for both cosmetic [205, 206] as well as therapeutic [176, 207-209] purposes. ME-based transdermal delivery of a wide variety of drugs have also been investigated *ex vivo* and *in vivo* [170, 181, 210-212]. Confocal laser scanning microscopy investigations revealed the involvement of paracellular and intercellular [213] as well as transfollicular pathways [214] during ME-mediated percutaneous absorption of topically applied drugs.

1.6.2. Polymeric Nanoparticles

NPs are solid colloidal particles with size in the range between 1 and 100 nm, the upper size limit being ~1000 nm [215, 216]. They are submicron-sized drug carriers and include both nanospheres (having matrix type of structure) and nanocapsules (vesicular systems). In polymeric NPs the drug is dissolved, entrapped, encapsulated or attached to a polymer NP matrix. Several biocompatible and biodegradable polymers have been used for the preparation of drug-loaded NPs. These include poly(lactic-co-glycolic acid) (PLGA) [217], poly(lactic acid) (PLA) [218], poly(E-caprolactone) (PCL) [219], polysaccharides such as chitosan [220], cellulose/cellulose derivatives [221, 222] and starch/modified starches [223, 224] and protein or polypeptides such as gelatin [225]. By virtue of their controlled/sustained release properties and biocompatibility and being promising nanocarriers, polymeric NPs have been extensively investigated in pharmaceutical and biomedical fields [216].

1.6.2.1. Preparation of Polymeric NPs

Polymeric NPs have been prepared by several methods which can be divided into two groups: those based on the polymerization of monomers (emulsion polymerization or interfacial polymerization) and those taking advantage of preformed polymers [226]. Those methods using preformed polymers can be categorized into two groups depending on the steps involved during NPs preparation: two-step (such as emulsification-solvent evaporation and

emulsification-solvent diffusion) and one-step (such as nanoprecipitation) methods. The later method does not require emulsion preparation prior to obtaining the particles [226, 227].

In the two-step emulsification-solvent evaporation technique the polymer organic phase containing the drug to be encapsulated is emulsified in an aqueous phase containing SAA using high-energy emulsification techniques (such as high-speed homogenization and ultrasonication). Evaporation of the organic solvent (either by continuous magnetic stirring at room temperature or under reduced pressure) results in the suspension of NPs in the aqueous phase [226, 228]. The size of the NPs depends on the type and amount of SAA, the viscosity of organic and aqueous phases and the stirring rate. This method has been widely used for the preparation of polymeric NPs. Emulsification-solvent evaporation method, however, can only be used for lipophilic drugs [216].

In emulsification-solvent diffusion method there are three phases: organic phase (polymer and drug dissolved in organic solvent partially miscible with water), aqueous phase (containing the SAA) and dilution phase (usually water). A rapid addition of the organic phase into the aqueous phase followed by high speed stirring result in the formation of O/W emulsion. Dilution of the emulsion with the dilution phase with mechanical stirring allow the migration of the organic solvent in the water leading to the formation of the NPs. Water-saturated organic solvent and organic solvent-saturated water are used for the preparation of organic and aqueous phases, respectively [227]. Here variables such as organic/aqueous phase ratio, organic phase addition rate and method, agitation rate and emulsion addition rate affect the physicochemical properties of the resulting NPs.

In nanoprecipitation (also termed solvent displacement, solvent diffusion or interfacial deposition) method, the polymer and drug are dissolved in a water-miscible solvent of intermediate polarity such as acetone and this solution is added into an aqueous solution, mostly containing SAA, in one shot, stepwise, drop wise or by controlled addition rate [226, 227]. This results in the interfacial deposition of the polymer due to the displacement of the organic solvent from a lipophilic solution to the aqueous phase and the NPs are formed instantaneously in an attempt to avoid the aqueous system [226]. The physicochemical properties of the NPs can be controlled by adjusting the process and formulation variables such as fluid dynamics, mixing speed, the nature and concentration of the components, organic/aqueous phase ratio, and organic phase injection rate [226, 229, 230]. Although nanoprecipitation method is widely used by virtue of its simplicity, quickness and

reproducibility, there are challenges associated with this method such as difficulties during mixing process for controlled fabrication of NPs and finding the right combination of drug/polymer/solvent/non-solvent system allowing the fabrication of drug encapsulated NPs. Hydrophilic drugs are also poorly encapsulated by this method due to their diffusion to the aqueous phase during polymer precipitation [226].

1.6.2.2. Characterization of NPs

Different analytical tools and testing approaches have been used to characterize NPs in terms of composition, morphology, size and size distribution, charge, physical state, and stability. The loading capacity (LC) and encapsulation efficiency (EE) of a NP-based delivery system should also be determined [231]. SEM is a common surface imaging technique used to determine the size and morphology of NPs. SEM also provides information on the purity of the NP sample and the degree of NPs aggregation. A useful morphologic characterization of NPs can also be made by TEM due to its high resolution. A two-dimensional TEM image formed from the electron transmission through the sample provides information on the inner structure of the NPs and also the polymeric wall thickness of nanocapsules [232, 233]. Another microscopic technique for the characterization of NPs surface morphology is atomic force microscopy (AFM), also known as scanning probe microscopy (SPM) as it scans a tiny probe across the surface of the sample being analyzed [231, 232]. Like SEM, the size and size distribution, shape and aggregation of NPs can be obtained from AFM images [226, 231]. AFM can be used to analyze both wet and dry samples and no special sample preparation procedure is required [231].

Although a number of different analytical tools including microscopy have been used to measure the size of NPs, dynamic light scattering (DLS) is probably the most appropriate and the most widely used approach for determination of size [231]. DLS provides size and size distribution of the whole particulate population in short experiment duration. Careful interpretation of the size information is needed as small aggregates or dust particles could shift the size distribution to larger values [226]. DLS covers the entire range of dimensions for NPs (1 to 1000 nm). The electrical properties of the NPs, which is mostly represented by ζ -potential, can be characterized by analytical instruments such as particle micro-electrophoresis [231]. The ζ -potential determines the surface charge and stability of the colloidal suspension and also affect the interaction of the NPs with biological systems [226]. The structural properties of NPs and drug-polymer molecular interactions are investigated

by using vibrational spectroscopies such as Fourier transform Infrared (FT-IR) and Raman spectroscopy [234]. Besides, DSC can be used to investigate the physical state and the possible drug-polymer interactions [235].

1.6.2.3. Starch-based NPs

1.6.2.3.1. Starch

Starch is one of the most abundant carbohydrates in plants occurring as granules [236]. It is a biopolymer comprising glucose units connected together by α -D-[1-4] and/or α -D-[1-6] linkages and consists of two main structural components, amylose and amylopectin, making up 98 to 99% of the dry weight of native granules. While amylose is essentially unbranched molecule with α -D-[1-4] linkage constituting 15 to 20% of starch, amylopectin is a larger highly branched molecule with α -D-[1-4] linear and α -D-[1-6] branching linkages [237]. Starch granules vary in terms of granule size (1 - 100 μ m), shape (polygonal, spherical, lenticular, etc), amylose/amylopectin ratio, structure and organization of the amylose and amylopectin molecules, the branching architecture of amylopectin, and the degree of crystallinity [237, 238].

1.6.2.3.2. Starch Modifications

Starch has been modified by physical, chemical and/or enzymatic techniques in attempt to correct the shortcomings associated with the native starch, improve its functional characteristics and/or impart certain desired properties [238, 239]. Physical modification involves physical treatment of starch granules using heat or moisture or by other physical means [240]. Pregelatinization is a popular physical method of starch modification. Chemical modification of starch is achieved via substitution of the free hydroxyl groups (by etherification or esterification), bridging of molecular chains using bi-functional and poly-functional compounds (intra-molecular and inter-molecular cross-linking), glucosidic bond cleavage (acid or enzymatic hydrolysis) or forming new functional groups (carbonyl group formation by oxidation) [239, 241]. The chemical modification of starch requires an effective destruction of starch granules to make the hydroxyl groups more accessible to the reactants [241]. The chemical and functional properties of modified starch depend on the origin of the starch, reaction conditions (reactant concentration, reaction time, pH and the presence of catalyst), type of substituent, extent of substitution, and the distribution of the substituent

in the starch molecule [239, 242]. The most common chemical modifications include acetylation, carboxymethylation, hydroxypropylation and cross-linking.

Acetylation is achieved by treatment of native starch with acetylating agents such as acetic anhydride [243, 244] or vinyl acetate [245] in the presence of catalyst (such as NaOH). The maximum possible degree of substitution (DS), which is the average number of moles of substituent per anhydroglucose unit, is 3 as each unit has three hydroxyl groups available for substitution [239, 246]. Starch acetates (SAs) with high DS have been shown to be promising pharmaceutical excipients due to their excellent bond-forming and drug-release sustaining abilities in tablet formulations [247] and controlled release film forming properties in tablets [248, 249] as well as in pellets or multi-particulate beads [250, 251].

1.6.2.3.3. Starch NPs

Due to its biocompatibility and biodegradability, starch has been investigated for various pharmaceutical and biomedical applications. It has been used as a carrier for drugs intended for tumor-targeting [252, 253], transdermal delivery [224] and transnasal mucoadhesive delivery [254]. The hydrophilic nature of starch, however, has limited its applications in nanotechnology. Therefore, as stated earlier, in attempt to enhance its functionality and expand its industrial applications, the native starch has been modified. Chemically modified starches such as acetylated starch [228, 255], propylated starch [224], dialdehyde starch [253], cross-linked starch [223, 254] and hydrophobic grafted and cross-linked starch [256] have been used in the fabrication of NPs loaded with various drugs. Starch-based NPs are also potential carriers for the dermal and transdermal drug delivery. Propyl starch NPs have shown to enhance the permeability of drugs into human skin [224]. SA is one the most common modified starches investigated for controlled drug delivery by virtue of its hydrophobicity and film-forming properties [247-251]. Recently the potential use of PEGylated SA NPs for oral delivery of insulin has been investigated [255]. In another study, SA NPs were fabricated using emulsification-solvent evaporation method in an attempt to optimize the process and formulation variables [228].

1.6.2.4. NPs in Dermal and Transdermal Drug Delivery

NPs have been extensively studied for oral and parenteral administration. The use of NPs for dermal and transdermal drug delivery also appears to be an interesting alternative to the application of colloidal systems [257]. The nano-encapsulation modifies the physicochemical

properties of the encapsulated drug and also facilitates its percutaneous delivery [258]. The NPs present an enormous surface area (resulting in a homogeneous release of encapsulated drug) and sustain the drug release (supply the skin with the drug over a prolonged period of time) [259, 260]. The NPs have been shown to be useful as reservoirs for controlled delivery of drugs into the SC, controlling the drug permeation into the deeper layers of the skin [261, 262]. The nano-encapsulation was found to increase the concentration of the drug in the SC [258]. The NPs are closely in contact with the SC, which increases the partition coefficient of the drug into the SC thereby facilitating the penetration of the drug into the SC [258, 262]. The rate and extent of penetration of drugs from NPs into the skin is governed by several factors including formulation composition, mechanism of encapsulation, size of the NPs and formulation viscosity [221, 263].

1.7. Rationale of the Study

As stated in section 1.2, in some skin diseases such as AD [47, 48] and psoriasis [22, 57], and with ageing [47, 264] the level of epidermal CERs is reduced and/or the SC lipid composition is altered resulting in defective skin barrier and skin dryness. Attempts have been made to treat skin barrier dysfunction and skin dryness associated with depletion and/or disturbance of SC lipids. Although direct replacement of the depleted CERs has been shown to be beneficial in improving skin barrier function and skin hydration [25], the commercial synthetic or animal-based CERs used in skin care products are associated with some limitations. The synthesis of CERs is an expensive and laborious procedure. Furthermore, animal-based CERs are associated with ethical and safety issues. Therefore, less expensive and safer alternative sources of CERs are needed. Since CERs isolated from edible plants are safe and structurally related to epidermal CERs, they are promising alternative sources of CERs. To date, however, little effort has been made to administer PhytoCERs topically for targeted delivery into the SC. Thus, PhytoCERs isolated from various plants should be investigated for topical delivery. To explore the potential use of topical PhytoCERs, robust and reliable analytical methods are needed for qualitative as well as quantitative analyses of PhytoCERs obtained from different plants. Furthermore, the transport of PhytoCERs across the various skin layers after topical application of PhytoCER-based formulations hasn't yet been investigated. Besides, to the best of our knowledge, to date, there is no study suggesting the best formulation strategy for the delivery of PhytoCERs into the SC of the skin. Further studies are, therefore, needed to provide supporting evidence for the skin health benefits of topically delivered PhytoCERs.

1.8. Research Questions

This PhD research will attempt to address the following four research questions that have emanated from the aforementioned research gaps.

1. How can PhytoCERs be characterized qualitatively and quantitatively?
2. Which plants are endowed with considerable amount of PhytoCERs?
3. How can PhytoCERs be quantified in different layers of the skin in skin permeation studies?
4. What is the best formulation strategy to deliver PhytoCERs into the SC of the skin?

1.9. Objectives of the Study

This study, therefore, aims at characterizing PhytoCERs and delivering them into the SC of the skin using nanocarriers. To address the four main research questions specified above, the following specific objectives were set:

1. Development of methods for structural characterization (LC-MS/MS) and quantification (AMD-HPTLC) of plant GlcCERs and analyzing the GlcCERs of selected plants;
2. Production and characterization of CERs from GlcCERs of selected plant;
3. Development and validation of LC-MS method for quantification of PhytoCERs in the skin permeation studies;
4. Investigation of *in vitro* and *ex vivo* skin penetration of PhytoCERs from nanocarriers such as MEs and NPs.

2. Isolation, Structural Characterization and Quantification of Plant GlcCERs

2.1. Introduction

Chronic skin conditions such as AD and psoriasis, and aged skin are characterized by defective skin barrier and skin dryness. The skin barrier dysfunction and dryness are associated with the depletion or disturbance of SC lipids, mainly CERs [265, 266]. The skin barrier function and hydration can be improved by skin care products and supplements containing CERs for which plants are interesting sources. PhytoCERs have attracted much attention in recent years due to their higher safety profile as they are mostly isolated from dietary sources. The beneficial effects of oral PhytoCERs for skin hydration and skin barrier reinforcement have also been documented in several studies [93, 94, 96]. Most of the commercial PhytoCERs are obtained from two sources: rice and wheat. However, very few efforts have been made to exploit CERs from other plants for dermal applications. Other plants should also be explored as there are enormous number of potential plants containing CERs.

PhytoCERs are mainly found in glycosylated form, the most abundant being GlcCERs [63]. In earlier studies, structural information of GlcCERs was mostly obtained after hydrolysis and GC-MS analyses of their derivatives making the pairing of specific SB with a FA in the intact molecular species more difficult [66, 76]. On the other hand, LC-MS/MS is a powerful, specific and sensitive technique for detection and identification of GlcCERs without preceding hydrolysis and derivatization [72]. While LC allows the separation of the complex mixtures of GlcCERs, tandem MS enables the identification of the various GlcCER species. The characteristic fragmentation patterns of GlcCERs through the transition of precursor ions to characteristic product ions of the SBs are the basis for structural identification [72, 136]. ESI has been the most commonly utilized ionization technique for LC-MS-based qualitative and quantitative analyses of SLs [72, 136, 145, 267]. On the other hand, APCI often gives good results for nonpolar compounds and thus is frequently used for the analysis of many lipid classes [146]. Despite the fact that APCI has greater applicability for the analysis of hydrophobic molecules, there are limited published data on the analysis of plant GlcCERs using LC/APCI-MS. In an attempt to explore alternative sources of CERs for dermal applications, the APCI and LC conditions were optimized for the structural characterization of GlcCERs isolated from the seeds of three plants (grass pea (*Lathyrus sativus* L.), Ethiopian mustard (*Brassica carinata*) and haricot bean (*Phaseolus vulgaris*)). In this context, the

collision energy was varied to monitor the fragmentation patterns of the GlcCER species at different dissociation levels. The in-source fragmentation, which is normally considered to be a disadvantage for APCI, also provided structural information in classifying the SBs. Furthermore, Automated Multiple Development-High Performance Thin Layer Chromatography (AMD-HPTLC) method was validated and used to quantify the GlcCER content of the plants.

2.2. Materials and Methods

2.2.1. Materials

The soybean GlcCER (> 99% by TLC), containing mainly d18:2/h16:0, was purchased from Avanti Polar Lipids (Alabaster, AL, USA). HPLC grade methanol and chloroform were purchased from VWR International GmbH (Darmstadt, Germany). Isopropanol and *n*-hexane were obtained from Grüssing GmbH (Filsum, Germany). Formic acid, silica gel 60 (0.063 - 0.200 mm), TLC (silica gel 60, F₂₅₄, 20 cm×20 cm) and HPTLC (silica gel 60 F₂₅₄, 20 cm×10 cm) plates were obtained from Merck KGaA (Darmstadt, Germany). Glyceroltrioleate, β -sitosterol glucoside and β -sitosterol were purchased from Sigma-Aldrich Chemie GmbH (Steinheim, Germany). Linoleic acid (\geq 98%) was obtained from AppliChem GmbH (Darmstadt, Germany). Cholesteryl oleate and squalene (\geq 97%) were supplied by Fluka Chemika (Buchs, Switzerland).

The plants used in the preliminary screening were obtained from different sources (Agricultural Research Center (ARC) of Ethiopian Institute of Agricultural Research (EIAR), Ethiopian Forestry Research Center (EFRC) and local markets in Ethiopia (the list of the plants are shown in Table A1, Appendix A). The seeds of the plants selected for further studies were collected from the seed banks of the various ARC, Ethiopia, between June and August 2015. The seeds were: Grass pea (*Lathyrus sativus* L., Fabaceae, variety name: ILAT-LS-LS-B2 (Wasie), local name: Guaya, breeder: Debrezeit ARC/EIAR), Ethiopian mustard (*Brassica carinata*, Brassicaceae, variety name: MS-YDX Zem-1-BCR-5 (Holleta-1), local name: Gomenzer, breeder: Holleta ARC/EIAR) and Haricot bean (*Phaseolus vulgaris*, Fabaceae, variety name: SER119 (Awash 1), breeder: Melkassa ARC/EIAR).

2.2.2. Methods

2.2.2.1. Extraction and Purification of GlcCER-enriched Lipid Fractions (GELFs)

The seeds of the plants were ground and the lipids in the powdered seeds (500 g) were extracted with 1500 mL of isopropanol/*n*-hexane/H₂O (55:20:25, v/v/v) as specified elsewhere [136] (ultrasonic assisted, 30 min). The extraction procedure was repeated for the marc. The extracts were filtered, pooled and evaporated to dryness. All the extractions were done in triplicate. The subsequent liquid-liquid extraction and column chromatographic purification were done following a method recently developed [268]. Briefly, the lipid extracts of the plant materials were fractionated in a mixture of CHCl₃, MeOH and H₂O (1:1:1, v/v/v), 500 mL each. The aqueous and CHCl₃ phases were separated and washed with CHCl₃/MeOH (1:1, v/v) and H₂O/MeOH (1:1, v/v) mixtures, 500 mL each, respectively. The CHCl₃ fractions were combined and evaporated to dryness. The CHCl₃ fractions were subjected to column chromatography (350 g of silica gel) with CHCl₃/MeOH stepwise gradient elution (first elution: 1500 mL of CHCl₃, second elution: 1500 mL of CHCl₃/MeOH (9:1, v/v), third elution: 1500 mL of CHCl₃/MeOH (8:2, v/v)). The fractions (50 mL) were collected. A scheme showing the extraction and purification of GlcCERs is presented in Fig. A1, Appendix A. The GlcCERs were detected on TLC (SiO₂, CHCl₃/MeOH 85:15) after immersion in CuSO₄/H₃PO₄ solution (10% CuSO₄ (w/v), 8% phosphoric acid (v/v) and 5% MeOH (v/v)) (for 20 s) and charring in an oven (at 150 °C for 10 min). A plant-derived GlcCER (soybean) was used as a reference standard.

2.2.2.2. Isolation of GlcCERs by Preparative LC/APCI-MS

Isolation of GlcCERs was achieved by preparative LC-MS using a 1260 Infinity LC coupled to a 6120 series single quadrupole mass spectrometer (Agilent Technologies, Waldbronn, Germany). The GlcCER-enriched lipid fractions (GELFs) were dissolved in *n*-hexane/isopropanol (7:3, v/v). The samples were eluted with solvents A: MeOH/isopropanol/H₂O (12:8:1, v/v/v) and solvent B: *n*-hexane/isopropanol (7:3, v/v) on YMC-Pack ODS-A 150 x 21 mm, 5 µm, 120 nm column (YMC Europe GmbH, Dinslaken, Germany) isocratically (90% solvent A and 10% solvent B) with a flow rate of 16 mL/min (a flow splitter with a split ratio of 1:1000 was used). The injection volume was 900 µL and the total run time was 15 min. A fraction collector linked to the LC-MS system by a capillary was used to collect the fractions at preprogrammed time intervals. Mass-based fraction collections were used to isolate the predominant haricot bean GlcCER (*m/z* 716). The mass

spectrometer was operated in the positive ion mode and the following APCI conditions were used: drying gas (N₂): 12 L/min, nebulizer gas (N₂) pressure: 40 psi, drying gas temperature: 250 °C, vaporizer temperature: 450 °C, capillary voltage: 4 kV and corona current: 5 µA.

2.2.2.3. LC/APCI-MS/MS-based Structural Characterization of Plant GlcCERs

The GELFs and isolated mixtures of GlcCERs of the various plant extracts were analyzed by LC-MS/MS. The system consisted of a 1220 Infinity LC (Agilent Technologies, Waldbronn, Germany) coupled with a LCQ ion trap mass spectrometer equipped with APCI source (Thermo Fisher, Bremen, Germany). A YMC-Pack ODS-AQ column (150 x 2.0 mm I.D., S-3µm, 200 Å pore size) (YMC Europe GmbH, Dinslaken, Germany) was used to separate the GlcCER species under the following chromatographic conditions: mobile phase of solvent A: H₂O (+ 0.1% formic acid) and solvent B: MeOH (+ 0.1% formic acid), flow rate: 0.3 mL/min, column temperature: 30 °C, injection volume: 10 µL and run time: 30 min. The separation was carried out using a gradient from 5% A to 100% B in 20 min and then 100% B was kept for the next 10 min. The MS/MS fragmentation experiments were conducted at different relative collision energies, between 10 and 100%, to monitor the progress of dissociations. The structural analysis of the GlcCERs was based on the characteristic product ions of the SBs obtained from the precursor ions (parent GlcCERs [M+H]⁺, loss of water [M+H-18]⁺, or loss of glucose [M+H-162]⁺). The MS was operated in the positive ion mode under the following APCI conditions: source heater temperature of 450 °C, capillary temperature of 200 °C, capillary voltage of 3 V, source (discharge) voltage of 6 kV, source (discharge) current of 6 µA, sheath gas flow rate of 70 AU and aux gas flow rate of 10 AU. MS full scan (*m/z* 100 - 2000) and MS/MS *m/z* range of 200 - 900 were used.

2.2.2.4. AMD-HPTLC-based Quantification of Plant GlcCERs

2.2.2.4.1. Instrumentation and Chromatographic Conditions

An AMD-HPTLC system with a software CAMAG winCATS Planar Chromatography Manager (Camag, Muttenz, Switzerland) was used for the quantification of plant GlcCERs. Before sample application, the HPTLC plate was prewashed (immersed in isopropanol for at least 2 h) and dried in an oven at 100 °C for 30 min. The plate was then cooled to room temperature and the samples were applied as 6 mm bands using a CAMAG Automatic TLC sampler 4. Chromatographic developments were conducted three times using a CAMAG AMD 2 using CHCl₃/MeOH/HAc (190:9:1, v/v/v) as a mobile phase over a distance of 70 mm for the first two steps and CHCl₃/MeOH/AC (76:20:4, v/v/v) for the last step (migration distance 30 mm).

Before each step the plate was automatically vacuum dried for 1.5 min and then conditioned in an acetic acid (4 M) atmosphere. The lipids were detected by immersing the HPTLC plates in aqueous $\text{CuSO}_4/\text{H}_3\text{PO}_4$ solution for 20 s by using automatic dipping device and charring in an oven at 150 °C for 20 min. Finally, the plate was scanned by a CAMAG TLC Scanner 3 in absorbance mode ($\lambda = 546 \text{ nm}$).

2.2.2.4.2. Method Validation

The HPTLC method was validated according to the EMA guideline on validation of bioanalytical methods, 2012 [269]. The linearity of the response over the concentration range of 20 to 1500 ng/band was investigated using soybean GlcCER standard ($n = 3$). The limits of detection (LOD) and quantification (LOQ) of the method were estimated by applying different volumes of blank ($\text{CHCl}_3/\text{MeOH}$ (1:1, v/v)) and standard solution (0.1 - 1 μL of 100 $\mu\text{g}/\text{mL}$ of soybean GlcCER in $\text{CHCl}_3/\text{MeOH}$ (1:1, v/v)) three times. The signal-to-noise (S/N) ratio of 3 and 10 were used for the estimation of LOD and LOQ, respectively. The within-run precision and accuracy were determined by using four concentration levels of GlcCERs (50, 200, 400 and 800 ng/band) in 5 determinations per each level on the same day. The four concentration levels, 5 determinations each, in three runs analyzed on three different days were used for the validation of between-run precision and accuracy. The relative standard deviation (RSD) and percentage recovery were used to report the precision and accuracy of the method, respectively.

2.2.2.4.3. Quantification of GlcCERs

The GELFs which mainly contain GlcCERs and other glycolipids such as sterol glycosides collected after column chromatography were used for the quantitative determination of GlcCERs. The samples (2 μL of 1 mg/mL of GELFs) and different volumes of standard solution (0.2 - 10 μL of 100 $\mu\text{g}/\text{mL}$ of soybean GlcCER) were applied as bands. After the three-step AMD and drying, the GlcCER bands were revealed by derivatization. Peak areas taken from densitometric scans were used for the quantification of GlcCERs in the plants. A separate calibration curve was obtained for each measurement (one calibration curve per plate) during quantification of GlcCERs.

2.3. Results and Discussion

2.3.1. Extraction and Purification of GlcCERs

The majority of the lipid extraction protocols utilize a mixture of CHCl_3 and MeOH. In this study, however, a solvent mixture of isopropanol/*n*-hexane/ H_2O (55:20:25, $v/v/v$) was used to extract the total lipids, mainly SLs, of plants as suggested by Markham *et al.* [136]. The subsequent liquid-liquid fractionation using $\text{CHCl}_3/\text{MeOH}/\text{H}_2\text{O}$ (1:1:1, $v/v/v$) mixture resulted in partitioning of lipids, including the neutral SLs (such as GlcCERs), into the CHCl_3 phase and removal of non-lipid contaminants in the aqueous phase. The total lipid extracts and CHCl_3 fractions were used during preliminary screening of plants for GlcCER content. Most of the plants were selected from Poaceae, Fabaceae and Brassicaceae families as previous reports have shown that these families are composed of plants which are rich sources of SLs [68, 87]. Table A1 (Appendix A) shows the TLC-based preliminary screening results of the CHCl_3 fractions of the extracts. The GlcCERs were not detected from the total lipid extracts at the applied concentration. Based on the preliminary results, the first four plants were selected for further studies: one from Poaceae family (oat), two from Fabaceae family (grass pea and haricot beans) and one from Brassicaceae family (Ethiopian mustard). The CHCl_3 fractions of these plants were further purified and GlcCER species were analyzed by LC/APCI-MS/MS.

The fractions enriched with GlcCERs were separated from other lipids (such as sterols, FAs, triacylglycerols and sterol esters) by using silica gel column chromatography (gradient elution from 100% CHCl_3 to $\text{CHCl}_3/\text{MeOH}$ (8:2, v/v)). The GELFs were collected from the last gradient $\text{CHCl}_3/\text{MeOH}$ (8:2, v/v). The amounts of total lipid extracts, CHCl_3 fractions and GELFs of the selected plants are presented in Table 2.1. Purification of GELFs with preparative LC-MS results in mixtures of the various GlcCER molecular species having closely related chemical structures. The GlcCERs differ from each other in terms of FA chain length, degree of unsaturation and hydroxylation.

Table 2-1: Amounts of total lipid extracts, CHCl₃ fractions, GELFs and GlcCERs in oat, grass pea, Ethiopian mustard and haricot bean (n = 3)

Plants	Total lipid extract (g/kg)	CHCl ₃ fraction (g/kg)	GELF (mg/kg)	GlcCERs (mg/kg)
Oat	59.3 (2.1)	19.2 (1.6)	649.6 (58.6)	193.5 (6.3)
Grass pea	73.4 (7.9)	20.3 (1.4)	1193.6 (25.1)	130.0 (8.1)
Mustard	234.4 (6.8)	133.1 (13.5)	1955.3 (52.0)	71.8 (1.4)
Haricot bean	77.1 (3.3)	18.4 (2.1)	584.5 (56.6)	161.2 (15.8)

The values in parentheses are the standard deviation (SD).

2.3.2. Structural Characterization of GlcCERs

A gradient LC/APCI-MS/MS method allowing separation, detection and structural characterization of the closely related GlcCER species was developed. The effects of chromatographic conditions such as mobile phase composition (H₂O/MeOH 3:97 to 7:93, v/v) and formic acid concentration (0.1% to 0.3%) on the degree of chromatographic separation of the GlcCERs were investigated. Higher degree of separation was obtained on C18 column using a gradient of 5% A (H₂O + 0.1% formic acid) to 100% B (MeOH + 0.1% formic acid) in 20 min followed by 100% B for 10 min. The elution order of the GlcCERs was according to the chain length of FAs.

APCI is a chemical ionization technique typically used for the analysis of hydrophobic molecules. Prior to analyzing the GlcCERs with LC/APCI-MS, attempts have been made to analyze the GlcCERs with LC/ESI-MS. However, the GlcCERs appeared to exhibit better ionization efficiency in APCI source compared to ESI and hence it was used for the investigation of GlcCERs in the plants. For GlcCERs derived from each plant, a series of MS/MS experiments with varying collision energies were carried out on individual GlcCER species to better monitor the dissociation processes. The lower relative collision energies (10%, 25% and 40%) were ineffective in fragmenting the precursor ions into the characteristic product ions. Higher relative collision energies (65 to 80%) were used for structural analysis.

The selected ionization conditions led to in-source fragmentation which is considered as a limitation of APCI [137]. However, in-source fragmentation (such as deglycosylation and

dehydration of GlcCERs) also provided us some structural information of GlcCERs and was used to classify the SBs into three categories (Table 2.2).

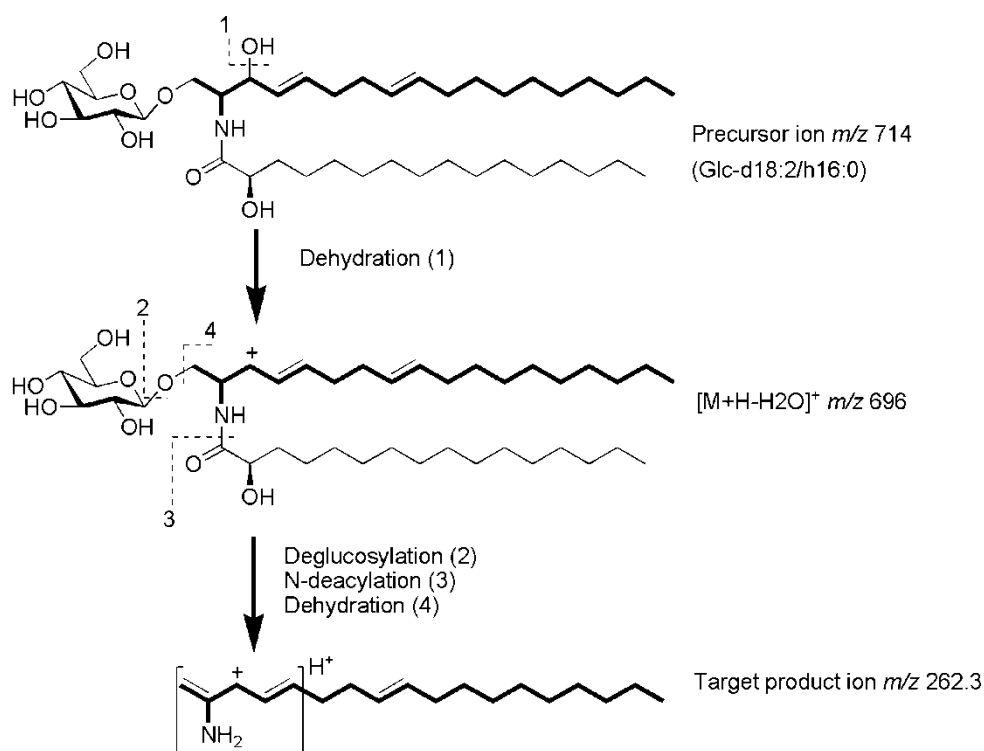
Table 2-2: Fragmentation characteristics of plant GlcCERs depending on the nature of C4 of the SBs (C4-hydroxylated, C4-desaturated and C4-saturated).

Nature of SB	Common SBs	Fragmentation	Precursor Ion ^a	Target Product Ion (<i>m/z</i>)			Product Ion
				[M+H-H ₂ O] ⁺	[M+H-2H ₂ O] ⁺	[M+H-3H ₂ O] ⁺	
C4-hydroxylated	t18:0, t18:1 ^{Δ8}	Readily deglucosylated	[M+H-Glc] ⁺		282.3, 280.3	264.3, 262.3	Abundant
C4-desaturated	d18:1 ^{Δ4} , d18:2 ^{Δ4,8}	Readily dehydrated	[M+H-H ₂ O] ⁺		264.3, 262.3		Abundant
C4-saturated	d18:0, d18:1 ^{Δ8}	Resistant to dehydration	[M+H] ⁺	284.3	266.3, 264.3		Very low abundance

^aFor C4-hydroxylated and C4-desaturated SBs, the product ions that lost Glc and water were subjected to MS/MS and the resulting target product ions were abundant.

In tandem MS experiments of GlcCER species with t18:1^{Δ8}, it was found that the corresponding product ion that lost Glc [M+H-Glc]⁺ is highly abundant, whereas other product ions, that could serve as marker ions (target product ions) for structural elucidation, were detected at very low intensities. Therefore, instead of using the parent ions ([M+H]⁺) as precursor ions, the ions that lost Glc [M+H-Glc]⁺ were used as precursor ions for further MS/MS experimentations. This led to the generation of abundant target product ions. Besides, as C4-desaturated SBs are readily dehydrated (which might be attributed to the electron donating property of the double bond), the predominant ions detected for GlcCERs consisting of these types of SBs were the ions that lost water [M+H-H₂O]⁺. Therefore, for these types of GlcCERs, the ions that lost water [M+H-H₂O]⁺ were used as precursor ions for MS/MS. The results indicate that GlcCERs containing C4-hydroxylated/desaturated SBs are readily deglucosylated/dehydrated and hence abundant target product ions were achieved from [M+H-Glc]⁺ and [M+H-H₂O]⁺, respectively. A previous study on other plants also indicated similar results [72]. On the other hand, as saturation of the double bond at C4 of SBs reduces the fragmentation efficiency to a very low level, the target product ions of GlcCERs containing C-4 saturated SBs were not abundant. To improve the sensitivity of the method and confirm the identity of GlcCER species containing these types of SBs, selected reaction monitoring (SRM) was used for the detection of selected target product

ions. Fig. 2.1 indicates the fragmentation of a representative plant GlcCER, d18:2^{Δ4,8} acylated with h16:0 [270].



Plant SBs

4, 8-Sphingadienine (d18:2)	m/z 262.3 (double dehydration)
8-Sphingenine (d18:1)	m/z 264.3 (double dehydration)
Sphinganine/dihydrosphingosine (d18:0)	m/z 266.3 (double dehydration)
4-Hydroxy-8-sphingenine (t18:1)	m/z 280.3/262.3 (double/triple dehydration)
4-Hydroxysphinganine/phytosphingosine (t18:0)	m/z 282.3/264.3 (double/triple dehydration)

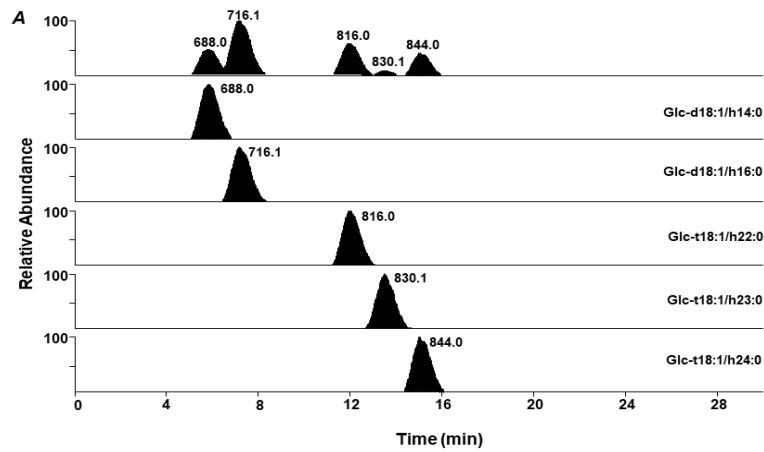
Target product ions

Figure 2-1: Suggested route of fragmentation of a representative plant GlcCER (d18:2/h16:0) under positive ionization mode [270]. As the SB of this GlcCER is readily dehydrated, the precursor ion (m/z 714) is detected at a very low abundance and the ion that lost water (m/z 696) is highly abundant.

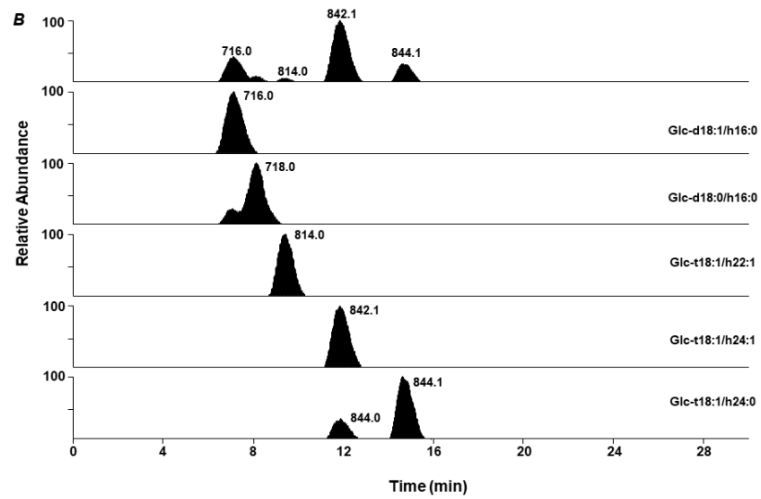
The base peak chromatograms and extracted ion chromatograms of GlcCERs obtained from grass pea, Ethiopian mustard and haricot bean are depicted in Fig. 2.2A to C. The LC-MS/MS-based structural characterization of oat GlcCERs and other related results will be discussed in the next chapter, as oat was the plant selected for further investigations.

Characterization and Quantification of Plant GlcCERs

Grass pea GlcCERs



Ethiopian mustard GlcCERs



Haricot bean GlcCERs

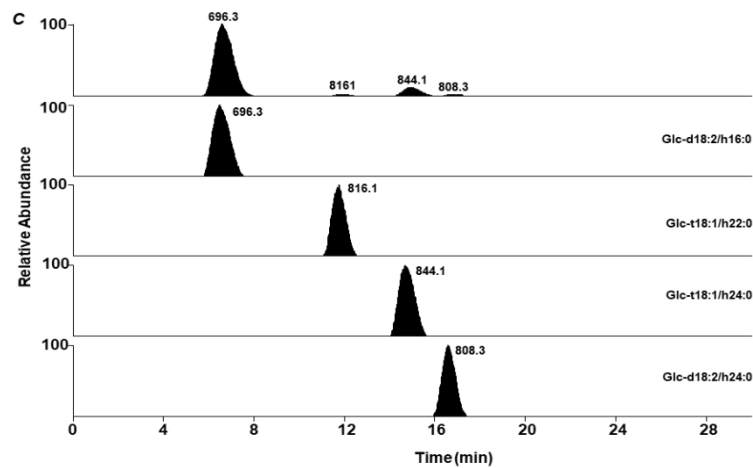


Figure 2-2: Base peak chromatogram (full scan: m/z 100 - 2000) and extracted ion chromatograms of GlcCERs derived from grass pea (A), Ethiopian mustard (B) and haricot bean (C) using YMC-Pack ODS-AQ column. Gradient eluent: solvent A: H₂O (+0.1% formic acid) and solvent B: MeOH (+0.1% formic acid), flow rate: 0.3 mL/min, column temperature: 30 °C and injection volume: 10 μ L.

Each isolated precursor ion of the three plants was subjected to MS/MS and the characteristic product ions detected during MS/MS analyses and the identified GlcCER species are presented in Tables 2.3 to 2.5. The chemical structures of the GlcCER species in the three plants are shown in Fig. 2.3. The representative tandem mass spectra of GlcCER-derived ions are shown in Fig. A3, Appendix A.

As can be seen from Table 2.3 to 2.5, both dihydroxy and trihydroxy SBs were found in GlcCERs derived from the three plants, the trihydroxy SBs (t18:1) being coupled with VLCFAs (C22-C24). The predominant GlcCER species in grass pea, Ethiopian mustard and haricot bean were composed of d18:1 linked to h16:0, t18:1 coupled with h24:1 and d18:2 linked to h16:0, respectively. VLCFAs (including odd carbon number FA) coupled with trihydroxy SBs were detected in grass pea GlcCERs. The fact that plant GlcCERs are mostly characterized by a double bond at position 8 on the sphingoid residue and grass pea GlcCERs containing d18:1 being resistant to dehydration (Table 2.2) suggest that the desaturation is at position 8. Unlike grass pea, Ethiopian mustard GlcCERs were found to contain C22 and C24 monounsaturated hydroxy FAs. Similarly, previous studies on plants of the Brassicaceae family such as *Arabidopsis thaliana* [271] and *Brassica oleracea* (broccoli) [78] were reported to have VLCFAs (\geq C20) with ω -9 desaturation.

Table 2-3: Grass pea GlcCER species identified by LC/APCI-MS/MS analyses.

GlcCER Species ^b	Retention Time (min)	Precursor and Product Ions m/z			Target Product Ion m/z
		[M+H] ⁺	[M+H-Glc] ⁺	[M+H-Glc- H ₂ O] ⁺	
Glc-d18:1/h14:0	5.02	688.0	526.3	508.3	264.3
Glc-d18:1/h16:0	6.63	716.1	554.3	536.3	264.3
Glc-t18:1/h22:0	11.76	816.1	654.3	636.3	280.3/262.3
Glc-t18:1/h23:0	13.30	830.1	668.3	650.3	280.3/262.3
Glc-t18:1/h24:0	14.94	844.0	682.3	664.3	280.3/262.3

^bGlc: glucose, for the SB: d (dihydroxy SB), 18 (SB carbon chain), 0, 1, 2 (number of denaturation on the SB); for the FA moiety: h (hydroxy FA), 14 - 24 (FA carbon chain) and 0 (number of denaturation on the FA).

Table 2-4: Ethiopian mustard GlcCER species identified by LC/APCI-MS/MS analyses.

GlcCER Species	Retention Time (min)	Precursor and Product Ions m/z		Target Product Ion m/z
		$[M+H]^+$	$[M+H-Glc]^+$	
Glc-d18:1/h16:0	7.14	716.1	554.3	264.3
Glc-d18:0/h16:0	8.13	718.0	556.3	266.3
Glc-t18:1/h22:1	9.43	814.1	652.3	280.3/262.3
Glc-t18:1/h24:1	11.84	842.1	680.3	280.3/262.3
Glc-t18:1/h24:0	14.64	844.1	682.3	280.3/262.3

Table 2-5: Haricot bean GlcCER species identified by LC/APCI-MS/MS analyses.

GlcCER Species	Retention Time (min)	Precursor and Product Ions m/z			Target Product Ion m/z
		$[M+H]^+$	$[M+H-H_2O]^+$	$[M+H-Glc]^+$	
Glc-d18:2/h16:0	6.49	714.1	696.3		262.3
Glc-t18:1/h22:0	11.75	816.1		654.3	280.3/262.3
Glc-t18:1/h24:0	14.72	844.1		682.3	280.3/262.3
Glc-d18:2/h24:0	16.54	826.0	808.3		262.3

Characterization and Quantification of Plant GlcCERs

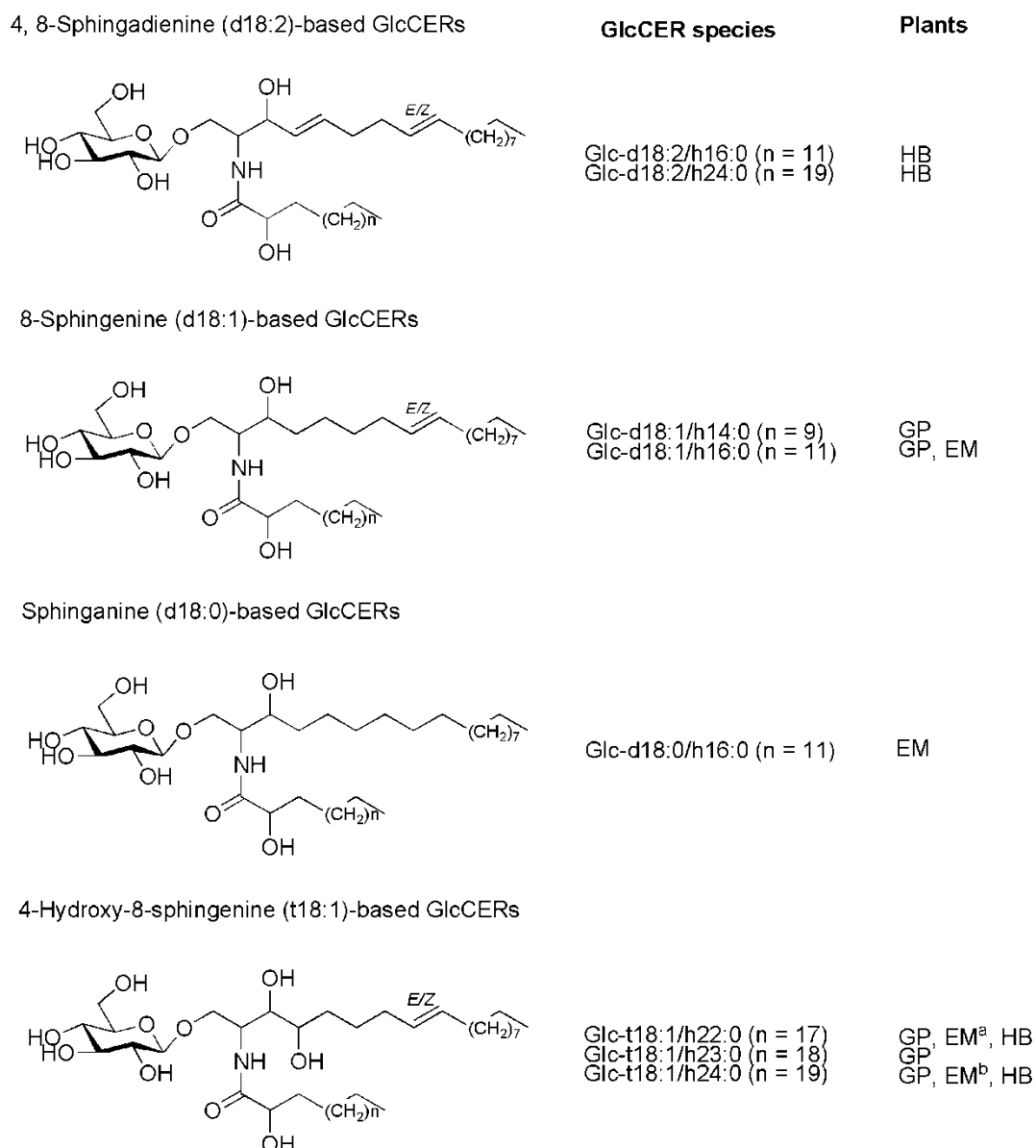


Figure 2-3: Individual GlcCER species identified from grass pea (GP), Ethiopian mustard (EM) and haricot bean (HB). ^aWith mono-unsaturated α -hydroxy FA, ^bboth saturated and mono-unsaturated α -hydroxy FAs.

The full-scan spectra of haricot bean-derived GELF revealed a highly abundant single GlcCER species ($[M+H-H_2O]^+$ m/z 696, identified as d18:2 coupled with h16:0, Fig. 2.2C). This predominant GlcCER species is structurally identical to soybean-derived GlcCER (d18:2/h16:0): the standard GlcCER used in the present study (Fig. A5, Appendix A). The GlcCERs derived from haricot bean exhibited identical chromatograms and fragmentation patterns with the standard GlcCERs (Fig. A6, Appendix A). Kojima *et al.* [90] described the SB and FA composition of GlcCERs isolated from kidney bean, one of the varieties of common bean, after hydrolyzing the GlcCERs and analyzing the resulting components and

derivatives. In this method it is difficult to pair a specific SB with a FA in the intact molecular species. LC-MS analysis can directly provide this information. Similar to our results from LC-MS/MS analyses, d18:2 and h16:0 were found to be the major SB and FA of kidney bean GlcCERs [90]. Unlike the seeds, the dominant SB and FA in GlcCERs from leaf of kidney bean were found to be trihydroxy bases (mainly t18:1^{Δ8E}) and α -hydroxylinolenic acid (h24:0), respectively [272]. These results confirm that the SB and FA compositions of plant GlcCERs are highly dependent on the type of the plant tissues, as indicated in earlier reports as well [63].

There are some structural similarities among the GlcCERs obtained from the two commercial plant sources (wheat and rice) and the GlcCERs isolated from the three plants. The major wheat GlcCERs comprised of d18:1^{Δ8} acylated with h16:0 and h20:0 [66, 68, 76]. The predominant grass pea GlcCER was also found to be Glc-d18:1/h16:0. Furthermore, the principal GlcCER species in rice consists of d18:2 acylated with h20:0 and hydroxylinolenic acid (h24:0) [72]. The haricot bean also predominantly contains Glc-d18:2/h16:0 (> 90%) (with a shorter FA chain length compared to rice GlcCERs).

As indicated in section 1.3.2, plant and mammalian CERs differ from each other in terms of hydroxylation, chain length and double bond in their FA and SB moieties. In PhytoCERs, 8E/8Z isomers of d18:2^{Δ4,8}, t18:1^{Δ8} and d18:1^{Δ8} represent the dominant bases [63]. However, like plant SBs, mammalian d18:1^{Δ4} and t18:0 are mostly coupled to short and long chain FAs, respectively [268]. The head groups of skin CERs contain hydroxyl groups capable of forming inter- and intra-molecular hydrogen bonds in the SC [5]. The number of hydroxyl groups was also shown to be substantial for the integrity of the barrier function of the SC [45]. Both skin and PhytoCERs have 3 or 4 hydroxy groups on their head groups which suggest the potential application of PhytoCERs in improving the skin barrier function of diseased and/or aged skin.

2.3.3. Quantification of GlcCERs

Previous investigations on plant SLs mainly focused on the structural analysis of GlcCERs, CERs and inositol phosphoryl-CERs. There are limited published data concerning quantitative analysis of plant GlcCERs. One of the reasons for this could be the limited commercial sources of individual GlcCER reference standards. However, few attempts have been made to quantify plant GlcCERs by HPLC with MS [86] and evaporative light scattering (ELSD) [87,

273] detections. As reference standards are not commercially available for individual GlcCER species in the plants investigated, it was difficult to quantify individual GlcCER species in each plant by LC-MS or HPLC-ELSD methods.

In this study, a three steps AMD-HPTLC method was used for the quantification of total GlcCERs in the plants. For soybean-derived GlcCER (d18:2/h16:0), the LOD and LOQ of the method were estimated to be 10 and 50 ng/band, respectively. Similar to previous reports on SC lipids [274, 275], the calibration curves were non-linear when the soybean GlcCER concentration varied over a wide range (nearly two orders of magnitude) and best fit for the polynomial regression model (> 0.999). The linearity range was found to be narrow (50 to 200 ng/band) with relatively smaller R^2 value (between 0.980 and 0.999). A representative calibration curve of soybean GlcCER is depicted in Fig. A7, Appendix A. The precision and accuracy results are shown in Table 2.6. The RSD of within-run and between-run precision ranged from 4.2 to 8.3 and 1.7 to 9.1, respectively. On the other hand, the recovery (%) ranged from 95.2% to 105.0% and 92.6% to 102.1% for within-run and between-run experiments, respectively. The results indicated that the method is accurate and precise for the quantification of plant GlcCERs.

Table 2-6: Precision and accuracy of HPTLC method for quantification of plant GlcCERs.

Nominal Concentration (ng/band)	Calculated Concentration (ng/band) (n = 5)		Recovery (%)		RSD (%) (n = 5)	
	Within-run	Between-run	Within-run	Between-run	Within-run	Between-run
50	47.6	46.3	95.2	92.6	8.3	9.1
200	210.0	204.2	105.0	102.1	4.2	5.0
400	402.6	401.6	100.7	100.4	5.7	1.7
800	778.0	765.1	97.3	95.6	4.7	2.4

The GlcCER content of the four plants is shown in Table 2.1. The highest amount of GlcCERs was obtained from oat grain (193.5 mg/kg of the grain, dry weight). Oat was, therefore, selected for further studies and will be discussed in the next chapter. The two plants in the Fabaceae family (haricot bean and grass pea) were found to contain relatively higher amount of GlcCERs (161.2 and 130.0 mg/kg of the seed, dry weight) compared to Ethiopian mustard (71.8 mg/kg). The GlcCER concentrations in these two plants were also comparable to the

GlcCER content in soybean, although the content of GlcCERs in plants in general varies depending on the genotype, growth condition and stage of maturity. A previous study has shown that the content of GlcCER in soybeans varies among the various genotypes in the range of 101 to 351 mg/kg seed (dry weight) [87]. In another study, the amounts of CER monohexoside in wheat flour and milled rice were shown to be 210 mg/kg and 25 mg/kg (dry weight) [273]. Generally, plants from Fabaceae (including soybean) and Poaceae (such as wheat and rice) families are common sources of commercial plant GlcCERs.

As GlcCERs occur in widely in Fabaceae family, the amounts of GlcCERs in five acacia species were also quantified by AMD-HPTLC. The results are presented in Table A2, Appendix A. The total amounts of GlcCERs ranged from 55 to 128 mg/kg of dry weight. These plants may also serve as source of CERs.

2.4. Conclusions

The RP LC-MS/MS method with APCI interface resulted in effective chromatographic separation and structural identification of plant GlcCERs. The extraction and purification protocols utilized in this study also isolated mixtures of closely related GlcCERs for LC-MS analysis. The various GlcCER species in the three plants (grass pea, Ethiopian mustard and haricot bean) contained four types of SBs (d18:0, d18:1, d18:2 and t18:1) acylated with C14-C24 hydroxy FAs. Haricot bean and grass pea GlcCERs primarily comprised of CERs with d18:2 coupled with h16:0 (> 90%) and d18:1 linked to h16:0, respectively, and these GlcCERs have similar structural features with the predominant GlcCERs obtained from commercial sources (soybean, rice and wheat). Compared to Ethiopian mustard, the two plants were also found to have higher quantities of GlcCERs comparable to the GlcCER content in the commercial sources. However, oat grain was selected for further investigations due to its high GlcCER content as well as the several documented dermatological benefits of oatmeal. The workflow consisting of an extraction protocol, a RP LC/APCI-MS/MS and HPTLC methods described here have been proven to be robust and reliable for the screening of GlcCERs in plants.

3. Isolation and Structural Characterization of Oat CERs for SC Delivery

3.1. Introduction

The dermatological benefit of colloidal oatmeal has been documented for decades [276-278]. It has a variety of dermatological benefits including moisturization, barrier protection and anti-inflammatory activity [277]. A clinical study demonstrated that a daily oat-based skin care regimen in atopic skin can improve the compromised skin barrier function [279]. In recent years, several clinical studies have also established the benefits of topical colloidal oatmeal formulations as adjunct treatment in AD [280-282]. An active moisturizing lotion containing colloidal oatmeal reduced the intensity, duration and frequency of itching and also improved the hydration of dry skin (xerosis) in a randomized controlled clinical study [283]. The antioxidant and anti-inflammatory effects of colloidal oatmeal were mainly attributed to the polyphenolic compounds (avenanthramides) present in oat grains [278, 284].

Oat grains contain high lipid content including polar lipids and FAs (3 - 18%) compared to other cereal grains [285]. The polar lipid content of oats is about 33% (8 - 17% glycolipids and 10 - 20% phospholipids) [286]. Oat grain lipids have the potential of reducing TEWL and restoring the skin permeability barrier. Although earlier studies have investigated the FA and SB compositions of GlcCERs derived from oat leaf [74, 80] and oat root [287], to our knowledge, the GlcCER composition of oat grain is not yet reported. Previous studies have shown that the GlcCER species obtained from various types of plant tissues display different SB and FA profiles. Seed tissues mainly consist of dihydroxy SBs and C16 - C20 saturated hydroxy FAs (the predominant being h16:0). On the other hand, trihydroxy SBs and VLCFAs (C20 - C26, both saturated and ω -9 monounsaturated hydroxy FAs) are enriched in leaf tissues [63, 79].

Oat belongs to Poaceae family which has been shown to have plants which are rich sources of GlcCERs such as wheat and rice. This was also supported by the quantitative results obtained in the previous section. Among the four plants, oat grain contained the highest quantity of GlcCERs. Considering the quantitative results and the reported dermatological benefits, investigation of oat grains may provide an alternative plant source of CERs that could have potential benefits in reducing TEWL and improving the barrier of diseased and/or aged skin. In this study, therefore, emphasis was given to this plant to exploit its potential

as a source of PhytoCERs for dermal applications. The GlcCERs were, therefore, extracted and isolated from Ethiopian oat grain (*Avena abyssinica*) and qualitatively and quantitatively analysed by LC/APCI-MS/MS and AMD-HPTLC methods, respectively. Furthermore, since CERs are needed for the SC delivery, a chemical method (acid-induced deglycosylation) was used to cleave the glycosidic linkage of the GlcCERs. The resulting predominant oat CERs were purified and their structures were further characterized by High Resolution Mass Spectrometry (HRMS) and NMR analyses.

3.2. Materials and Methods

3.2.1. Materials

Soybean GlcCER containing mainly d18:2/h16:0 (> 99%) (Avanti Polar Lipids, Alabaster, AL, USA), CER [AP] and CER [AS] (Evonik-Industries, Essen, Germany) and N-(R,S)- α -hydroxyhexadecanoyl-D-*erythro*-dihydrosphingosine (BIOTREND Chemikalien GmbH, Köln, Germany) were used as reference standards. 1, 4-dioxane anhydrous (99.8%) and 4.0 M HCl in dioxane were obtained from Sigma-Aldrich Chemie GmbH (Steinheim, Germany). The extraction solvents, isopropanol and *n*-hexane, were purchased from Grüssing GmbH (Filsum, Germany). The following solvents were used for the purification and analysis of GlcCERs: chloroform, methanol (VWR International GmbH, Darmstadt, Germany) and formic acid (Merck KGaA, Darmstadt, Germany).

3.2.2. Methods

3.2.2.1. Extraction and Purification of Oat GlcCERs

The extraction and purification of oat GlcCERs were carried out following the method described in section 2.2.2.1 [288]. Briefly, the dehulled oat grain was ground and the powdered grain (1 kg) was extracted with isopropanol/*n*-hexane/H₂O (55:20:25, v/v/v, 3 L). The dried lipid extract (59.3 g) was fractionated in a mixture of CHCl₃, MeOH and H₂O (1:1:1, v/v/v, 0.5 L each). The aqueous and CHCl₃ phases were separated and washed with CHCl₃/MeOH (1:1, 0.2 L each) and H₂O/MeOH (1:1, 0.2 L each) mixtures, respectively. The CHCl₃ fractions were combined and evaporated to dryness. The dried non-polar fraction (19.2 g) was further purified with column chromatography (400 g of Silica gel 60 (0.063 - 0.200 mm)) with CHCl₃/MeOH stepwise gradient elution (first elution: CHCl₃, 1.5 L; second elution:

CHCl₃/MeOH (9:1, v/v), 1.5 L; third elution: CHCl₃/MeOH (8:2, v/v), 1.5 L). The resulting GELF was subjected to a second similar gradient column chromatography to get oat GlcCERs.

3.2.2.2. Structural Identification of GlcCERs by LC/APCI-MS/MS Analyses

The separation and structural characterization of oat GlcCER species were carried out by the LC/APCI-MS/MS method described in section 2.2.2.3 [288].

3.2.2.3. Quantification of Oat GlcCERs

The quantification of oat GlcCERs was carried out by the validated HPTLC method described in section 2.2.2.4 [288].

3.2.2.4. Cleavage of Glycosidic Linkage (Deglycosylation)

The oat GlcCERs was first dissolved in anhydrous 1, 4-dioxane (30 mg/mL) at room temperature and the GlcCERs solution was mixed with solutions of different acid concentrations (0.25, 0.5, 1.0, 2.0 and 4.0 M HCl in dioxane) (1:1, v/v) in Eppendorf tubes. The reaction mixtures were shaken with a thermomixer for 1h at 25 °C and 800 RPM. Finally, the reactions were quenched by ice water bath and the content of the reaction mixtures were neutralized with saturated NaHCO₃ solution. The concentration of the acid that led to cleavage of the glycosidic linkage, 4.0 M HCl, was used to investigate the effect of temperature on the production of CERs. In this, the acid-GlcCER mixtures (1:1, v/v) were shaken in the thermomixer (800 RPM) for 1h at five different temperatures (25, 35, 45, 55, 65 °C). The effect of reaction time (0.5 - 24h) on the production of CERs was also studied at 25 °C using 4.0 M HCl solution in dioxane. In all the cases the progress of the reactions were monitored by TLC and LC-MS analyses.

3.2.2.5. Purification of Oat CERs

The reaction mixtures were exhaustively extracted with CHCl₃ (three times) on a separatory funnel to separate the CERs from the hydrophilic components of reaction mixture (including the sugar moiety). The CHCl₃ phase was washed with saturated NaCl solution (brine), dried under nitrogen stream and purified by a TLC-guided column chromatography using a gradient elution: first elution CHCl₃, second elution CHCl₃/MeOH (9:1, v/v), third elution CHCl₃/MeOH (8:2, v/v). The fraction containing CERs was analyzed by LC-MS. CER [AP] C-

18 and CER [AS] C-18 and α -hydroxy CER (N-(R,S)- α -hydroxyhexadecanoyl-D-*erythro*-dihydrosphingosine) were used as reference standards.

3.2.2.6. Preparative LC/APCI-MS

The two predominant oat CERs (m/z 554 and m/z 610) were separated by preparative LC-MS using a 1260 Infinity LC (Agilent Technologies, Waldbronn, Germany) coupled to a 6120 series single quadrupole mass spectrometer. The sample was dissolved in MeOH/isopropanol/*n*-hexane (90:10:1, *v/v/v*) and eluted in a gradient mode with solvent A: H₂O (+0.1% formic acid) and solvent B: MeOH (+0.1% formic acid) (Table 3.1) on YMC-Pack ODS-A 150 x 21 mm, 5 μ m, 120 nm column (YMC Europe GmbH, Dinslaken, Germany) with a flow rate of 16 mL/min (flow splitter with a split ratio of 1:1000 was used). The injection volume was 900 μ L and the total run time was 30 min. The mass spectrometer was operated in a positive ion mode under the following APCI conditions: drying gas (N₂): 12 L/min, nebulizer gas (N₂) pressure: 40 psi, drying gas temperature: 250 °C, vaporizer temperature: 450 °C, capillary voltage: 4 kV and corona current: 5 μ A. The scanning mode: SIM (m/z 554 and m/z 610).

Table 3-1: Preparative LC/APCI-MS gradient system for the isolation of predominant oat CERs.

Time (min)	A [%]	B [%]
0	10	90
5	10	90
10	5	95
30	0	100
31	10	90
40	10	90

3.2.2.7. Structural Characterization of Oat CERs

The structure of oat CERs identified by LC/APCI-MS/MS was confirmed by ESI-HRMS, ¹H and ¹³C NMR, ¹H COSY and HMBC spectral analyses. High resolution mass spectra were acquired in positive ionization mode using an Orbitrap XL mass spectrometer (Thermo Fisher Scientific, Bremen, Germany) equipped with a nano-ESI source (Proxeon, Odense, Denmark). Samples were dissolved in MeOH and measured with static nano-ESI (spray

voltage 1.3 kV, capillary temperature 200 °C) using in-house pulled gold coated glass emitters. Spectra were acquired in full MS (m/z 150 - 800) at a resolution of 100,000 at m/z 400. The NMR spectra were obtained on Varian Gemini 2000 and Varian Inova 500 instruments using $CDCl_3$. The operating frequencies were 500 MHz for 1H NMR and 101 MHz for ^{13}C NMR.

3.2.2.8. HPLC-Evaporative Light Scattering Detector (ELSD)

The purity of oat CERs was determined by 1100 Series HPLC (Agilent technologies, Waldbronn, Germany) with ELSD (Alltech ELSD 2000, Deerfield, USA) using a normal phase Nucleodur (5 μ m, 100Å pore size, 125 mm x 2 mm ID) column. The samples were dissolved in $CHCl_3$ and gradient elution was performed using 100% solvent A ($CHCl_3$) to 100% solvent B ($CHCl_3/n$ -propanol/HAc (80/20/2, $v/v/v$)) in 15 min at a flow rate of 1.0 mL/min. The injection volume was 20 μ L and the column temperature was 30 °C. The parameters for ELSD were set as follows: heated drift tube temperature: 50 °C, gas flow rate: 1.5 L/min and gain setting: 6.

3.3. Results and Discussion

3.3.1. LC/APCI-MS/MS-based Structural Identification of GlcCERs

The total lipid, mainly SLs, in oat grain was extracted by a solvent mixture of isopropanol/*n*-hexane- H_2O (55:20:25, $v/v/v$) as suggested by Markham *et al.* [136]. The liquid-liquid extraction ($CHCl_3/MeOH/H_2O$ (1:1:1, $v/v/v$)) resulted in partitioning of lipids, including the neutral SLs such as GlcCERs, into the $CHCl_3$ phase and removal of non-lipid contaminants in the aqueous phase. The $CHCl_3$ phase was subjected to silica gel column chromatography (gradient elution from 100% $CHCl_3$ to $CHCl_3/MeOH$ (8:2, v/v)) to separate the GELF from the other lipids (such as sterols, FAs, triacylglycerols and sterol esters). The TLC chromatogram of the GELF, isolated oat GlcCERs and CERs (after acid treatment) are shown in Fig. 3.1.

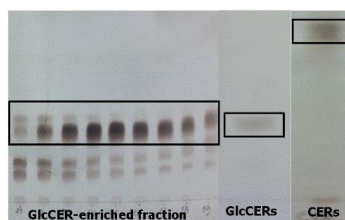


Figure 3-1: TLC chromatograms of oat GELF, isolated GlcCERs and CERs (after acid treatment).

The GELF is mainly composed of a mixture of structurally related GlcCERs varying in terms of FA chain length and degree of unsaturation on the SB. The oat GlcCERs had the same R_f value as the reference standard (soybean GlcCER). The individual GlcCERs were separated on a RP column and each GlcCER species was subjected to a series of MS/MS experiments of different collision energies (10 - 100%) to better monitor the dissociation processes. Since lower relative collision energies (10%, 25% and 40%) were ineffective for the precursor-to-product ion transitions, higher energies (65 to 80%) were used for structural characterization. The GlcCERs containing C4-desaturated SBs were readily dehydrated in APCI source. As a result the ions that lost water $[M+H-H_2O]^+$ were detected as predominant ions and hence these ions were subjected to MS/MS as precursor ions. On the other hand, during tandem MS experiments the target product ions of GlcCERs having C4-saturated SBs were not abundant due to their poor fragmentation efficiency. For these types of GlcCERs, SRM was used for the target product ions to improve the sensitivity of the method and confirm the identity of the GlcCERs.

The base peak chromatogram and extracted ion chromatograms of oat GlcCER species are depicted in Fig. 3.2. About 12 GlcCER molecular species (Fig. 3.3) were identified by pairs of precursor-to-target product ion transitions observed during tandem MS experimentations of individual GlcCER.

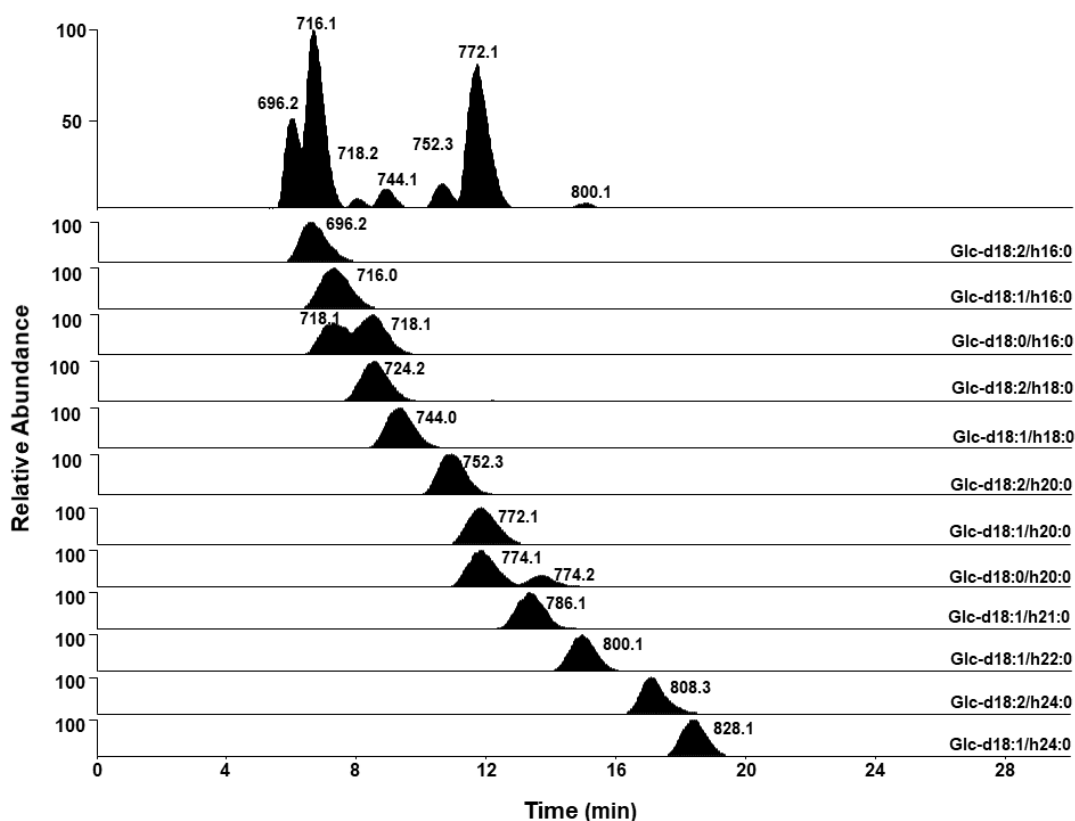


Figure 3-2: Base peak chromatogram (full scan: m/z 100 - 2000) and extracted ion chromatograms of oat GlcCERs using YMC-Pack ODS-AQ column. Gradient eluent: solvent A: H₂O (+0.1% formic acid) and solvent B: MeOH (+0.1% formic acid), flow rate: 0.3 mL/min, column temperature: 30 °C and injection volume: 10 μ L.

The target product ions detected during MS/MS analyses and the identified GlcCER species are presented in Table 3.2. Representative tandem mass spectra of oat GlcCERs are shown in Fig. A4, Appendix A. All the detected oat GlcCER species are composed of C18 dihydroxy SBs amide linked with saturated α -hydroxy FAs (C16-C24). The two principal oat GlcCER species were found to contain a d18:1 linked to h16:0 and h20:0. The fact that plant GlcCER are mostly characterized by a double bond at position 8 on the sphingoid residue and d18:1-based oat GlcCERs were found to be resistant to dehydration in the ion source (C-4 desaturated SBs are readily dehydrated) suggest that the desaturation is at position 8. One of the oat GlcCER species (d18:2/h16:0) is structurally identical to the standard GlcCER used in the present study (soybean GlcCER) and it exhibited identical chromatogram and fragmentation pattern with the standard GlcCER (Fig. A6, Appendix A).

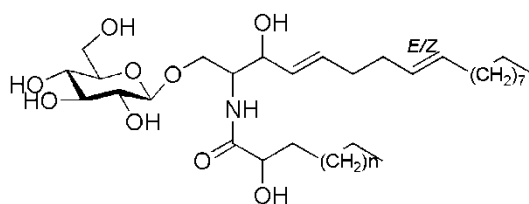
Table 3-2: Identification of oat-derived GlcCER species by LC/APCI-MS/MS analyses.

GlcCER Species ^a	Retention Time (min)	Precursor and Product Ions <i>m/z</i>				Target Product Ion <i>m/z</i>
		[M+H] ⁺	[M+H-H ₂ O] ⁺	[M+H-Glc] ⁺	[M+H-Glc-H ₂ O] ⁺	
Glc-d18:2/h16:0	5.89	714.0	696.2		534.3	262.3
Glc-d18:1/h16:0	6.41	716.0		554.3	536.3	264.3
Glc-d18:0/h16:0	7.78	718.1		556.3	538.3	266.3
Glc-d18:2/h18:0	7.84	742.2	724.2		562.3	262.3
Glc-d18:1/h18:0	8.70	744.1		582.3	564.3	264.3
Glc-d18:2/h20:0	10.29	770.1	752.3		590.3	262.3
Glc-d18:1/h20:0	11.23	772.1		610.3	592.5	264.3
Glc-d18:0/h20:0	13.28	774.1		612.3		266.3
Glc-d18:1/h21:0	14.36	786.1		624.3	606.3	264.3
Glc-d18:1/h22:0	14.56	800.1		638.3	620.3	264.3
Glc-d18:2/h24:0	16.68	826.1	808.1		646.3	262.3
Glc-d18:1/h24:0	17.90	828.1		666.3	648.3	264.3

^aFor the SBs: d (dihydroxy), 18 (carbon chain), 0, 1, 2 (number of denaturation on the SBs); for the FA moieties: h (α -hydroxy FAs), 16 - 24 (FA carbon chain) and 0 (number of denaturation on the FAs); Glc: glucose, The two GlcCER species written in bold are the predominant GlcCERs.

In contrast, other studies indicated that trihydroxy SBs (mainly t18:1 ^{Δ 8E/Z} which accounts for more than 60% of the SB composition) are the predominant species of GlcCERs isolated from leaf of *Avena sativa*. The oat leaf GlcCERs have also VLCFA (\geq C20) with high concentrations of ω -9-desaturation, especially C24:1 [74, 78, 80]. The only SB found in oat root-derived GlcCERs was d18:2 linked to hydroxy FAs, the predominant (>90%) being h24:1 [287, 289]. All these results confirm that the SB and FA compositions of plant GlcCERs are highly dependent on the type of the plant tissues.

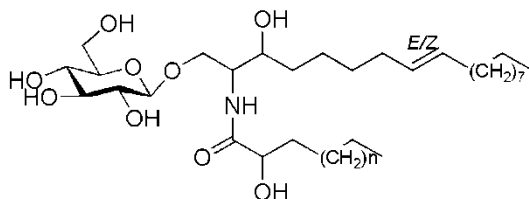
4, 8-Sphingadienine (d18:2)-based GlcCERs



GlcCER species

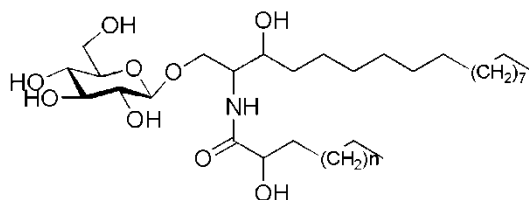
Glc-d18:2/h16:0 (n = 11)
 Glc-d18:2/h18:0 (n = 13)
 Glc-d18:2/h20:0 (n = 15)
 Glc-d18:2/h24:0 (n = 19)

8-Sphingene (d18:1)-based GlcCERs



Glc-d18:1/h16:0 (n = 11)
 Glc-d18:1/h18:0 (n = 13)
 Glc-d18:1/h20:0 (n = 15)
 Glc-d18:1/h21:0 (n = 16)
 Glc-d18:1/h22:0 (n = 17)
 Glc-d18:1/h24:0 (n = 19)

Sphinganine (d18:0)-based GlcCERs



Glc-d18:0/h16:0 (n = 11)
 Glc-d18:0/h20:0 (n = 15)

Figure 3-3: Individual oat GlcCER species identified by LC-MS/MS.

There are structural similarities among the GlcCERs obtained from wheat, rice and oat. Similar to oat, the major wheat GlcCERs comprised of d18:1^{Δ8} acylated with h16:0 and h20:0 [66, 68, 76]. Furthermore, the predominant GlcCER species in rice consists of d18:2 acylated with h20:0 and hydroxylignoceric acid (h24:0) [65, 72]. Here it is also worth mentioning that, although plant and mammalian CERs differ from each other in terms of chain length and double bond in their FA and SB moieties, they have similar head groups. Similar to CER [AS], the head groups of oat CERs consist of three hydroxyl groups. As stated earlier, the head groups of epidermal CERs are capable of forming inter- and intra-molecular hydrogen bonds in the SC [5] which are shown to be crucial for the integrity of the barrier function of the SC [14, 15, 45]. Therefore, further investigations are needed to understand the influence of structural variations between PhytoCERs and epidermal CERs on the stabilization of SC lipid bilayer.

3.3.2. Quantification of Oat GlcCERs

The total amount of GlcCERs was found to be 193.5 mg/kg of oat grain (dry weight). The high GlcCER level in oat grain, compared to the other plants investigated earlier (haricot bean: 161.2 mg/kg, grass pea: 130.0 mg/kg and Ethiopian mustard: 71.8 mg/kg) [288], support the claimed dermatological benefits of oatmeal. The contents of CER monohexoside in wheat flour and milled rice, determined by HPLC-ELSD, were shown to be 210 mg/kg and 25 mg/kg (dry weight), respectively [273]. Another HPLC-ELSD-based quantification has also shown that the GlcCER content in soybeans varies among the various genotypes in the range of 101 to 351 mg/kg seed (dry weight) [87]. The high GlcCER content of the oat grain is one of main reasons for selecting this plant for further investigations, in addition to the several clinical studies proving the dermatological benefits of topical oat-based formulations.

3.3.3. Deglucosylation of Oat GlcCERs

The limited published data on the topical administration of PhytoCERs as a replacement of CERs lost due to some skin diseases and ageing could be partly attributed to the fact that the PhytoCERs predominantly exist in glycosylated form. For plant GlcCERs to be directly delivered into the SC of the skin, cleavage of the sugar moiety (either chemically or enzymatically or chemo-enzymatically) is inevitable.

Various researchers have been using the classical methods of hydrolysis (acid/alkaline) for qualitative analysis of plant GlcCERs. As GlcCERs are moderately resistant to acid hydrolysis, vigorous acid conditions are required. However, these drastic acidic conditions might induce unintended chemical alterations, racemization and allylic rearrangements (formation of 3-O-methyl and 5-O-methyl ethers caused by the reaction of allylic alcohol group with methanol in methanolic acids and formation of 5-hydroxy isomers and dienic compounds in aqueous systems) [290-295] (Fig. B2, Appendix B). As some of the derivatives are closely related, they have similar chromatographic properties making the purification of the target CERs more difficult. An effective and practically applicable method for the cleavage of glycosidic linkage producing a good yield of CERs with less unintended by-products would be valuable.

The deglucosylation of oat GlcCERs was, therefore, carried out in non-aqueous/non-methanolic systems to reduce the unintended effects. The oat GlcCERs were dissolved in anhydrous 1, 4-dioxane and the resulting solution was treated with HCl solution in dioxane.

The production of the two predominant oat CERs (d18:1/h16:0 and d18:1/h20:0) was monitored by LC-MS analysis (Fig. 3.4). The LC-MS analyses of acid-treated oat GlcCER samples indicated that lower HCl concentrations (0.25 - 2.0 M) are ineffective for the cleavage of glycosidic linkage. Therefore, 4.0 M HCl in dioxane was used to investigate the effects of temperature and reaction time on the production of CERs. The unintended strong acid effects were found to be aggravated by high temperatures (35 - 65 °C) and, hence, further experiments were carried out at 25 °C. Shorter reaction times led to incomplete reaction. A long reaction time (18h) was needed for nearly complete conversion of GlcCERs into CERs. As can be seen from the full scan base peaks of acid-treated GlcCERs, while the signal intensities of GlcCER peaks (I) decline to a very low levels, new peaks, which didn't appear prior to the acid treatment, were detected after the acid treatment (II) (Fig. 3.5A).

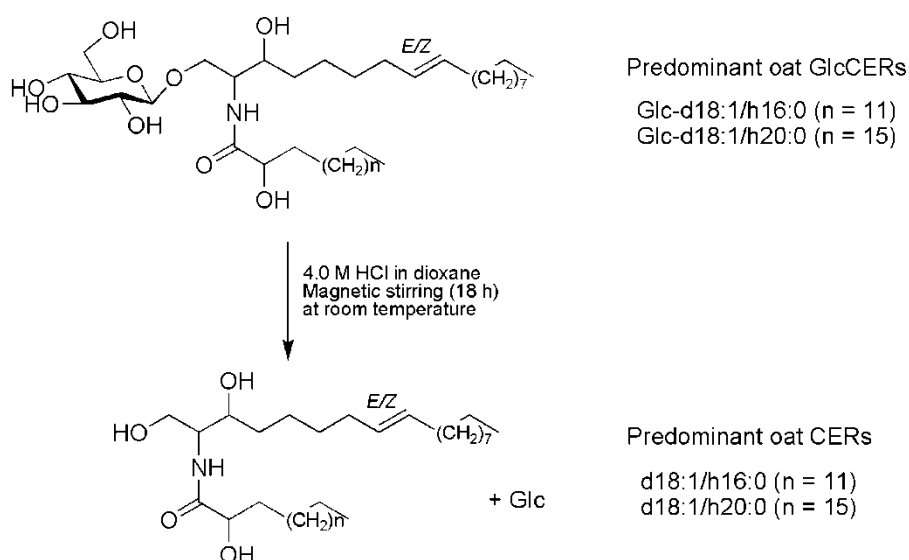


Figure 3-4: Acid-induced hydrolysis of predominant oat GlcCERs

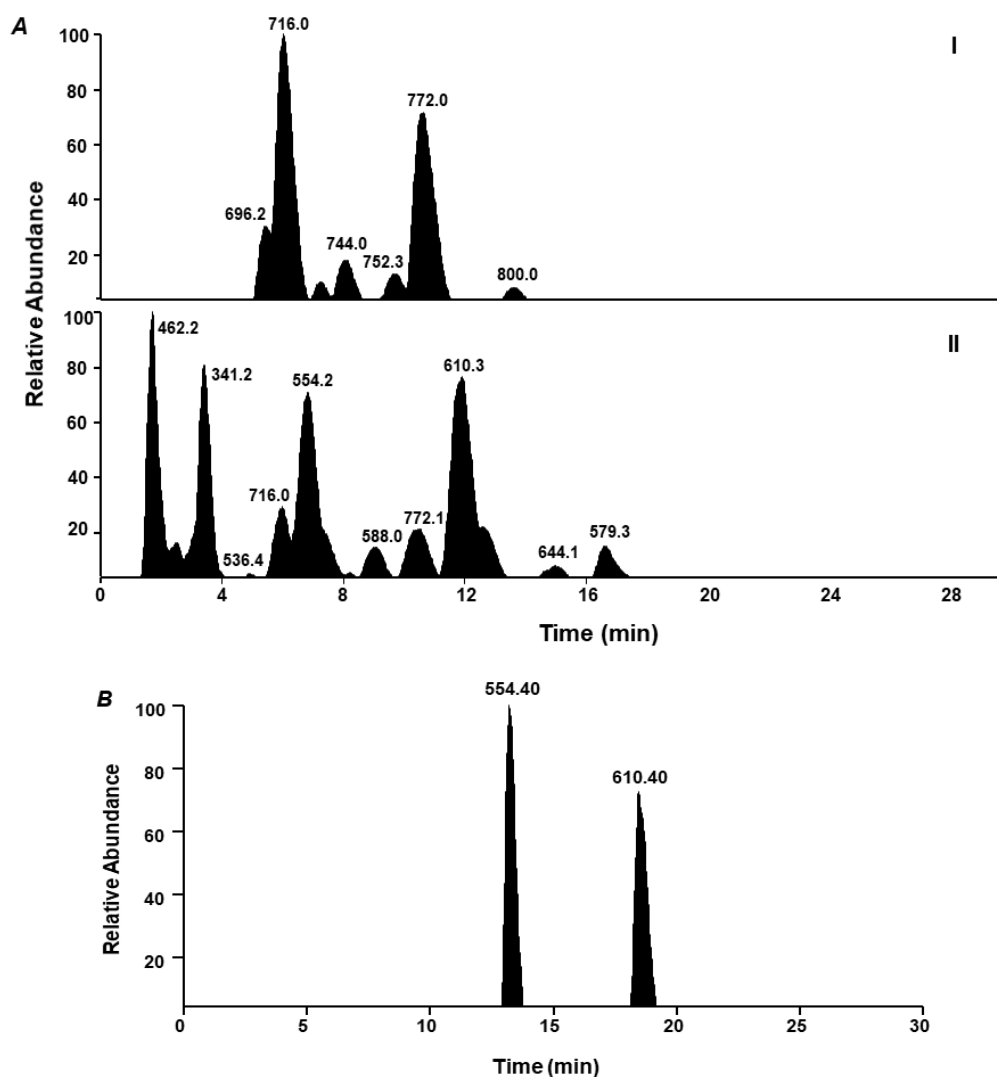


Figure 3-5: Full scan (m/z 100 - 2000) base peaks obtained before (AI) and after (AII) acid treatment of oat GlcCERs. In the acid treated samples (AII), the CERs in the reaction mixture were extracted with CHCl_3 . The SIM (m/z 554 and m/z 610) chromatograms of the two predominant oat CERs after column chromatographic purification (B).

Two peaks were detected in the SIM chromatograms (m/z 554 and m/z 610) of each of the predominant oat CERs, one at the same retention times as the parent GlcCERs and another at longer retention times indicating the two possible sources of CERs: acid-induced and source fragmentation-induced CER production. Acid-induced CERs, which are more lipophilic than the parent GlcCERs, were eluted later than the parent GlcCERs after they are separated in the column. However, the source-induced CERs and the corresponding parent GlcCER species were eluted at the same retention times (Fig. 3.6). The subsequent post-reaction

purification procedure with column chromatography and preparative LC-MS led to the isolation of the two predominant oat CERs (Fig. 3.5B).

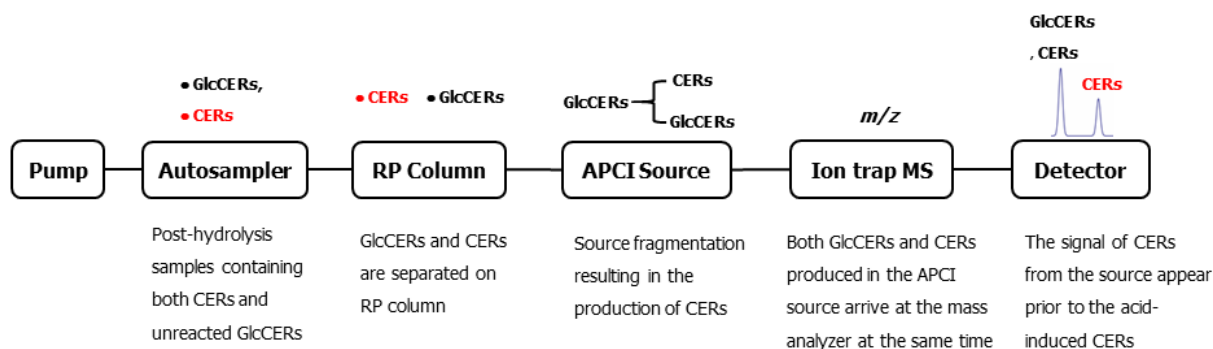


Figure 3-6: A scheme showing the two possible sources of CERs (CERs obtained from acid-induced deglycosylation (red) and CERs produced by APCI source fragmentation) while analyzing acid-treated samples by LC-APCI/MS.

The other CERs derived from oat GlcCERs consisting of SBs with allyl (enol) group such as Glc-d18:2/h16:0 were not detected after the reactions suggesting the possible allylic-group degradations and rearrangements in the strong acidic conditions. The involvement of aqueous system during work-up procedure (during quenching the reaction mixture with saturated NaHCO_3 solution and liquid-liquid extraction) might have caused these rearrangements. Table 3.3 summarizes the stability of GlcCERs in the ion source, CID (in ion trap instrument) and acidic conditions with respect to the nature of the SBs. The chemical structures of d18:1 $^{\Delta 8}$ -based GlcCERs and d18:2 $^{\Delta 4,8}$ /t18:1 $^{\Delta 8}$ -based GlcCERs are shown in Fig. 3.7.

Table 3-3: Stability of d18:1 $^{\Delta 8}$ -based GlcCERs and d18:2 $^{\Delta 4,8}$ /t18:1 $^{\Delta 8}$ -based GlcCERs in the ion source, CID and strong acidic conditions.

	C4-saturated SBs	C4-desaturated/hydroxylated SBs
Typical plant SBs	d18:1 $^{\Delta 8}$	d18:2 $^{\Delta 4,8}$ and t18:1 $^{\Delta 8}$
In source fragmentation	Resistant to dehydration	Readily dehydrated/deglucosylated
MS/MS fragmentation efficiency ^a	Resistant to fragmentation and very low product ions	Readily fragment and result in abundant product ions
Acid Hydrolysis	Result in cleavage of glycosidic linkage	Allylic degradations in dihydroxy CERs Almost complete loss of trihydroxy CERs

^aOat GlcCERs were resistant to MS/MS fragmentation in ion trap instrument. However, oat CERs were easily dissociated into the product ions in the triple quadrupole instrument.

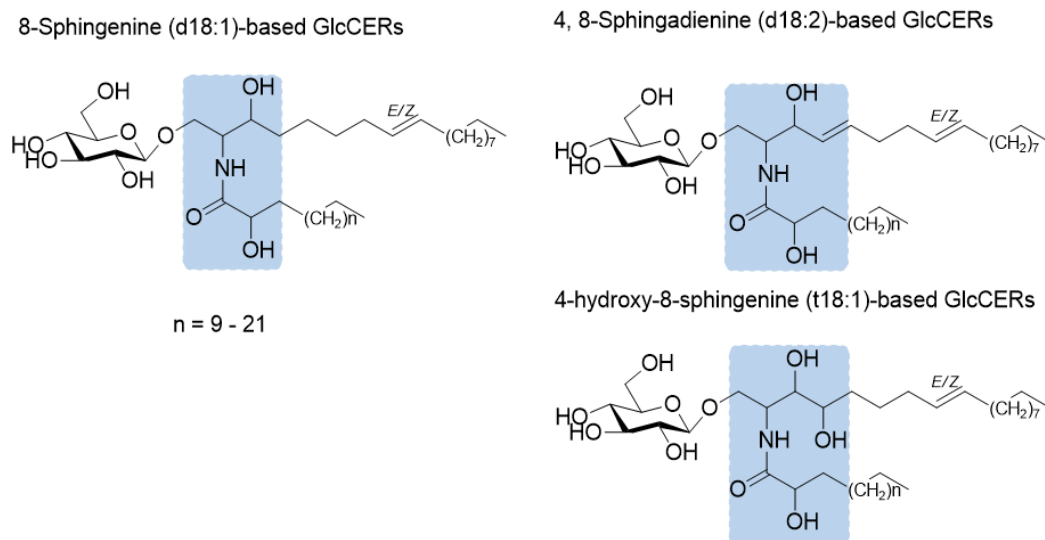


Figure 3-7: Chemical structure of d18:1^{A8}-based GlcCERs and d18:2^{A4,8} /t18:1^{A8}-based GlcCERs

The other more selective and efficient approach for the production of CERs from GlcCERs is enzymatic hydrolysis. There are few reports indicating the use of this method for production of CERs. The β -glucosidase isolated from ox brain and β -galactosidase obtained from rat brain were used to hydrolyze CER glucoside and CER lactoside, respectively [296, 297]. In another study, an enzyme extracted from rat brain was used to hydrolyze SPM into CER and phosphorylcholine [298]. Recently, a human recombinant glucocerebrosidase (imiglucerase, Cerezyme) was used for hydrolysis of plant GlcCERs [268].

3.3.4. Further Structural Characterization of Oat CERs

The structural information obtained from LC-MS/MS analysis of oat CERs (Fig. 3.8) was supported by ESI-HRMS and 1D and 2D NMR analyses (Table 3.3). The molecular formulae of oat CERs assigned by positive mode ESI-HRMS ($C_{34}H_{67}NO_4$ and $C_{38}H_{75}NO_4$) at m/z 554.5133 (calculated 554.5143) and m/z 610.5784 (calculated 610.5769) were identical to the ones identified by LC/APCI-MS/MS. The ESI-HRMS spectra of the two predominant oat CERs are depicted in Fig. B3 and Fig. B4, Appendix B. Additional structural information was obtained from 1H , ^{13}C , 1H COSY NMR and HMBC spectral analyses (Fig. B5 - B8, Appendix B).

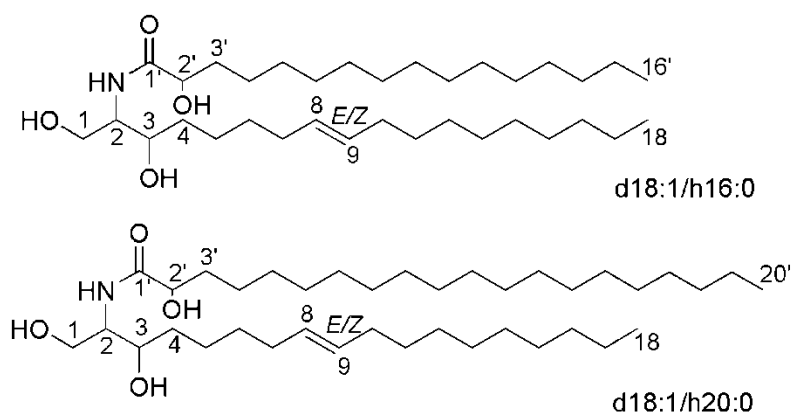


Figure 3-8: Chemical structure of predominant oat CERs.

The ^1H NMR spectra showed several overlapped signals of methylene hydrogens at δ 1.20-1.41 and signals of the terminal methyl hydrogens at δ 0.88 (3H-16' or 20'/3H-18) in the two aliphatic chains. The signals for the double bond appeared at δ 5.35. The signals for methylene hydrogens adjacent to the double bond (H-7 and H-10) appeared at δ 2.04 and have exhibited coupling with the double bond hydrogens in ^1H COSY spectra. In addition to the carbon signals of methylene groups in the range of δ 22.6 - 34.1, ^{13}C NMR spectra exhibited signals at δ 174.6 (C-1') for carbonyl amide, at δ 130.2 (C-8) and 130.0 (C-9) and 128.0 (C-8) and 127.9 (C-9) for a double bond, at δ 77.2 (C-3) and 72.3 (C-2') for the two oxymethylenes, at δ 62.6 (C-1) for an oxymethylene and δ 14.1 for the two terminal methyls (C-18 and C16'/18'). The NMR spectra of the two CERs are similar indicating the similarity of the structure, the difference being the four methylene groups on the FA chain. The two predominant oat CERs were identified as N-(1,3-dihydroxyoctadec-8-en-2-yl)-2-hydroxyhexadecanamide (APCI-MS m/z 554.3) and N-(1,3-dihydroxyoctadec-8-en-2-yl)-2-hydroxyicosanamide (APCI-MS m/z 610.3). The purity of both CERs was $> 99\%$ (a representative HPLC-ELSD chromatogram of oat CER is shown in Fig B9, Appendix B). The appearance of double peaks for each CER (m/z 554 and m/z 610; SIM mode) during preparative LC-MS isolation and the four carbon signals on ^{13}C NMR spectrum (at δ 130.8 and 130.3 for *E* isomers; 129.7 and 129.2 for *Z* isomers) indicate that both CERs are mixtures of *E/Z* isomers.

Table 3-4: ^1H and ^{13}C chemical shift (CDCl_3) of oat CER (d18:1 $^{\Delta 8E/Z}$ /h16:0).

	δ_{H} [ppm]	δ_{C} [ppm]
Sphingoid Base		
1a, 1b	3.42 (dd)	62.6
2 - 4	3.60 - 3.85	34.1 (C-4), 77.2 (C-3)
5, 6	1.20 - 1.41	22.6 - 31.9
7, 10	2.04 (m), 2.04 (m)	22.6 - 31.9
8, 9	5.35 (m), 5.35 (m)	128.0, 127.9 and 130.2, 130.0
11-17	1.20 - 1.41	22.6 - 31.9
18	0.88 (m)	14.1
Fatty Acid		
1'	-	174.6
2'	4.20 (m)	72.3
3'a, 3'b	1.62 (m)	33.8, 34.1
4' - 15'	1.20 - 1.41	22.6 - 31.9
16'	0.88 (m)	14.1

3.4. Conclusions

The LC/APCI-MS/MS-based separation and structural characterization of oat GlcCERs have shown three types of C18 dihydroxy SBs (d18:0, d18:1 and d18:2) amide linked to hydroxy FAs (C16-C24). The principal oat GlcCERs species comprised of d18:1 coupled with h16:0 and h20:0 which are similar to the predominant GlcCERs obtained from commercial sources such as wheat. The total GlcCER content of oat was also comparable to the GlcCER content in the commercial sources. The ESI-HRMS and NMR analyses of isolated oat CERs, after deglycosylation of GlcCERs, supported the structural information obtained from LC-MS/MS. The results suggest that oat is a potential alternative source of GlcCERs for dermal application.

4. Development and Validation of LC/APCI-MS Method for the Quantification of Oat CERs in Skin Permeation Studies

4.1. Introduction

It has been shown that the level of epidermal CERs is reduced in skin diseases such as AD [47, 48] and psoriasis [22, 57] and with increasing age [47, 264] resulting in defective skin barrier and skin dryness. It has also been documented that replenishing the depleted epidermal CERs with exogenous CERs has beneficial effects in improving skin barrier and skin hydration [25]. Recently, CER-containing topical products are proliferating for the management of skin conditions associated with perturbed levels of SC lipids [115, 118-120].

As indicated earlier, CERs isolated from natural sources such as edible plants are highly safe and their skin barrier improving effect has attracted much attention in recent years [299]. Unlike the oral PhytoCERs, little effort has been made to deliver PhytoCERs topically as a replacement therapy for the depleted epidermal CERs in diseased and/or aged skin. As PhytoCERs such as oat CERs are structurally related to SC CERs, the topical delivery of PhytoCERs can potentially stabilize SC lipid lamellae. However, *in vitro* as well as *in vivo* studies are required to document their role in stabilizing the bilayer structure of the SC. Further studies are also needed to investigate the rate and extent of permeation of PhytoCERs from pharmaceutical formulations and cosmetic products into the various skin layers. This is due to the fact that the CERs used to replenish the depleted CERs have to be delivered deep into the SC-SG interface where the SC lipid organisation into lipid bilayers takes place [7, 25]. Except for a few recent studies [123, 124], most of the previous studies showing the beneficial effects of topical formulations containing CERs were unable to confirm the permeation of the CERs into the SC and deeper layers of the skin.

Previously, analytical methods have been developed for the determination of endogenous CERs in the SC including LC/APCI-MS [23, 147, 149, 300], LC/ESI-MS [12, 20, 301, 302] and AMD-HPTLC [275, 303]. *Ex vivo* or *in vivo* CER skin permeation studies, however, require analytical methods that can selectively detect and quantify the exogenous CERs permeated into the SC without any interference from skin constituents including the epidermal lipids. *Ex vivo* skin permeation studies also require sensitive analytical methods as small size skin layers (skin slices representing the SC, viable EP and DR) containing minute quantities of CERs are obtained from Franz diffusion cells. In the literature, LC-MS methods are reported

for the quantification of exogenous deuterated CER [NP] [304] and a novel dimeric CER [305] in the skin. To our best knowledge, however, no other studies have shown a method for quantitative analysis of PhytoCERs in the various skin layers.

One of the major challenges we faced in developing a method for quantitative determination of PhytoCERs in biological systems was unavailability of phyto-identical CER reference standards on the market. There are structural variations among the commercially available CERs and PhytoCERs. While the commercially available CER standards usually have d18:1^{Δ4} SB, PhytoCERs typically contain d18:2^{Δ4,8}, d18:1^{Δ8} and t18:1^{Δ8} SBs [288]. In LC-MS-based analysis, these structural variations on the SBs could affect the MS signal intensity (associated with the stability of CERs in the ion source and CID). For instance, unlike CERs with C4-saturated SBs, CERs containing C-4 desaturated/hydroxylated SBs are readily dehydrated/deglucosylated (ion source fragmentation) (Table 3.3) [71, 72, 288]. Besides, in ion trap instrument, d18:1^{Δ8}-based GlcCER ions were found to be resistant to fragmentation in CID resulting in very low product ions making SRM scan mode difficult in LC-MS/MS analysis of these type of GlcCERs [288, 306]. On the other hand, d18:2^{Δ4,8}/t18:1^{Δ8}-based GlcCER ions are readily fragmented in the CID resulting in abundant product ions. The stability of d18:1^{Δ8}-based GlcCERs was also observed in the strong acidic conditions where the d18:2^{Δ4,8}/t18:1^{Δ8}-based GlcCERs are prone to degradations in acidic conditions resulting in the loss of the CERs.

To avoid these signal variabilities, one can consider synthesizing phyto-identical CERs. However, the existence of α -hydroxy FAs and SBs desaturated at position 8 in PhytoCERs make the synthetic procedure laborious and expensive. Therefore, it was indispensable to isolate GlcCERs from a plant, Ethiopian oat (*Avena abyssinica*), cleave the glycosidic linkage of GlcCERs and characterize the resulting CERs. Thus, the well characterized oat CERs (Fig. 4.1) were used as reference standards for the development and validation of the LC-MS method. Since the predominant oat CERs contain d18:1^{Δ8} SB, which are resistant to dissociation in ion trap instrument, we were unable to use SRM scan mode in the LC-MS analysis of oat CERs in the skin samples. Therefore, SIM mode was used for quantification of oat CERs in skin permeability studies.

APCI is frequently used for the analysis of many lipid classes [23, 137, 146, 147, 149, 150]. Since APCI was shown to be a good ionization technique for PhytoCERs [288, 306] and due

to its potential to reduce matrix effects [300], it was used in this study. As compared to ESI, the ionization process in APCI is also mostly independent of the nature of mobile phase used and the tendency of forming adducts is also less pronounced [137, 146, 148]. The present work is, therefore, aimed at developing and validating an LC/APCI-MS method for the detection and quantification of oat CERs in the SC and other layers of the skin. The method was also used to investigate the skin permeation of PhytoCERs after applying an amphiphilic cream containing oat CERs to the surface of *ex vivo* human skin.

4.2. Materials and Methods

4.2.1. Materials

Formic acid, 4.0 M HCl in dioxane and 1, 4-dioxane anhydrous (99.8%) were obtained from Sigma-Aldrich Chemie GmbH (Steinheim, Germany). HPLC grade methanol and chloroform were purchased from VWR International GmbH (Darmstadt, Germany). Isopropanol and *n*-hexane were obtained from Grüssing GmbH (Filsum, Germany). LC-MS grade methanol, silica gel 60 (0.063 - 0.200 mm) and TLC (silica gel 60, F₂₅₄, 20 cm×20 cm) plates were obtained from Merck KGaA (Darmstadt, Germany). Ethanol was supplied by Brüggemann GmbH & Co. KG (Heilbronn, Germany). CERs isolated from oat grain (oat CER I and oat CER II, Fig. 4.1) were used as reference standards (> 99% by HPLC- ELSD).

4.2.2. Methods

4.2.2.1. Isolation and Structural Characterization of Oat GlcCERs

The isolation and structural identification of oat GlcCERs were carried out following the methods described previously [306].

4.2.2.2. Cleavage of Glycosidic Linkage of Oat GlcCERs

The oat GlcCERs were dissolved in anhydrous 1, 4-dioxane (30 mg/mL) at room temperature and the solution was mixed with 4.0 M HCl in dioxane (1:1, *v/v*) in a round bottom flask. The reaction mixture was stirred on a magnetic stirrer at 500 rpm for 18 h at room temperature. The reaction mixture was kept in an ice water bath and the content of the mixture was neutralized with saturated NaHCO₃ solution. The reaction mixture was exhaustively extracted with CHCl₃ (three times) on a separatory funnel to separate the CERs from the hydrophilic components of reaction mixture (including the sugar moiety). The CHCl₃

phase was washed with saturated NaCl solution (brine) and dried under nitrogen stream. The progress of the reaction was monitored by TLC and LC-MS analyses. The scheme for the preparation and purification of oat CERs is shown in Fig. B1, Appendix B.

4.2.2.3. Isolation of Predominant Oat CERs

Isolation of the resulting oat CERs from the rest of reaction products in the CHCl_3 phase was achieved by TLC-guided column chromatography using a gradient elution: first elution with CHCl_3 followed by a second elution with $\text{CHCl}_3/\text{MeOH}$ (9:1, v/v). The two predominant oat CERs (m/z 554 and m/z 610) were separated by preparative LC/APCI-MS described in section 3.2.2.6 [306].

4.2.2.4. LC/APCI-MS Method Development

The method development and validation were started with LCQ ion trap instrument specified in section 2.2.2.3. Since the instrument was out of order, later we were forced to shift into a triple quadrupole instrument. Therefore, a system consisting of LC coupled to a triple quadrupole MS (Thermo Fisher Scientific TSQ Quantum Ultra, Bremen, Germany) equipped with APCI source was used for the development and validation of the method. A YMC-Pack ODS-AQ column (150 x 2.0 mm I.D., S-3 μm , 200 Å pore size) (YMC Europe GmbH, Dinslaken, Germany) was used to separate the oat CERs under the following chromatographic conditions: mobile phase of solvent A: H_2O (+ 0.1% formic acid) and solvent B: MeOH (+ 0.1% formic acid), flow rate: 0.3 mL/min, column temperature: 40 °C, injection volume: 10 μL and run time: 30 min. The separation was carried out using a gradient elution as follows: 10 % solvent A and 90% solvent B isocratic elution in the first 5 min followed by a gradient elution from 90% solvent B to 95% solvent B in the next 5 min and then from 95% B to 100 % B in the final 20 min. The post run equilibration time was 10 min. The MS was operated in the positive ion mode with SIM (m/z 554 and m/z 610) under the following APCI conditions: source vaporizer temperature of 450 °C, capillary temperature of 275 °C, source (discharge) current of 6 μA , sheath gas pressure of 55 psi and ion sweep gas pressure of 30 psi.

4.2.2.5. Extraction of SC Lipids

An ethical clearance was obtained from the Ethics Committee of the Faculty of Medicine, Martin Luther University Halle-Wittenberg for the SC lipid extraction and *ex vivo* permeability

studies. The SC lipids were extracted from a full-thickness skin sample and the skin of six volunteers. The full-thickness human skin from which the subcutaneous tissue was removed was extracted with 5 mL of *n*-hexane/ethanol (2:1, v/v) at room temperature overnight. The extract was filtered through a 0.45 µm syringe filter (PERFECT-FLOW® PTFE, WICOM Germany GmbH, Heppenheim, Germany) and dried under a nitrogen stream at 40 °C. The SC lipids from the skin of human subjects were extracted following a protocol described elsewhere [275]. Briefly, round glass cylinders were kept over the volar forearm of the six volunteers and tightly pressed to the skin to prevent lateral leakage, the cylinders were filled with 5 mL of *n*-hexane/ethanol (2:1, v/v) and the lipid was extracted for 5 min over extraction area of 6.158 cm². The SC extracts were taken with micropipette and dried under nitrogen stream at 40 °C. The residues were reconstituted in 1 mL of MeOH, filtered through 0.45 µm syringe filter and stored at -25 °C until use.

4.2.2.6. Method Validation

The LC/APCI-MS method was validated for selectivity, linearity, matrix effect, accuracy, precision, detection limit, quantitation limit and carry-over effect according to the EMA guideline on validation of bioanalytical methods, 2012 [269].

Calibration curve and linearity

Calibrations curves were constructed using different concentrations of the two oat CERs (30 - 1050 ng/mL) in MeOH. The linearity range was tested based on the average peak areas versus the concentration (ng/mL) of oat CERs using linear regression analysis and calibration curve parameters (correlation coefficient, slope and intercept) were calculated. The concentrations of the calibration standards were back calculated from the peak areas using the regression equations and the mean accuracy values were determined.

Limits of detection and quantification

The LOD and LOQ were determined according to the 1996 Analytical Detection Limit Guidance [307]. The LOD and LOQ of the method were estimated at spike level of 25 ng/mL (selected from a series of dilutions based on S/N ratio). The peak areas of 7 replicas of oat CER solutions (25 ng/mL) were determined and the corresponding concentrations were back calculated. From the average and SD of the back calculated concentrations, the LOD (LOD

= t -value \times SD, where t is Student's t value for 6 degrees of freedom ($n = 7$) and LOQ (LOQ = $10 \times$ SD) of the method were estimated. Finally, the spike level requirements were checked: whether the S/N ratio is in the range of 2.5 to 10, the spike level is in the appropriate range (which is $\text{LOD} < \text{spike level} < 10 \times \text{LOD}$) and the percentage recoveries (= average/spike level \times 100) are reasonable.

Precision and accuracy

The within-run precision and accuracy were determined by analyzing in a single run 5 samples per level at 4 concentrations covering the calibration curve range (at the LOQ (30 ng/mL), three times the LOQ (90 ng/mL), medium (400 ng/mL) and at 75% of the upper calibration curve range (800 ng/mL)). The four concentrations, 5 samples for each level in three runs analyzed on three different days, were used for the validation of between-run precision and accuracy. While the precision of the method was expressed as RSD, the accuracy was reported as percent of the nominal value (percent recovery).

Selectivity

The selectivity of the method was determined using the full-thickness skin and SC extracts obtained from different sources. The interference of the constituents of each of the extracts in the analysis of the target CERs was separately evaluated.

Carry-over

The carry-over effect of the method was assessed by injecting blank samples after running a high concentration sample of oat CERs spiked in the skin lipid extract (three times) and observing the occurrence of MS signals within the retention windows of the target CERs.

Matrix effect

The matrix effect was investigated using skin lipid extracts obtained from six different persons spiked with oat CERs. For each CER, the matrix factor (MF), ratio of the peak area in the presence of matrix (matrix spiked with oat CERs) to the peak area in the absence of matrix (pure solution of oat CERs), was calculated for each lot of matrix and the mean and RSD of the MF were obtained. The spiking was done at low ($3 \times$ lower LOQ) and high (close to the upper LOQ) concentrations.

4.2.2.7. Application of the Method for *ex vivo* Skin Permeation Studies

4.2.2.7.1. Preparation of Oat CER-based Cream

Oat CERs enriched fraction containing ca. 25% of total oat CERs was used for the formulation of cream. Oat CERs enriched fraction (10 mg) was incorporated into 4 g of an amphiphilic cream (Basiscreme, *Deutscher Arzneimittel Codex* (DAC), Caesar & Loretz GmbH, Hilden, Germany) which contains white soft paraffin (25.5%), glycerol monostearate (4%), cetyl alcohol (6%), polyoxyethylene glycerol monostearate (7%), medium-chain triglycerides (7.5%), propylene glycol (10%) and distilled water (40%).

4.2.2.7.2. *Ex vivo* Skin Permeability Studies

The permeation of oat CERs into the skin was investigated using an excised human skin in which the subcutaneous layer was removed. The skin was stored at -20 °C until use. The skin was first defrosted and mounted on a Franz diffusion cell (Crown Glass Company, Somerville, NJ, USA). A defined amount of the formulation, 20 mg of amphiphilic cream containing oat CERs, was applied evenly on the outer surface of the skin (3.1416 cm²) facing the donor compartment which was kept on filter gauze (Sartolon polyamide, pore size 0.45 µm; Sartorius Stedim Biotech GmbH, Gottingen, Germany). The acceptor compartment contained distilled water and was stirred continuously. The cell was kept at 32 °C using circulating water. The permeation experiments were carried out for 30, 100 and 300 min. Following the incubation period, the formulation remaining on the surface of the skin was removed by a cotton swab and three 6 mm diameter discs (0.2827 cm²) were cut out using a Kromayer punch (Stiefel-Laboratorium, Offenbach, Germany). The discs were sectioned into different slices using a cryo-microtome (Jung, Heidelberg, Germany). While the upper 10 µm thick slice represents the SC, the next four 20 µm thick slices were considered as viable epidermal layer (EP) (two slices for each epidermal sub-layers EP1 and EP2). Each of the DR sub-layers (DR1 to 3) were represented by five 40 µm thick slices. The lipids in each skin layer and the remaining piece of tissue of the skin was extracted with 1 mL of *n*-hexane/ethanol (2:1, v/v) overnight, filtered through 0.45 µm syringe filter and dried under nitrogen stream at 40 °C. The dried lipid extract was re-dissolved in 0.25 mL of MeOH and the amount of oat CERs was quantified by LC/APCI-MS. The cotton swab and the filter gauze were extracted with 5 and 2 mL of *n*-hexane/ethanol (2:1, v/v), respectively, and treated like the skin slices. The liquid collected from the acceptor compartment (20 mL) was also

treated like the other skin layers after freeze drying (Alpha 2 - 4 LSC Christ, Martin Christ Gefriertrocknungsanlagen GmbH, Osterode am Harz, Germany). The freeze-dried residue was dissolved in 2 mL of MeOH, filtered through 0.45 μm syringe filter, dried under nitrogen stream at 40 $^{\circ}\text{C}$, re-dissolved in 0.25 mL of MeOH and analyzed. The quantity of oat CERs in each skin slice, the total quantity of oat CERs distributed across the various skin sub-layers, total quantity of oat CERs recovered and the extraction recovery were calculated as follows:

Quantity of oat CERs in each skin slice

$$= (\text{Quantity of oat CERs in each slice}/0.2827 \text{ cm}^2) \times 3.1416 \text{ cm}^2$$

Total quantity of oat CERs distributed across the various sub-skin layers

$$\begin{aligned} &= (\text{Total quantity of oat CERs in the skin slices}/0.2827 \text{ cm}^2) \times 3.1416 \text{ cm}^2 \\ &= [\text{Quantity in (SC + EP1 + EP2 + DR1 + DR2 + DR3 + RT)}/0.2827 \text{ cm}^2] \times 3.1416 \text{ cm}^2 \end{aligned}$$

where RT is the remaining skin tissue

Total quantity of oat CERs recovered

$$= \text{Quantity of oat CERs in (various skin sub-layers + cotton swab + filter gauze + acceptor fluid)}$$

Extraction Recovery (%)

$$= (\text{Total quantity of oat CERs recovered}/\text{nominal quantity of oat CERs applied}) \times 100$$

4.3. Results and Discussion

4.3.1. Preparation of oat CERs Reference Standards

As reported earlier [306], about 12 GlcCER species were identified by LC/APCI-MS/MS in oat grain. The two predominant oat GlcCER species were Glc-d18:1 $^{\Delta 8}$ /h16:0 and Glc-d18:1 $^{\Delta 8}$ /h20:0. As the CERs are needed for the SC delivery as a replacement of the native CERs lost due to some skin diseases and ageing, cleavage of the sugar moiety in the GlcCER species was necessary. Hence, the glycosidic linkage of oat GlcCERs was cleaved under strong acidic conditions. The resulting predominant oat CERs (CER I and CER II, Fig. 4.1) and their structures were further characterized by ESI-HRMS and NMR analyses [306]. The purity of the CERs was found to be > 99% as determined by HPLC-ELSD. The well characterized CERs isolated from oat grain were used as reference standards for the development and validation of the method.

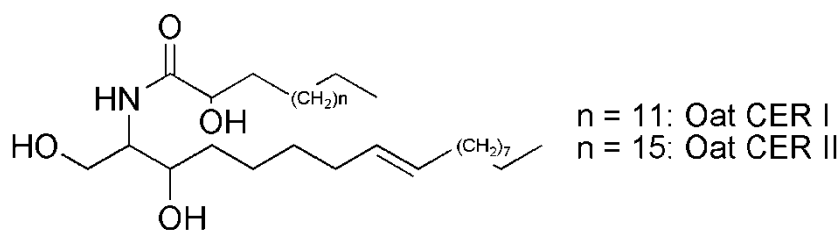


Figure 4-1: Chemical structures of major oat CERs

4.3.2. Method Development

During method development, different RP-HPLC columns were tested with various eluents in gradient mode of elution. The effects of mobile phase composition (H₂O/MeOH, varied from 0:100 to 10:90) and formic acid concentration (0.1%, 0.2% and 0.3% in both H₂O and MeOH) on the degree of separation of the target oat CERs and other components of SC extracts were investigated. The oat CERs were better separated from SC components on YMC-Pack ODS-AQ column using a gradient of 5% A (H₂O + 0.1% formic acid) to 100% B (MeOH + 0.1% formic acid) in 20 min. The degree of separation was even improved when the run starts with 10% A for the first 5 min (isocratic), followed by a gradient from 10% A to 5% A for the next 5 min and then the gradient mentioned earlier for 20 min. The positive mode APCI ionization allowed detection of the target CERs easily without significant peak area fluctuations. The APCI conditions such as ionization temperature and voltage parameters were also adjusted to improve the peak intensity of the target CERs. Higher degree of ionization was obtained at APCI vaporizer temperature of 450 °C and capillary temperature of 275 °C.

As indicated earlier, the method development was first started with ion trap instrument. In LCQ ion trap instrument, the predominant oat CERs, which contain d18:1Δ8 SB, were found to be resistant to MS/MS fragmentation. Therefore, it was difficult to use SRM scan mode in LC-MS/MS-based quantification of oat CERs in the skin samples. Thus, SIM mode was used for the quantification of oat CERs in skin permeability studies. At the later stage of method development and validation, the ion trap instrument became nonfunctional. Hence, another instrument with triple quadrupole mass analyzer was used to complete the method validation process. The oat CERs were easily dissociated into the product ions in the triple quadrupole instrument.

4.3.3. Method Validation

In order to validate the method developed and demonstrate its reliability for the quantification of oat CERs in the skin layers, the system was challenged with skin lipid extracts obtained from different individuals. The lipid extracts of the SC, deeper skin layers (epidermal and dermal skin slices) and full-thickness skin were also used as matrix. One of the common solvent mixtures for the extraction of SC lipids, *n*-hexane/ethanol [23, 275, 304], was used for the extraction of skin lipids. The lipid extracts which contains mainly CERs, FAs and cholesterol were used to investigate the selectivity, matrix effect and other parameters of analytical method validation.

Selectivity

As stated earlier, the method is mainly meant for the quantification of oat CERs permeated into the skin following the application of various topical formulations and skin-care products. One of the limitations in investigating CER penetration into the skin is the lack of sensitive analytical method differentiating exogenous CERs from endogenous CERs and other lipids. Therefore, a new method was needed to separate the skin components from the target oat CERs. The potential interference of the components of each skin lipid extract with the two oat CER peaks was individually analyzed. The full scan chromatograms of SC and full thickness skin lipid extracts are shown in Fig. 4.2A and B, respectively. Representative LC/MS chromatograms of SC extract spiked with low and high concentrations of oat CERs are depicted in Fig. 4.2C-E. As can be seen from the chromatograms obtained in SIM mode (m/z 554 and m/z 610), no other interfering peak has been detected within the retention windows of both target CERs. Therefore, the method effectively differentiated the oat CERs from the endogenous components of all the extracts including CERs.

Among the epidermal CERs, the d18:1 Δ^4 -based CERs containing h16:0 and h20:0 (CER [AS]-C16 and CER [AS]-C20) are isobaric or isomeric with oat CERs, the difference being the position of the double bond on the SB. As the ionization conditions of APCI are somewhat harsher compared to ESI [23], d18:1 Δ^4 containing epidermal CERs are readily dehydrated in the ion source unlike the oat CERs containing C-4 saturated/C-8 desaturated SB. As a result of ion source fragmentation, the abundant ions detected for CERs consisting of d18:1 Δ^4 were the ions that lost water $[M+H-H_2O]^+$ and, hence, parent skin CERs $[M+H]^+$ are detected at

low intensities (particularly in SC extracts spiked with low concentrations of oat CERs) during SIM mode scanning (m/z 554 and m/z 610).

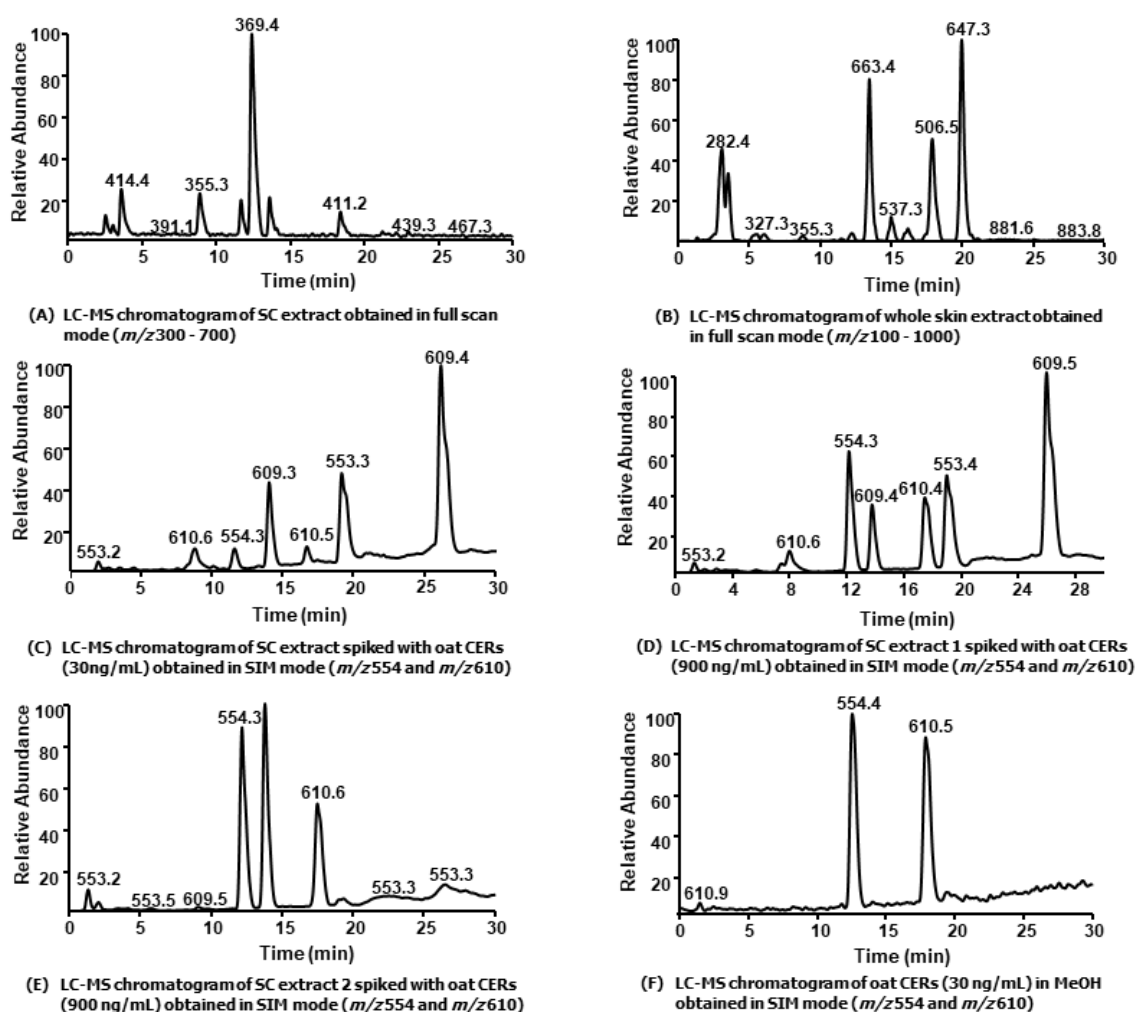


Figure 4-2: LC-MS chromatograms of skin lipid extracts obtained in full scan mode and SC extracts spiked with oat CERs acquired in SIM mode.

To confirm the specificity of the method, SC extracts spiked with oat CERs were analyzed by Q1 full scan followed by LC-MS/MS at different collision energies (20 - 50 V). Fig. 4.3A and B depict the dissociation of oat CERs in triple quadrupole instrument. The oat CERs were fragmented into characteristic product ions. The well chromatographic separation of oat CERs avoided the possible interference from isobaric compounds in the skin samples. The proposed fragmentation mechanism is shown in Fig. 4.3 C.

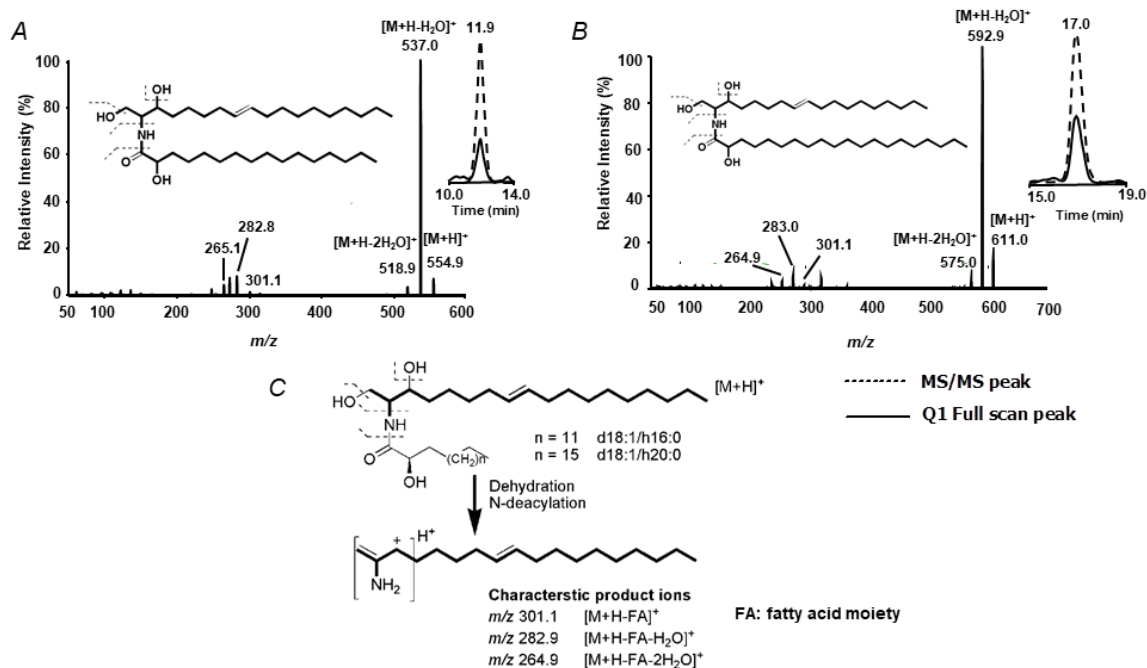


Figure 4-3: MS/MS fragmentation of oat CERs in triple quadrupole instrument (A and B) at CID 20 V and suggested fragmentation pattern (C) [270].

Matrix effect and carry-over

During the method development, emphasis was given to avoid the possible interferences and matrix effects of the components of the SC extracts. As stated earlier, the method separates the components in the SC extracts from target oat CERs. The MF was determined from the peak areas of matrix spiked with CERs (90 and 900 ng/mL oat CERs) and solution of CERs in MeOH. As can be seen from Table 4.1, the mean MF values were found to be around 100% at 90 ng/mL spiking level. The mean MF values of spiking at high concentration level (900 ng/mL) were also nearly 100% (data not shown). The RSD value also shows that the ionization of CERs was not significantly affected by the presence of matrix. These results indicated that the matrix effect was insignificant.

Table 4-1: The S/N, LOD/LOQ, Recovery and MF of the LC/APCI-MS method for quantification of oat CERs in the skin.

	S/N	LOD (ng/mL)	LOQ (ng/mL)	Percentage Recovery	Mean of MF (%)*	RSD of MF (%)*
CER I	8.1	10.0	30.8	103.7	101.1	5.2
CER II	8.0	9.3	29.5	94.9	102.5	4.2

*for extracts spiked with 90 ng/mL of oat CERs

The carry-over effect of the method was assessed by injecting high concentration of oat CERs (1050 ng/mL) followed by blank samples (MeOH and SC extracts). No peak was detected in the retention windows of the oat CERs indicating that the method is free of carry-over effect.

LOD and LOQ

The estimated LOD and LOQ of the method are shown in Table 4.1. The spike level (25 ng/mL) was in the recommended range i.e., $LOD < \text{spike level} < 10 \times LOD$ with reasonable percentage recoveries (103.7% and 94.9% for oat CER I and CER II, respectively). Accordingly, the method's LOD and LOQ were estimated to be around 10 and 30 ng/mL for each oat CER, respectively. The method was found to be sensitive enough to detect and quantify the trace amounts of oat CERs in the deeper layers of the skin, as supported by the results from the skin permeability studies described below.

Linearity

The LC-MS method showed linear responses over a concentration range from 30 ng/mL to 1050 ng/mL for both CERs. The linear equations obtained for oat CER I and CER II were $Y = 4582.5X + 2658.1$ (with R^2 of 0.9997) and $Y = 3538.2X - 38379.6$ (with R^2 of 0.9991), where Y is the peak area and X is the concentration of CERs (ng/mL), respectively. The mean accuracy and the RSD values of the back calculated concentrations of the calibration standards are shown in Table 4.2. The RSD values of the back calculated concentrations are within the acceptable limits ($\pm 15\%$ of the nominal value).

Table 4-2: Back calculated concentrations of the calibration standards and the corresponding calculated mean accuracy values.

Nominal Concentration (ng/mL)	Back calculated concentration (ng/mL)		Mean Accuracy (%)		RSD (%)	
	CER I	CER II	CER I	CER II	CER I	CER II
30	29.5	28.5	98.4	95.1	8.2	6.0
50	49.8	50.8	99.6	101.6	2.3	4.1
100	101.3	98.5	101.3	98.5	2.5	3.6
200	186.6	183.0	93.3	91.5	7.6	7.8
400	416.0	403.0	104.0	100.7	8.9	8.8
500	515.7	520.7	103.1	104.1	8.1	8.7
900	912.3	915.6	101.4	101.7	4.3	5.8
1050	1048.1	1053.6	99.8	100.3	1.1	2.0

Precision and accuracy

The results of the method's precision and accuracy are presented in Table 4.3. The RSD of within-run and between-run precision ranged from 1.2% to 7.3% and 1.2% to 7.8%, respectively. On the other hand, the recovery (%) ranged from 94.1% to 109.2% and 92.5% to 109.4% for within-run and between-run experiments, respectively. The results suggest that the method is accurate and precise for the quantification of oat CERs in the skin layers.

Table 4-3: Within-run and between-run precision and accuracy of LC/APCI-MS method for the quantification of oat CERs in the skin layers.

Nominal Concentration (ng/mL)	Oat CERs	Calculated Concentration (ng/mL) (n = 5)		Recovery (%)		RSD (%) (n = 5)	
		Within-run	Between-run	Within-run	Between-run	Within-run	Between-run
30	CER I	28.8	29.3	95.9	97.6	7.3	3.5
	CER II	32.8	32.8	109.2	109.4	3.7	4.8
90	CER I	84.7	83.2	94.1	92.5	2.6	3.5
	CER II	95.1	97.3	107.5	108.1	1.2	5.5
400	CER I	421.2	429.1	105.3	107.3	2.4	7.8
	CER II	425.3	430.3	106.3	107.6	4.0	6.0
800	CER I	829.4	830.8	103.7	103.9	2.2	1.8
	CER II	836.0	872.8	104.5	109.1	1.5	1.2

4.3.4. Application of LC/APCI-MS Method in *ex vivo* Permeation Studies

As mentioned earlier, recently there has been a proliferation of CER-based topical skin-care products. However, in most of the cases, the permeation of CERs into the SC and deeper layers of the skin from these products has not been investigated. The skin permeation of exogenous CERs such as PhytoCERs from the various topical dosage forms needs to be investigated to demonstrate their potential application in improving the barrier function of diseased, aged and/or affected skin. Even though the CERs are intended for the SC delivery (mainly at the SC-SG interface where the SC lipids organize into the lipid bilayer), depending upon the delivery systems used and the components of the formulations, the CERs can possibly penetrate into the deeper layers of skin. Different formulation strategies such as colloidal systems have been designed for controlled delivery of CERs into the SC and improve their poor solubility and permeation [123, 124].

The CER skin permeation studies, therefore, require sensitive and selective analytical methods for quantifying the exogenous CERs in the SC, viable EP and DR of the skin. Against this background, the applicability of the current LC-MS method for the investigation of PhytoCERs permeation across the different layers of skin was studied. It has been shown that CERs have poor penetration across the skin from conventional formulations such as ointments and creams [123, 308] and, hence, the oat CERs were incorporated into amphiphilic cream in attempt to detect and quantify the small quantities of CERs distributed across the skin layers (SC, viable epidermal sub-layers (EP1, EP2), dermal sub-layers (DR1, DR2, DR3)) using the validated LC-MS method.

The extraction of oat CERs from the skin samples was carried out by using *n*-hexane/ethanol (2:1, v/v) as this solvent mixture was shown to be an effective solvent for the extraction of CERs from the skin [23, 123, 304, 305]. The extraction was carried out overnight after sonication at 40 °C for 30 min to exhaustively extract oat CERs. The actual concentrations of oat CERs measured in the skin slices ranged from 49 ng/mL to 675 ng/mL. Since the concentrations of oat CERs extracted from the cotton swab were out of the calibration range, appropriate dilution were made before quantification.

The extraction recovery were found to be 83.4%, 87.9% and 83.2% for the three incubation periods (30, 100 and 300 min), respectively. Despite the fact that over 85% of the oat CERs remained in the cream after the three incubation periods, the method quantified the minute

quantities of oat CERs that penetrated into and distributed across the skin layers (Table 4.4 and Fig. 4.4 A and B).

Table 4-4: Amount of oat CERs permeated across the skin layers and sub-layers following topical application of amphiphilic cream after 300 min incubation period.

	Samples/skin slices	Amount of oat CERs (ng)*	
		CER I (SD)	CER II (SD)
Unpenetrated	Cotton swab	4319.5 (89.0)	4504.5 (44.3)
SC	A 10 µm thick slice	15.9 (1.5)	35.1 (1.5)
Viable EP1	Two 20 µm thick slices	15.0 (1.3)	32.5 (2.2)
Viable EP2	Two 20 µm thick slices	13.5 (1.7)	32.6 (2.0)
DR1	Five 40 µm thick slices	87.3 (2.1)	129.7 (4.3)
DR2	Five 40 µm thick slices	53.6 (3.7)	91.3 (5.2)
DR3	Five 40 µm thick slices	21.1 (1.0)	47.4 (3.0)
Remaining skin tissue	Remaining skin tissue	81.5 (1.3)	107.4 (1.4)
Penetrated CERs	Filter gauze	124.7 (10.3)	18.6 (0.6)
Penetrated CERs	Acceptor fluid	13.8 (0.1)	13.0 (0.3)

*The quantities of oat CERs in the skin slices were corrected for the applied skin area i.e., (quantity of oat CERs in each slice/0.2827 cm²) × 3.1416 cm².

The main barrier (rate-limiting step) in CER transport across the skin is the SC. The small portion of oat CERs which has overcome the SC barrier distributes into the viable EP and DR layers as well as the acceptor. The longer the penetration time the higher the possibility of detecting the CERs in the acceptor fluid. Oat CERs were not detected in the acceptor fluid after 30 and 100 min of incubation periods (only detected in filter gauze). The thickness of the remaining skin tissues varies in the skin samples used in the three incubation periods. The thickness variation affected the quantities of oat CERs considered as DR (Fig. 4.4A). Fig. 4.4B shows the permeation profile of oat CERs without considering the remaining skin tissues (DR = DR1 + DR2 + DR3). The extent and depth of permeation depend also on several other factors including the physicochemical properties of the active, the biological factors and the delivery system used. The normalized amount of oat CERs (ng/10 µm skin slice) permeated and distributed across the various skin layers is shown in Table 4.5. The interesting thing we can see from the Table is that the portion of oat CERs penetrated into the skin is mainly concentrated in the SC where the CERs are needed. Therefore, formulation strategies enhancing the penetration of oat CERs and localizing them in the SC should be

designed and further investigated. The method clearly indicated the depth and extent of penetration of oat CERs into excised human skin. The method, therefore, can be used to investigate the skin distribution of PhytoCERs from the various dermal and transdermal formulations including nano-sized systems such as MEs and NPs which are shown to improve the skin permeability of drugs.

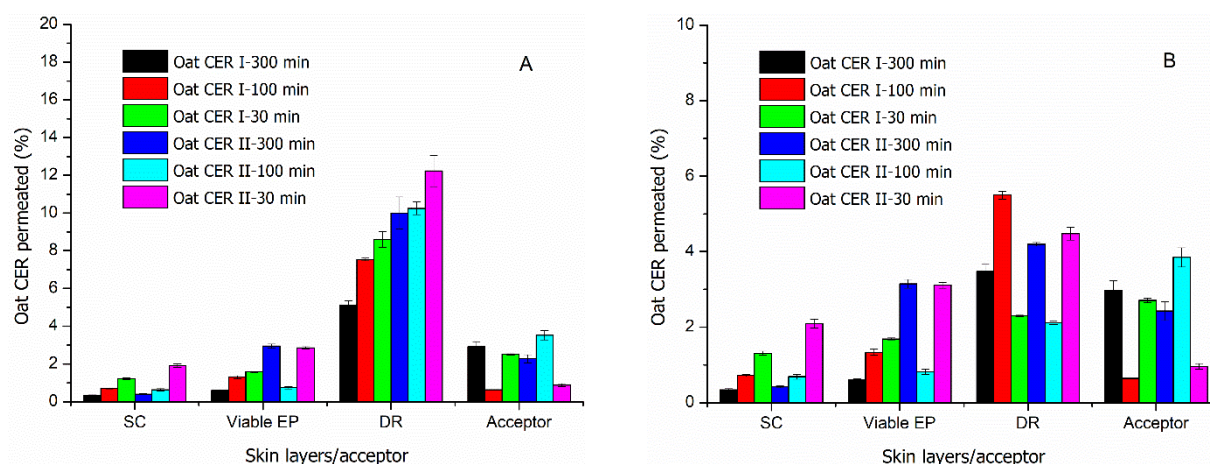


Figure 4-4: Percentage of oat CERs permeated (\pm SD) into the various layers of the skin from an amphiphilic cream containing oat CERs: SC, viable EP (EP1 + EP2), DR (For A: DR1 + DR2 + DR3 + remaining skin tissue and for 'B' without the remaining skin tissue) and acceptor (filter gauze + acceptor fluid).

Table 4-5: Skin thickness normalized amount of oat CERs (ng/10 μ m skin slice) permeated across the skin layers following topical application of amphiphilic cream (Incubation periods: 30, 100, 300 min).

Skin layers*	Normalized amount of oat CERs (ng/10 μ m skin slice) (SD)					
	300 min		100 min		30 min	
	Oat CER I	Oat CER II	Oat CER I	Oat CER II	Oat CER I	Oat CER II
SC	15.86 (1.53)	35.15 (1.47)	57.68 (3.10)	19.46 (1.47)	29.72 (2.83)	90.32 (6.13)
Viable EP	3.56 (0.24)	8.14 (0.52)	9.28 (0.06)	18.13 (0.68)	4.40 (0.37)	16.76 (0.56)
DR	2.70 (0.11)	4.47 (0.09)	1.69 (0.01)	3.06 (0.03)	1.52 (0.03)	3.22 (0.11)

*SC (10 μ m skin slice), viable EP (4 \times 20 μ m skin slices), DR (15 \times 40 μ m skin slices)

4.4. Conclusions

A simple, sensitive, selective, precise and accurate LC/APCI-MS method with no or minimal matrix effect was developed and validated for the quantification of oat CERs in the skin layers. The applicability of the method to real samples was tested using an amphiphilic cream containing oat CERs. The method selectively quantified the amounts of oat CERs distributed across the various skin layers. The results of method performance evaluation suggest that the current method can be used to investigate the penetration of oat CERs into the skin from the various topical dosage forms to demonstrate the *ex vivo* or *in vivo* dermal bioavailability of oat CERs.

5. Delivery of Oat CERs into the SC of the Skin using Nanocarriers: Formulation, Characterization and *in vitro* and *ex-vivo* Penetration Studies

5.1. Introduction

The SC lipid matrix is composed of approximately equimolar ratios of CERs, cholesterol, and free FAs. CERs play important structural roles in maintaining the skin barrier function and water-retaining properties [81]. Even though the unique lamellar arrangement of SC lipid matrix has not yet been fully elucidated, it has been shown that the deficiency or disturbance of SC lipids may lead to disruption of lipid organization which, in turn, affects the skin barrier function and skin hydration [25, 47, 48]. One of the approaches used to treat the skin barrier dysfunction and skin dryness associated with depletion and/or disturbance of SC lipids such as CERs is direct replacement of the depleted lipids [25]. Although several topical formulations containing CERs, pseudo-CERs, or agents correcting the depleted CERs have been produced, many of these products lack documented evidence to establish their cutaneous efficacy [120].

The depleted native skin CERs can potentially be replaced with PhytoCERs such as oat CERs. The beneficial effects of oral intake of PhytoCERs for skin hydration and skin barrier reinforcement have been indicated in several studies [93, 94, 96]. So far, however, little effort has been made to investigate the possibility of delivering PhytoCERs topically for the stabilization of SC lipid lamellae in diseased, aged and/or affected skin. *In vitro* as well as *in vivo* studies are, therefore, needed to investigate the skin permeation profile of PhytoCERs and for better understanding of the influences of the structural variations between plant and human skin CERs on the stabilization of SC lipid bilayer.

Most of the studies supporting the beneficial effects of CER-based topical formulations were unable to show the depth and extent of permeation of the CERs into the skin. The CERs replenishing the depleted CERs in the SC have to be delivered deep into the SG-SC interface where the SC lipid organisation into lipid bilayers takes place [7, 25, 122]. Since the penetration of CERs across the skin from conventional formulations such as ointments and creams is poor [123, 308], other formulation strategies such as colloidal systems have been investigated to improve the poor solubility, facilitate the permeation and target the delivery of CERs into the SC [123, 125-127].

Nano-sized carriers such as MEs and NPs have been shown to be promising vehicles for dermal and transdermal delivery of drugs [257]. MEs are optically isotropic, transparent one phase systems which are formed spontaneously by mixing appropriate amounts of lipophilic and hydrophilic components with SAA/co-SAA [125]. They have the advantages such as high drug-loading capacity, drug-permeation enhancing effects, long-term stability and ease of preparation [161, 171, 309]. The high drug solubilization capacity is attributed to the enormous interfacial area and existence of microenvironments of different polarity within the same single-phase system [161]. A wide range of hydrophilic and lipophilic actives can be solubilized in MEs as there are plenty of combinations of ME constituents which principally can form MEs [162]. Previously lecithin-based MEs (LBMEs) have been formulated and characterized for controlled delivery of CER [AP] into the SC [127].

Polymer-based NPs are another interesting nanocarriers for effective delivery of drugs to a target site. In dermal and transdermal delivery, they present enormous surface area allowing homogeneous drug release [259, 260]. They also act as reservoirs for controlled delivery of drugs into the SC, controlling the drug permeation into the deeper layers of the skin [261, 262]. The NPs are closely in contact with the SC, which increases the partition coefficient of the drug into the SC thereby facilitating the penetration of the drug into the SC [258, 262]. Starch has been used as a nanocarrier for drugs destined for tumor-targeting [252, 253], transdermal delivery [224] and transnasal mucoadhesive delivery [254]. As indicated earlier, the native starches have been modified chemically, physically and/or enzymatically to provide the required functionality and expand their applications in nanotechnology. Chemically modified acetylated starch is one the most common starches investigated for controlled drug delivery by virtue of its hydrophobicity and film-forming properties [247-251]. It has also been used in the fabrication of NPs [228, 255, 310, 311].

In an attempt to deliver oat CERs into the SC, in this study, therefore, LBMEs and starch-based NPs containing oat CERs were formulated and characterized. Besides, the *in vitro* release and penetration (using artificial multilayer membrane system) and *ex vivo* skin permeation (using excised human skin) of oat CERs were also investigated.

5.2. Materials and Methods

5.2.1. Materials

CER [AP] and CER [AS] were obtained from Evonik-Industries (Essen, Germany). HCl (4.0 M in dioxane), 1, 4-dioxane anhydrous (99.8%), Pluronic® F-127 and 1,2-pentanediol were obtained from Sigma-Aldrich Chemie GmbH (Steinheim, Germany). Euxyl® PE 9010 was supplied by Schülke & Mayr GmbH (Norderstedt, Germany). Carbopol®980 Polymer was obtained from Lubrizol Advanced Materials Europe BVBA (Brussels, Belgium). Miglyol® 812 and collodion 4% were purchased from Caesar & Loretz GmbH (Hilden, Germany). Phosal®75 SA (phosal) was kindly donated by Phospholipid GmbH (Köln, Germany). Octanol and dodecanol were obtained from Sasol Germany GmbH (Brunsbüttel, Germany). DMSO was obtained from Fluka Chemie GmbH (Buchs, Switzerland). Tris (hydroxymethyl)-aminomethane, formic acid, silica gel 60 (0.063 - 0.200 mm) and TLC (silica gel 60, F₂₅₄, 20 cm×20 cm) plates were obtained from Merck KGaA (Darmstadt, Germany). Ethanol was supplied by Brüggemann GmbH & Co. KG (Heilbronn, Germany). Ethylacetate was obtained from Overlack GmbH (Leipzig, Germany). Cassava tubers were collected from Sawula, Gamo Gofa Zone, Southern Ethiopia.

5.2.2. Methods

5.2.2.1. Preparation of CERs from Oat GlcCERs

The method described previously was used to cleave the sugar moiety of oat GlcCERs (section 4.2.2.2) [306]. The GELF of oat was acid treated (4.0 M HCl in dioxane) and the oat CERs enriched fraction was extracted from the reaction mixture by using CHCl₃ and purified with column chromatography. The oat CERs enriched fraction was used for the preparation of the formulations.

5.2.2.2. Isolation and Acetylation of Cassava Starch and Determination of DS

Cassava starch was isolated from cassava tubers (*Manihot esculenta Crantz*) following the method described previously [312]. The preparation of cassava SA and determination of DS were carried out according to the methods specified elsewhere [228]. The acetylation of cassava starch was achieved using acetic anhydride as acetylating agent (1:4 starch to agent ratio) and 50% (*w/w*) aqueous NaOH solution as a catalyst at 90 °C. SAs with three different

DS (1.74, 2.15 and 2.72) were prepared at three different reaction times (3, 6 and 9 h). The DS of SAs was determined by saponification titration method.

5.2.2.3. Preparation of Oat CER-based Formulations

5.2.2.3.1. Preparation of LBMEs and ME Gel

Oat CER MEs were prepared by mixing all the components of the MEs (oil, hydrophilic phase and SAA) in vials and sonicating the mixtures for 30 min at 40 °C (Table 5.1). Carbopol®980 gel (1%) was used as a thickening agent for the preparation of ME gel. LBME1 and Carbopol®980 gel (1%) were mixed (in 1:2 ratio) and the pH was adjusted with 7.5 % of Tris for the gel formation. The ME gel was preserved with Euxyl® PE 9010 (1% of the total ME gel).

Table 5-1: Compositions of LBMEs

MEs	Miglyol®812 (%, w/w)	Phosal®75 SA (%, w/w)	Water-PD* (1.5:8.5) (%, w/w)	Total oat CERs (%, w/w)
LBME1	5	35	60	0.25
LBME2	10	40	50	0.25
LBME3	15	45	40	0.25

*PD: 1,2 pentanediol

5.2.2.3.2. Preparation of Starch-based NPs and NP Gel

Oat CER-loaded SA NPs were prepared by emulsification solvent evaporation method. Both oat CERs and SAs with three different DSs (1.74, 2.15 and 2.72) were dissolved in ethylacetate (1 mg/mL). The solution of oat CERs was mixed with SA solutions (in 1:4 ratio of oat CERs to SAs). The mixture of the two organic systems was emulsified with aqueous solution containing Pluronic® F127 (1.5 mg/mL) in 1:4 ratio via high shear homogenization (at 18000 RPM for 5 min) followed by sonication (15 min). The organic solvent was removed by continuous stirring of the dispersion overnight in a fume hood. The resulting concentrated colloidal dispersion was diluted with double distilled water and filtered through 0.45 µm syringe filter.

The NP gel was prepared by incorporating one part of the NPs suspension (SANP-DS 2.72) into two parts of Carbopol®980 gel (1%). The aqueous system was neutralized by 7.5 % of

Tris to get the gel formulation. Euxyl® PE 9010 (1%) was used as a preservative. A pure gel containing equal portion of distilled water instead of NPs suspension was prepared for comparison purpose.

5.2.2.3.3. Preparation of oat CER-based Amphiphilic Cream

Oat CERs enriched fraction (10 mg) was incorporated into 1 g of an amphiphilic cream (DAC). The cream is composed of white soft paraffin (25.5%), glycerol monostearate (4%), cetyl alcohol (6%), polyoxyethylene glycerol monostearate (7%), medium-chain triglycerides (7.5%), propylene glycol (10%) and distilled water (40%).

5.2.2.4. Characterization of Oat CER Formulations

5.2.2.4.1. Cross-Polarized Light Microscope

The isotropicity of MEs was verified by cross-polarized light microscope (Zeiss AxioLab Pol, Carl Zeiss MicroImaging GmbH, Jena, Germany). A drop of each sample was put on a slide, covered by a slide cover and was observed under the cross-polarized light microscope.

5.2.2.4.2. Dynamic Light Scattering (DLS)

The droplet size of the MEs was determined by a light scattering hardware set-up (ALV-Laser, Langen, Germany) allowing simultaneous static and DLS measurements. A sample cell made of Suprasil® quartz glass (Hellma, Mühlheim, Germany) was placed on a motor-driven precision goniometer and was allowed for temperature equilibration (15 min). The motor-driven goniometer enabled the photomultiplier detector to be moved from 20° to 150° scattering angles. A green Nd: YAG DPSS-200 laser (532 nm, Coherent, Auburn, USA) with an output of 200 mW was used as a light source. The second order intensity time correlation functions (g^2) was recorded with an ALV-5000E Multiple Tau Digital Correlator with fast option, with a sampling time of 60s. The measurements were made at five different angles (30, 40, 50, 60 and 70°) at 25 °C and the results were analyzed by using ALV-5000 Multiple Tau Digital Correlator (ALV-Laser Vertriebsgesellschaft M-B.H., Langen, Germany).

The particle size and size distribution of NPs were determined by DLS using particle size analyzer (Malvern, Zetasizer Nano ZS, Herrenberg, Germany). Scattered light was collected at fixed angle at 25 °C. Prior to size measurements, the NP suspensions were diluted with double distilled water and filtered through 0.45 µm syringe filters.

5.2.2.4.3. Viscosity

The viscosity of the formulations was measured using rotational viscometer (Anton Paar GmbH, Graz, Austria). A cup and bob viscometer with Couette geometry was used for measuring the viscosity of the MEs at 16 varying shear rates ($1 - 1000 \text{ s}^{-1}$) at $25 \text{ }^\circ\text{C}$. The average and RSD of the readings were calculated as all the formulations exhibited Newtonian type of flow.

Rheological measurements of the gel formulations were carried out at $25 \text{ }^\circ\text{C}$ by a rotational viscometer equipped with a cone-and-plate geometry of 25 mm diameter (the cone angle was 1°). First strain sweep measurement was carried out a fixed angular frequency (10 rad/s) and varying deformation amplitude (%) to determine the critical strain level. Then all the formulations were subjected to frequency sweep measurements at a fixed deformation amplitude in the linear range (below the critical strain level) by varying the angular frequency (100 to 0.1 rad/s). Steady shear measurements with increasing and decreasing shear rates (hysteresis loops) were also made for each gel formulation. Each measurement consisted of three parts: a stepwise increase in shear rate from 1 s^{-1} to 100 s^{-1} with 21 measurement points (the measurement time for each rate was 5 s), 10 measurement points with a constant shear rate of 100 s^{-1} for 5 seconds each, and finally, a stepwise decrease in shear rate from 100 s^{-1} to 1 s^{-1} with 21 points (with 5 s measurement time for each rate).

5.2.2.4.4. Refractive Index

The refractive index of the MEs was obtained using an Abbe refractometer (Carl-Zeiss, Jena, Germany) at $25 \text{ }^\circ\text{C}$. The average and the RSD of the readings ($n = 3$) were calculated.

5.2.2.4.5. Stability

The physical stability of the MEs over a period of time was evaluated by visual inspection at ambient conditions. The physical changes such as turbidity, phase separation, flocculation and/or precipitation were indicator for instability.

5.2.2.4.6. Environmental Scanning Electron Microscopy (SEM)

The SEM images of starch samples were obtained using Environmental Scanning Electron Microscopy (ESEM) FEI/Philips XL-30 ESEM (Leuven, Belgium) at low accelerating voltage

(1.00 KV) to inhibit the surface charging and to better see the fine surface structures of the particles.

5.2.2.4.7. Encapsulation Efficacy and Loading Capacity of NPs

The EE and LC of the NPs were determined indirectly by quantifying the amount of untrapped oat CERs in the NPs. The NPs colloidal dispersion was centrifuged at 16,000 g for 2 h (Eppendorf Centrifuge 5415 R, Hamburg, Germany), the supernatant was withdrawn and dried under nitrogen stream at 40 °C. The residue was re-dissolved in CHCl₃/MeOH (1:1, v/v) and the amount of oat CERs was determined by AMD-HPTLC. To determine the weight of NPs recovered, NPs suspension was prepared separately, filtered (0.45 μm syringe filter), freeze-dried and the weight of the dried NPs was taken. Finally, the EE (%) i.e., (total oat CERs - untrapped oat CERs)/total oat CERs × 100 % and LC (%) i.e., (entrapped CERs/weight of NPs × 100 %) were calculated.

5.2.2.4.8. Automated Multiple Development (AMD)-HPTLC

AMD-HPTLC method described elsewhere [288, 306] was used for the quantification of oat CERs in determining the EE and LC of the NPs. Different volumes of standard CER solution (1 - 15 μL of 100 μg/mL of CER [AS]) and 2 μL samples were applied on prewashed and dried HPTLC plate (TLC silica gel 60 F254, 20 cm×10 cm, Merck KGaA) as 6 mm bands using a CAMAG Automatic TLC sampler 4. A three steps chromatographic development (CAMAG AMD 2) was conducted using CHCl₃/MeOH/HAc (190:9:1, v/v/v) as a mobile phase (migration distance of 70 mm) for the first two steps and CHCl₃/MeOH/AC (76:20:4, v/v/v) for the last step (migration distance 30 mm). The HPTLC plates were automatically vacuum dried for 1.5 min and conditioned in an acetic acid (4M) atmosphere prior to each development. The post-chromatographic derivatization (immersion of the plates in aqueous CuSO₄/H₃PO₄ solution for 20 s and charring in an oven at 150 °C for 20 min) revealed grey-brown bands. The peak areas from densitometric scans of the plates (CAMAG TLC Scanner 3) in absorbance mode (λ=546 nm) were used for quantification. The software used was CAMAG winCATS Planar Chromatography Manager (Camag, Muttenz, Switzerland).

5.2.2.5. *In vitro* Release and Penetration of Oat CERs

5.2.2.5.1. Preparation of Dodecanol-Collodion Model Membrane

A model membrane system consisting of dodecanol and collodion was prepared by spreading 100 g of a membrane solution over a glass surface (50 cm × 30 cm) using a film applicator with adjustable clearance. The film was allowed to dry in a fume hood overnight, removed from the glass surface and cut into 40 mm diameter discs. The membrane solution (100 g) was prepared by mixing 50 g of 4% (*w/w*) collodion solution with 50 g of 8% (*w/w*) dodecanol mixture (dodecanol/octanol/DMSO, 8:1:1, *v/v*) in diethylether/ethanol (8.5:1.5, *v/v*).

5.2.2.5.2. *In vitro* Release and Penetration Studies

The multi-layer membrane model described earlier [313] was used to investigate the *in vitro* release and penetration of oat CERs from various formulations. The model comprises circular 40 mm penetration cells arranged one over the other in a penetration cell stand. Each cell consists of a covering plate, a stencil, four layers of membrane films and a base plate. The formulation (an amount equivalent to 50 µg of total oat CERs) was uniformly spread through the stencil (with a square opening of 4 cm² at the centre) which was kept above the upper membrane and the whole cell was covered by the covering plate. A nitrocellulose film was placed between the lower membrane and the base plate to prevent any possible adhesion. The cells were kept at 32 °C in a thermostatic chamber for predetermined time intervals (15, 30 and 60 min) allowing release and penetration of oat CERs. The cells were taken out, the unabsorbed formulation over the surface of the top membrane was removed by a cotton swab, the membranes were separated and the oat CERs in each layer as well as remained unabsorbed were extracted with 1 mL (3 mL for the cotton swab) of *n*-hexane/ethanol (2:1, *v/v*) (with sonication at 40 °C for 30 min) in test tubes. The extracts were dried under nitrogen stream at 40 °C and the dried residues were re-dissolved in CHCl₃/MeOH (1:1, *v/v*) (4 mL was used for cotton swab and the top layer and 2 mL for the three bottom layers). The samples were filtered through 0.45 µm syringeless filters (Whatman Mini-UniPrep™, Dassel, Germany) and the amount of oat CERs was quantified by an LC/APCI-MS method. One-way ANOVA (*p* < 0.05) followed by Tukey's test as post hoc analysis was used to indicate the existence of significant differences between sets of data.

5.2.2.6. *Ex vivo* Skin Permeability Studies

The diffusion set up described in section 4.2.2.7.2 was used for the *ex vivo* permeation studies of oat CERs. The permeation of oat CERs into the skin was investigated using an excised human skin in which the subcutaneous tissue was mechanically dissected and discarded. Circular piece of skin (2 cm in diameter, 3.14 cm²) was punched, wrapped in tin foil, sealed in an occlusive polyethylene bag and stored at -20 °C. At the time of investigation, the skin specimen was defrosted at room temperature and mounted on a Franz diffusion cell with the SC side facing the donor compartment. The dermal side of the skin and the acceptor compartment were separated by filter gauze. The acceptor compartment contained 20 mL of distilled water and the hydrodynamics was maintained by continuous stirring. The cell was kept at 32 °C using circulating water. A defined amount of each formulation (ca. 20 mg) containing 0.25% of total oat CERs was applied evenly on the outer surface of the skin. The permeation experiments were carried out for 300 min. Following the incubation period, the formulation remaining on the surface of the skin was carefully removed by a cotton swab and three 6 mm diameter discs (0.2827 cm²) were cut out using a Kromayer punch. The discs were sectioned into different slices using a cryo-microtome. While the upper two 10 µm thick slices represent the SC, the next four 20 µm thick slices were considered as viable epidermal layer (EP). Each of the DR sub-layers (DR1 to 3) were represented by five 40 µm thick slices. The lipids in each skin layer and the remaining piece of tissue of the skin was extracted with 1 mL of *n*-hexane/ethanol (2:1, v/v) overnight, filtered through 0.45 µm syringe filter and dried under nitrogen stream at 40 °C. The dried lipid extract was re-dissolved in 0.25 mL of CHCl₃/MeOH (1:1, v/v) and the amount of oat CERs was quantified by LC/APCI-MS. The cotton swab and the filter gauze were extracted with 5 and 2 mL of *n*-hexane/ethanol (2:1, v/v), respectively, and treated like the skin slices. The liquid collected from the acceptor compartment (20 mL) was freeze-dried. The freeze-dried residue was dissolved in 2 mL of CHCl₃/MeOH (1:1, v/v), filtered through 0.45 µm syringe filter, dried under nitrogen stream at 40 °C, re-dissolved in 0.25 mL of CHCl₃/MeOH (1:1, v/v) and analyzed. The amounts of oat CERs obtained from the three punch biopsies of each skin slice and the remaining skin tissue (amount/0.2827 cm²), filter gauze, acceptor fluid and the cotton swab were used to calculate the total oat CERs recovered. The nominal amount of oat CERs applied to the skin (amount/3.1416 cm²) was used to calculate the extraction recovery (%). The amount of oat CERs obtained from each slice was used to calculate the percent permeability of oat CERs. Prior to the *ex vivo* permeability studies, an ethical

clearance was obtained from the Ethics Committee of the Faculty of Medicine, Martin Luther University. One-way ANOVA ($p < 0.05$) followed by Tukey's test as post hoc analysis was used to indicate the existence of significant differences between sets of data.

5.2.2.7. LC/APCI-MS

The amounts of oat CERs released and penetrated across the artificial multi-layer membrane and excised human skin were quantified by the LC/APCI-MS method developed and validated earlier (section 4.2.2.4).

5.3. Results and Discussion

5.3.1. Preparation and Characterization of Formulations

PhytoCERs were proposed to be an alternative source of CERs for the formulation of products improving skin hydration and reinforcing the skin barrier [288, 299]. Among the several plants we have investigated qualitatively and quantitatively, oat was found to be a good alternative source of GlcCERs [288, 306]. As reported earlier [306], the two predominant oat GlcCER species were Glc-d18:1^{Δ8}/h16:0 and Glc-d18:1^{Δ8}/h20:0. For plant GlcCERs intended for direct SC delivery, cleavage of the glycosidic linkage is inevitable. Therefore, oat GELF (which contains mainly oat GlcCERs) was subjected to acid treatment to cleave the sugar moiety. The resulting oat CERs enriched fraction was standardized against pure oat CERs. The oat CERs enriched fraction containing ca. 25% of total oat CERs was used for the preparation of the various formulations. Among the SC CERs, the d18:1^{Δ4}-based CERs (particularly CER [AS] with h16:0 and h20:0) are isobaric or isomeric with oat CERs.

The depth and extent of skin permeation depend upon different factors including the delivery system used and the components of the formulation. Different formulation approaches including colloidal carriers such as MEs have been designed to overcome the protective barrier of the SC and deliver CERs into the skin [123, 124]. The formulations are designed to enhance the permeation of CERs into the SC and deliver the CERs at the SC-SG interface. At the same time, the formulations should also control the penetration of CERs into the deeper layers of the EP and DR. NPs are the other nanocarriers which are shown to be useful for delivering lipophilic drugs into the SC, retarding their permeation into the deeper skin layers, as they control the drug release and act as reservoirs of the drugs [261].

It has been shown that lecithin-based SAAs enhance the solubility and penetration of CER [AP] into the SC [127]. Besides, phosal® 75 SA, miglyol® 812 and water/1,2-pentanediol mixture were also shown to be the preferred SAA, oily and hydrophilic phases, respectively for the preparation of stable LBMEs containing CERs with high loading capacity. Therefore, in the current study these ingredients were used for the formulation of oat CERs containing oil in water (O/W) MEs. Under cross-polarized light microscope, the MEs were clear systems that appeared as dark background. The viscosity, droplet size and stability profile of the MEs are presented in Table 5.2. Although all the MEs had relatively lower viscosities, those MEs with higher amounts of SAA demonstrated higher viscosities. All the ME formulations exhibited Newtonian type of flow which is typical characteristic of MEs [126, 127]. The droplet size of the MEs was determined without diluting the formulations to avoid the possible change in the microstructure of the MEs as suggested by Sahle *et al.* [127]. For all the MEs, the apparent diffusion coefficients (from which the size of the ME droplets was determined using Stokes-Einstein equation) obtained at various angles (30, 40, 50, 60 and 70°) showed no significant difference and, hence, the average and RSD of the droplet diameter was taken. The angular independence of the diffusion coefficients suggest that ME droplets are spherical in shape [123, 126, 127]. The PCS results were also used as a means of identifying the nanostructure of MEs. Unlike droplet MEs, bicontinuous (BC) MEs were shown to have a very high pseudo-droplet diameter and RSD which was attributed to the dynamics and structural alterations of the BC channels. Besides, the apparent diffusion coefficients of BC MEs vary with the scattering angles [123, 126, 127]. Both features were not observed in the current oat CER MEs i.e., they are O/W MEs. All the LBMEs containing oat CERs were stable over a period of one year; no evidence of sedimentation of droplets or precipitation of the oat CERs was observed.

Table 5-2: Viscosity, refractive index, droplet size and stability of oat CERs O/W MEs (n = 3).

MEs	Viscosity (% RSD) (mPa s)	Refractive Index (RSD)	Droplet Size (% RSD) (nm)	Stability (Months)
LBME1	43.6 (0.308)	1.442 (0.000)	195.0 (5.9)	> 12
LBME2	51.1 (0.469)	1.444 (0.000)	184.8 (12.8)	> 12
LBME3	59.4 (0.429)	1.448 (0.000)	196.0 (7.6)	> 12

On the other hand, oat CER NPs were fabricated following previously optimized emulsification-solvent evaporation method [228] using acetylated cassava starch and Pluronic® F127 as polymer and SAA, respectively. The physicochemical properties of cassava have been characterized elsewhere [312]. The granule size of cassava starches obtained from different sources ranged from 11 to 15 μm . The scanning electron microscope (SEM) images of native cassava starch showed spherical granules. The SEM images of SAs with three different DS (1.74, 2.15 and 2.72) are given in Fig. C1, Appendix C. Upon acetylation, the starch granules were disrupted and fused together [314]. This effect is more pronounced at higher degree of acetylation. These SAs were used for the preparation of oat CER NPs. The particle size, PDI, EE and LC of the NPs containing oat CERs are presented in Table 5.3. As can be seen from the results, the oat CER EE and LC of SA increased drastically with an increase in the DS. Previously SAs with high DS have been used for the fabrication of NPs [228, 255, 310, 311]. They are suitable for controlled release applications due to their hydrophobic nature and film-forming properties [247-251]. The NPs prepared from SA with DS 2.72 also exhibited lower PDI compared to the NPs prepared from SAs with medium DS (1.74). Similar finding was also reported elsewhere [228]. Therefore, SA with high DS (2.72) was used for the preparation of NP gel.

Table 5-3: Particle size, PDI, oat CERs EE and LC of SA NPs (n = 3).

NPs	Particle size (nm) (SD)	PDI (SD)	EE (% w/w) (SD)	LC (% w/w) (SD)
SANP-DS 1.74	159.4 (0.829)	0.262 (0.010)	2.2 (0.8)	0.03 (0.01)
SANP-DS 2.15	175.3 (1.799)	0.204 (0.017)	23.1 (4.9)	0.24 (0.05)
SANP-DS 2.72	161.8 (2.854)	0.171 (0.004)	85.2 (1.9)	0.88 (0.02)

Since the MEs and the aqueous NPs dispersions possess a low viscosity, they need to be incorporated into convenient topical dosage forms to obtain the desired semisolid consistency [123, 315]. Previously, ME gels [123] and NP gels [260, 315-317] were prepared to provide appropriate characteristics for cutaneous application. Therefore, both oat CERs containing MEs and NPs were incorporated into Carbopol®980-based gel systems to provide the required rheological characteristics and for targeted delivery of oat CERs into the SC of the skin. During incorporation of the nanocarriers into the semisolid systems, any possible interactions between the formulation ingredients can potentially affect the semisolid consistency of the formulations [315]. Therefore, the rheological properties of the gel

formulations (ME gel and NP gel) were investigated and compared with a pure gel containing water instead of the NPs dispersion.

For all the gel formulations, first strain sweep measurements were made and the results are depicted in Fig. 5.1. All formulations showed linear deformation behavior (i.e., moduli were independent of the strain amplitude) below ca. 10 % and a strong decrease in modulus (shear thinning behavior) above the critical strain level (non-linear range). Below the critical strain level, the structure of the gel formulations is intact, they behave solid-like, and storage modulus $G' > \text{loss modulus } G''$.

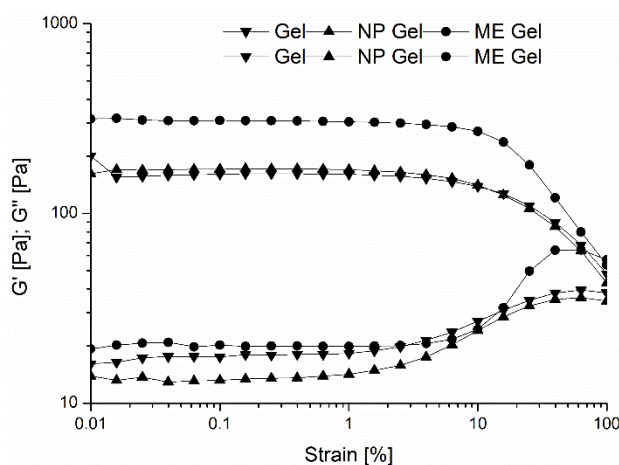


Figure 5-1: Strain sweep of gel formulations at 25 °C after a week of storage (0.01 - 100 % at 10 rad/s).

Therefore, a deformation amplitude of 1 % was selected for the next frequency sweep (i.e., measurement with varying frequency at fixed amplitude) in the linear range from which the storage modulus G' and loss modulus G'' were obtained. As shown in Fig. 5.2, the storage modulus G' was higher than the loss modulus G'' in all of the formulations i.e., the samples behave as elastic gels. However, the modulus values were low (ca. 100 - 200 Pa) showing that the formulations are very soft gels. Over the range of angular frequencies from 100 to 0.1 rad/s the G' values showed a weak frequency dependence indicating that the systems are within the gel state, above the threshold for the critical gel. The G' values of pure gel and NP gel were very similar suggesting the compatibility of the formulation ingredients in the NP gel. However, the G' values for ME gel were clearly higher than the pure and NP gels by about a factor of 1.5.

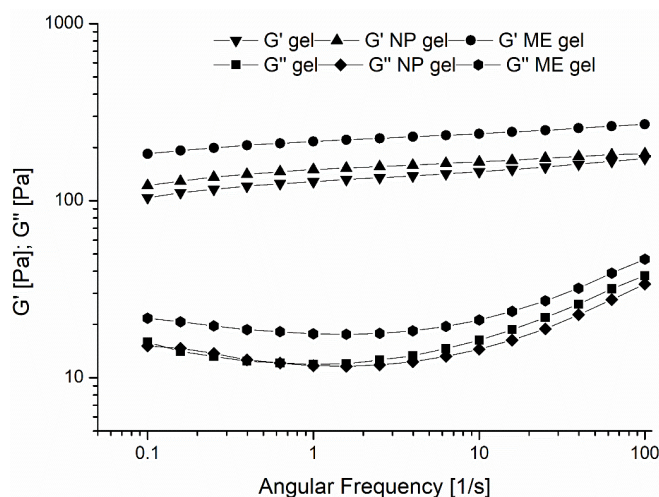


Figure 5-2: Frequency sweep for the gel formulations (G' and G'' as a function of angular frequency at 1% strain measured at 25 °C after a week of storage).

After a month of storage, the oscillatory shear experiments under small deformation (1%) showed similar results for the NP gel. On the other hand, the ME gel showed about three times smaller G' and G'' values than the values after a week of storage. However, the formulation still exhibited gel-like behavior with dominating elastic modulus i.e., the real part of modulus G' was higher than the imaginary part G'' .

The results of the shear stress and viscosity at different shear rates showed a strong shear thinning behavior, i.e. the viscosity decreases with increasing shear rate and the shear stress grows slower than linearly with shear rate (Fig. 5.3 and Fig. 5.4). The large shear deformation destroyed some internal structure in the samples. But in all cases the traces of shear stress for increasing and decreasing shear rate overlap with only minor difference. The gel formulations, therefore, didn't exhibit thixotropic behavior (at least on the time scale of 5 s). The incorporation of NP dispersions also didn't modify the kind of flow exhibited by the pure gel i.e., the non-Newtonian behavior of the gel.

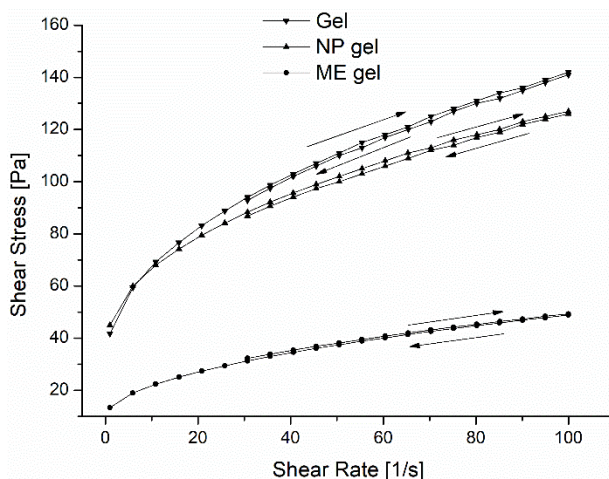


Figure 5-3: Hysteresis loop of the gel formulations (shear stress a function of shear rate measured at 25 °C after a month of storage).

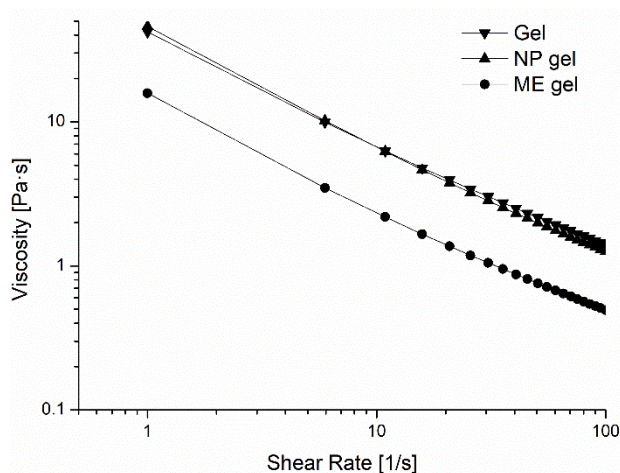


Figure 5-4: Viscosity versus shear rate for gel formulations (at 25 °C after a month of storage).

In an attempt to suggest appropriate formulation strategies to deliver oat CERs into the SC, these gel formulations as well as their corresponding ME and NP suspension were used for further *in vitro* release and penetration and *ex vivo* permeation studies. The formulations, therefore, include ME (LBME1), ME gel (LBME1 gel), NPs (CSANP-DS 2.72), NP gel (CSANP-DS 2.72 gel) and an amphiphilic cream (reference formulation). In all the formulations, the final concentration of oat CERs was 0.25%.

5.3.2. *In vitro* Release and Penetration of Oat CERs

The CERs incorporated into the various topical dosage forms have to be released and penetrate the SC barrier before reaching the target lipid lamellae at the SC-SG interface. A

system for modelling CER penetration and permeation into and through human skin, such as multilayer membrane model, is useful before conducting *ex vivo* and *in vivo* permeation studies. The *in vitro* release and penetration of oat CERs from the various formulations was carried out using a multi-layer membrane model described elsewhere [313]. The artificial membrane is composed of dodecanol as lipid and collodion as a matrix former. The dodecanol mixture used in the preparation of the membrane contains 10 % octanol and 10 % DMSO. While the former provides membrane stability, the later enhances the solubility of CERs in the membrane reducing the number of membranes needed to maintain the sink condition [126, 127].

The release and penetration of oat CERs from the five formulations specified earlier are depicted in Fig. 5.5. The release and penetration of oat CERs from the ME was higher than the amphiphilic cream and the NP/NP gel formulations. The *in vitro* penetration-enhancing effect of MEs has also been indicated in the earlier studies [126, 127]. Compared to the ME and cream, the release from the NPs was slower which can be attributed to the controlled release characteristics of the NPs. Furthermore, minute quantities of oat CERs incorporated in the NP gel formulation penetrated into the lower layers of the multi-layer membranes. This could be explained by the high viscosity of the NP gel.

Formulation and Skin Permeation Studies

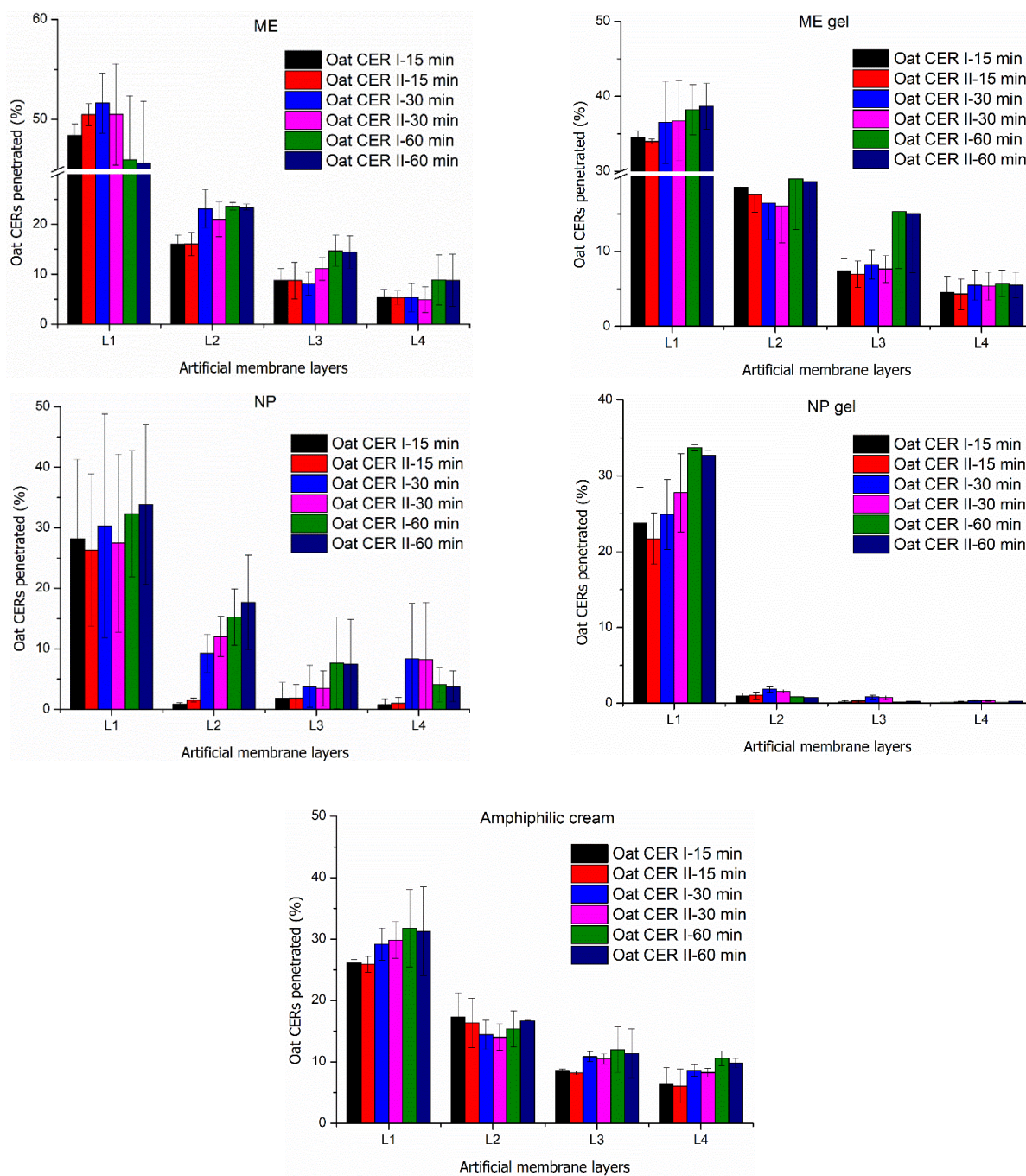


Figure 5-5: Release and penetration of oat CERs into the artificial multilayer membranes from various formulations

The total oat CERs release and penetration profile from the various formulations is shown in Table 5.4. As can be seen from the Table, over 90 % of oat CERs incorporated in ME were released and penetrated into the four-layer membrane system after 60 min. When the ME was incorporated into gel, the amount of oat CERs released and penetrated in 60 min was

reduced to ca. 79 %. On the other hand, only 59 - 63 % oat CERs in the NPs were released and penetrated in 60 min, which was drastically reduced to 34 % in the NP gel system. Thus, the results showed that while ME improved the release and penetration of oat CERs into the model membrane, the NPs retarded the release of oat CERs.

.Table 5-4: Total oat CERs released and penetrated (%) into the four-layer membrane system at three different incubation periods (15, 30 and 60 min) (n = 3).

Formulations	Total oat CERs released and penetrated (%)					
	15 min		30 min		60 min	
	CER I	CER II	CER I	CER II	CER I	CER II
ME	78.7 (3.7)	80.6 (5.2)	88.3 (7.3)	83.7 (5.2)	93.2 (1.9)	92.3 (2.7)
ME gel	65.1 (1.2)	62.9 (1.6)	66.7 (10.0)	65.8 (9.8)	79.0 (3.3)	78.6 (3.2)
NP	31.6 (16.6)	30.7 (15.6)	51.8 (15.1)	51.2 (11.0)	59.4 (11.3)	62.8 (15.0)
NP gel	25.0 (8.1)	23.3 (4.0)	29.5 (2.3)	30.4 (5.3)	34.8 (0.3)	34.0 (0.5)
Cream	58.3 (0.2)	56.6 (2.2)	63.1 (3.5)	62.6 (3.9)	69.7 (9.3)	69.1 (9.8)

5.3.3. *Ex vivo* Permeability of Oat CERs

In attempt to repair the skin barrier, prevent moisture loss and increase the skin hydration level, CERs have been included in several commercial topical products. Even though CER-containing products have been proliferating on the market in recent years, there are limited clinical evidence showing the depth and extent of permeation of the exogenous CERs into the skin [308]. Few reports have shown the transport of exogenous CERs in *ex vivo* human skin [123, 124]. It has been shown that the depth and extent of permeation of CER [NP] from the various types of MEs are dependent on the nanostructure and viscosity of the formulations [123]. ME gels were also prepared to increase the viscosity of the MEs thereby reducing the depth of CER [NP] penetration into the deeper layers of the skin.

The permeation profile of oat CERs into *ex vivo* human skin from the five formulations is depicted in Fig. 5.6. The *ex vivo* skin permeation of oat CERs loaded into ME and NPs and the corresponding gel formulations was compared with the reference formulation (amphiphilic cream) over a period of 300 min. The extraction recovery were found to be

87.4%, 87.2%, 90.1%, 95.7% and 88.0% for the ME, ME gel, NPs, NP gel and the reference cream, respectively.

As can be seen in Fig. 5.6, the ME enhanced the permeation of oat CERs into the SC and other layers of the skin compared to the cream and the gel formulations. Higher amounts of oat CERs were found in the acceptor compartment from ME suggesting the need to use more viscous systems to reduce the depth of penetration and to target the upper part of the skin. ME gel has reduced the permeation of oat CERs into the deeper layers of skin compared to the ME. As compared to NP gel, however, ME gel enhanced the degree of permeation of oat CERs into the deeper layer of the skin. This is also in agreement with *in vitro* penetration results where the ME gel had a better penetration-enhancing effect compared to NP gel. The NP gels are interesting carriers for targeting the upper layer of the skin as they act as reservoirs for the controlled release of CERs into the SC. They retain the CERs in the upper layer of the skin without increasing transdermal transport. The high specific area of the NPs also facilitates the contact of the encapsulated actives with the SC [258, 260]. The depth of penetration and extent of transport of actives from NPs into the skin depend on several factors including size, formulation viscosity and encapsulation mechanism [261]. Further investigations are, therefore, needed to establish their use in delivery of CERs into the SC of the skin.

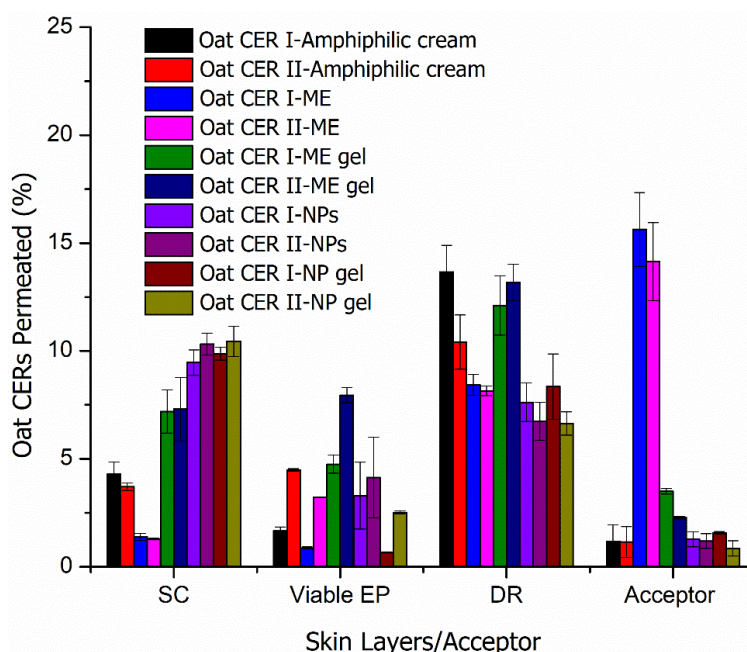


Figure 5-6: Percentage of oat CERs permeated into different layers of the skin from the various formulations: SC (SC1 + SC2), viable EP (EP1 + EP2), DR (DR1 + DR2 + DR3 + remaining skin tissue) and acceptor (filter gauze + acceptor fluid).

In a previous study done elsewhere [123], during quantification of CER [NP] in the various skin layers, the SC was represented by 10 tape strips. In our case, however, two 10 μm thick skin slices were considered as SC which allowed us measure the sectional skin concentrations of oat CERs normalized to the thickness of the skin slices. Fig. 5.7 depicts the skin thickness normalized distribution of oat CERs across the various skin layers (the amounts of oat CERs (ng) per thickness of the skin slices (μm)). As can be seen from the figure, the oat CERs in the gel formulations of both ME and NP were able to penetrate the SC barrier and concentrate in the primary target site of the skin i.e., the SC. On the other hand, the oat CERs in the ME have permeated into the deeper layers of the skin and higher amount of oat CERs was found in the acceptor compartment. Thus, the deepest permeation was obtained from ME, whereas the gel formulations were effective in reducing the depth of permeation.

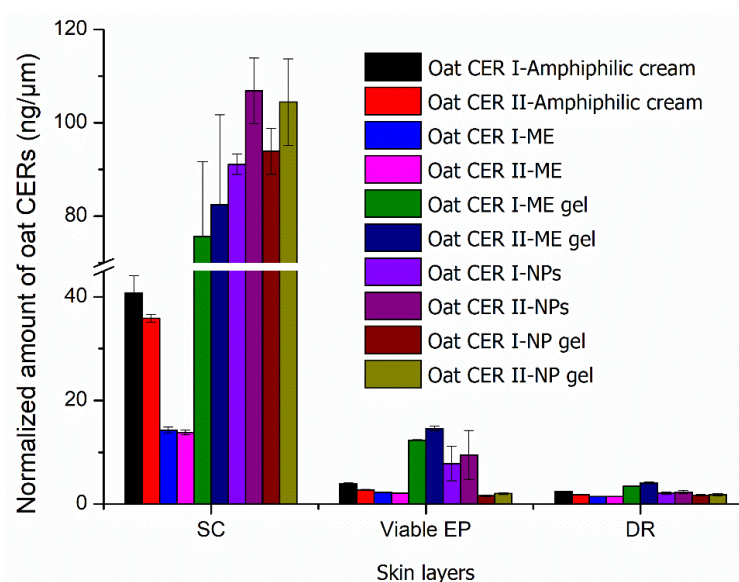


Figure 5-7: Skin thickness normalized distribution of oat CERs across the various skin layers (SC: $2 \times 10 \mu\text{m}$ thick slices, viable EP: $4 \times 20 \mu\text{m}$ thick slices and DR: $15 \times 40 \mu\text{m}$ thick slices).

5.3.4. Conclusions

With the objective of delivering oat CERs into the SC of the skin, MEs and NPs as well as the corresponding gels were formulated and characterized. The mean droplet size of the MEs was between 185 - 196 nm. The NPs prepared from SA with high DS (2.72) exhibited high EE and LC with mean particle size of 162 nm. While MEs display Newtonian type flow, the gel formulations containing ME and NPs exhibited non-Newtonian pseudoplastic type of flow. The *in vitro* studies have shown that the extent of release and penetration of oat CERs from the various formulations over an hour depend on the type of formulation. The ME was shown

to improve the penetration of oat CERs into the multilayer membrane compared to the other formulations. On the other hand, the NP and the NP gel sustained the release of oat CERs, the effect being more pronounced in the gel formulation by virtue of its viscosity. The results of *ex vivo* permeability of oat CERs from the ME and NPs were also in consistent with the *in vitro* results. Similar to the *in vitro* artificial membrane, oat CERs from ME gel have shown better extent of permeation compared to the NP gel in the *ex vivo* human skin. The skin layers thickness normalized permeability revealed the accumulation of oat CERs from the gel formulations in the SC. Therefore, they can be used as means of localizing the CERs into the upper epidermal layers. However, further optimization of the formulations is suggested to reduce the penetration of oat CERs into the deeper layers of the skin. In conclusion, this study provided an insight into the skin permeation profile of oat CERs which is crucial to demonstrate their potential use in improving the barrier of diseased and/or aged skin.

6. Summary

CERs play a crucial role in the skin barrier function and skin hydration. Some skin diseases such as psoriasis and AD, and ageing are associated with depleted CER levels and altered CER compositions. The depleted skin CERs can potentially be substituted by topical delivery of skin-similar CERs obtained from semi-synthetic or biotechnological sources. The commercial CERs are, however, expensive and, hence, cheaper CERs are needed. Plants are interesting alternative sources of CERs for topical formulations intended to reinforce the impaired skin barrier. The present work, therefore, aimed at exploring alternative CERs from plants and delivering them into the skin using nanocarriers. The workflow involved isolation, structural characterization, quantification and formulation of PhytoCERs and investigation of their permeation into the skin.

LC-MS/MS and AMD-HPTLC methods were used for the qualitative and quantitative analyses of GlcCERs isolated from four plants (grass pea, Ethiopian mustard, haricot bean and oat). The plants were found to contain four types of C18 di/trihydroxy SBs (d18:2, d18:1, d18:0 and t18:1) amide-linked to C14-C24 hydroxy FAs. While the dihydroxy SBs were coupled to short chain FAs, the trihydroxy SBs were acylated with VLCFAs (C22-C24). The predominant GlcCERs in grass pea, Ethiopian mustard and haricot bean were found to be Glc-d18:1/h16:0, Glc-t18:1/h24:1 and Glc-d18:2/h16:0, respectively. All oat GlcCERs consisted of C18 dihydroxy SBs, the two predominant species being Glc-d18:1/h16:0 and Glc-d18:1/h20:0. The predominant GlcCER species identified in the four plants have similar structural features with the commercial plant GlcCERs such as soybean, rice and wheat GlcCERs. The quantitative analysis showed oat grain has the highest amount of total GlcCERs compared to the other seeds and the content is also comparable to the GlcCER contents in the commercial plant sources. Therefore, oat was selected for further investigations.

Since the GlcCERs are not suitable for direct SC targeting, the sugar moiety of oat GlcCERs was cleaved chemically (by strong acid treatment) and the predominant oat CERs were purified. The production of oat CERs was confirmed by LC/APCI-MS, ESI-HRMS and NMR analyses. Prior to incorporating oat CERs into the various topical formulations, an LC/APCI-MS method for quantitative analysis of oat CERs in skin permeation studies was developed and validated using a well characterised oat CERs (d18:1/h16:0 and d18:1/h20:0) as reference standards. The method was shown to be sensitive (with LOD and LOQ of 10 and 30ng/mL, respectively), selective, precise, accurate and applicable to the intended purpose.

This method was used for the quantification of oat CERs during the *in vitro* release and penetration and *ex vivo* skin permeation studies.

The two principal oat CERs were incorporated into two types of nanocarriers namely MEs and NPs and the formulations were characterized. The mean droplet size of the MEs was between 185 - 196 nm. Generally, the MEs had low viscosity and exhibited Newtonian type of flow. On the other hand, NPs prepared from SA with high DS (2.72) showed high EE and LC with mean particle size of 162 nm. Since the MEs and the aqueous NPs dispersions possess a low viscosity, gel formulations containing the ME and the NPs were also prepared using Carbopol®980 as a gelling agent to acquire the required consistency for topical applications. The gel formulations exhibited non-Newtonian pseudoplastic flow behavior (shear thinning systems). The incorporation of NP dispersions did not modify the kind of flow exhibited by the pure gel devoid of the NPs.

The release and penetration of oat CERs from four formulations (ME, ME gel, NPs, and NP gel) was assessed *in vitro* using a four-layer membrane model over 60 min and the results were compared with an amphiphilic cream. The ME enhanced the release and penetration of oat CERs into the various layers of the membrane compared to the other formulations. The slowest release was obtained from the NP gel which could be explained by the controlled release properties of NPs and the high viscosity of the formulation. The depth and extent of permeability of oat CERs was also investigated *ex vivo* using excised human skin mounted on Franz diffusion cell. Similar to the *in vitro* results, ME enhanced the permeation of oat CERs into the skin. The normalized percent permeability (normalized to skin thickness) showed the accumulation of oat CERs in the upper layer of the skin, particularly in the SC. This effect is more pronounced in the NP/NP gel formulations. This is interesting as the oat CERs are needed to be delivered into the SC. Therefore, the gel formulations are promising in localizing the SC lipids into the upper epidermal layers and reducing the depth of permeation. However, further optimization of the formulations is suggested to reduce the penetration of the oat CERs into the deeper skin layers. In conclusion, this study encompassing qualitative and quantitative analyses of PhytoCERs as well as their incorporation into nanocarriers has provided the first insight into the direct delivery of PhytoCERs into the SC of the skin. Besides, the extraction and purification protocols, the LC/APCI-MS/MS and AMD-HPTLC methods used in this work have been proven to be robust and reliable and they can be used for isolation, structural characterisation and quantification of GlcCERs from other plants.

7. Zusammenfassung

Ceramide (CER) spielen eine entscheidende Rolle bei der Funktion der Hautbarriere und der Hauthydratation. Einige Hauterkrankungen wie Psoriasis und atopische Dermatitis und Alterung sind mit abnehmenden CER-Spiegeln und veränderten CER-Zusammensetzungen verbunden. Die dezimierten Haut-CER können potentiell durch topische Abgabe von hautähnlichen CER aus semisynthetischen oder biotechnologischen Quellen ersetzt werden. Die kommerziellen CER sind jedoch teuer und daher sind günstigere Varianten von Interesse. Pflanzen sind interessante alternative Quellen von CER für topische Formulierungen, die die beeinträchtigte Hautbarriere verstärken sollen. Die vorliegende Arbeit zielte daher darauf ab, alternative CER aus Pflanzen (PhytoCER) zu untersuchen und diese mithilfe von Nanoträgersystemen in die Haut abzugeben. Der Arbeitsablauf beinhaltete Isolierung, strukturelle Charakterisierung, Quantifizierung und Formulierung von PhytoCER und Untersuchung ihrer Permeation in die Haut.

Flüssigchromatographie mit Tandem-Massenspektrometrie-Kopplung (LC-MS/MS) und Automatisierte Mehrfachentwicklungs-Hochleistungs-Dünnschichtchromatographie (AMD-HPTLC) Methoden wurden für die qualitative und quantitative Analyse von aus vier Pflanzen isolierten Glucosylceramide (GlcCER) (Graserbse, äthiopischer Senf, Bohne und Hafer) eingesetzt. Es wurde herausgefunden, dass die Pflanzen vier Typen von C18-Di/Trihydroxy-Sphingoid-Basen (d18:2, d18:1, d18:0 und t18:1) amidverknüpft an C14-C24-Hydroxy-Fettsäuren enthalten. Während die Dihydroxy-Sphingoid-Basen an kurz-kettige Fettsäuren gekoppelt wurden, wurden die Trihydroxy-Sphingoid-Basen mit sehr langkettigen Fettsäuren (C22-C24) acyliert. Die vorherrschenden GlcCER in Graserbse, äthiopischem Senf und Haricotbohne waren Glc-d18:1/h16:0, Glc-t18:1/h24:1 bzw. Glc-d18:2/h16:0. Alle Hafer GlcCER bestanden aus C18-Dihydroxy-Sphingoid-Basen, wobei die beiden vorherrschenden Spezies Glc-d18:1/h16:0 und Glc-d18:1/h20:0 waren. Die vorherrschenden GlcCER-Spezies, die in den vier Pflanzen identifiziert wurden, haben ähnliche strukturelle Merkmale wie die kommerziellen pflanzlichen GlcCER, wie GlcCER aus Sojabohnen, Reis und Weizen. Die quantitative Analyse ergab, dass Haferkorn im Vergleich zu den anderen Samen die höchste Menge an Gesamt-GlcCER aufweist und der Gehalt auch mit den GlcCER-Gehalten in kommerziellen Pflanzenquellen vergleichbar ist. Daher wurde Hafer für weitere Untersuchungen ausgewählt.

Da die GlcCER nicht für ein *stratum corneum* (SC)-Targeting geeignet sind, wurde die Zuckereinheit von Hafer-GlcCER chemisch abgespalten (durch eine starke Säurebehandlung) und die verbleibenden Hafer-CER aufgereinigt. Die Produktion von Hafer-CERs wurde durch LC-MS-, Hochauflösende Massenspektrometrie (HRMS)- und NMR-Analysen bestätigt. Vor der Einarbeitung von Hafer-CER in die verschiedenen topischen Formulierungen wurde eine LC-MS-Methode zur quantitativen Analyse von Hafer-CER in Hautpermeationsstudien entwickelt und mit Hilfe gut charakterisierter Hafer-CER (d18:1/h16:0 und d18:1/h20:0) als Referenzstandards validiert. Die gewählte Methode war empfindlich (mit Nachweisgrenze und Bestimmungsgrenze von 10 bzw. 30 ng/ml), selektiv, präzise, genau und auf den beabsichtigten Zweck anwendbar. Diese Methode wurde für die Quantifizierung von Hafer-CER während der *In-vitro*-Freisetzung sowie für die Penetrations- und *Ex-vivo*-Hautpermeationsstudien verwendet.

Die beiden wichtigsten Hafer-CER wurden in zwei Nanosystemen, Mikroemulsionen (ME) und Nanopartikel (NP), inkorporiert und charakterisiert. Die mittlere Tropfengröße der ME betrug zwischen 185 - 196 nm. Im Allgemeinen hatten die ME niedrige Viskosität und zeigten newtonisches Fließverhalten. Andererseits zeigten NP, welche aus Stärkeacetat mit hohem Substitutionsgrad (2.72) hergestellt wurden, hohe Verkapselungseffizienz und Beladungskapazität, bei mittlerer Partikelgröße von 162 nm. Da die ME und wässrige NP-Dispersionen eine niedrige Viskosität besitzen, wurde für die Herstellung von Gelformulierungen, die die ME und NP enthielten, Carbopol®980 als Gelbildner verwendet, um die erforderliche Konsistenz für topische Anwendungen zu erhalten. Die Gelformulierungen zeigten nicht-newtonisches pseudoplastisches Fließverhalten (scherverdünnende Systeme). Das Fließverhalten wurde durch Einbringen der NP-Dispersionen im Vergleich zu reinem Gel ohne NP nicht verändert.

Die Freisetzung und Penetration von Hafer-CER aus vier Formulierungen (ME, ME gel, NP und NP-Gel) wurden *in vitro* in einem Vierschicht-Membranmodell über 60 min untersucht und die Ergebnisse mit einer amphiphilen Creme verglichen. Die ME verbessern die Freisetzung und Penetration der Hafer-CER in die verschiedenen Schichten der Membran im Vergleich zu den anderen Formulierungen. Die langsamste Freisetzung zeigte das NP-Gel, was mit den Eigenschaften der kontrollierten Freisetzung aus den NP und der hohen Viskosität der Formulierung erklärt werden kann. Die Tiefe und das Ausmass der Permeabilität der Hafer-CER wurde auch *ex vivo* an Ausschnitten menschlicher Haut auf einer Franz'schen Diffusionszelle untersucht. Gleich den Ergebnissen der *in vitro*

Untersuchung verbesserten ME das Eindringen der Hafer-CER in die Haut. Die normalisierte prozentuale Permeabilität (normalisiert im Bezug auf die Dicke der Haut) zeigte die Anreicherung von Hafer-CER in den oberen Hautschichten, besonders im SC. Dieser Effekt ist bei den NP- und NP-Gel-Formulierungen stärker ausgeprägt. Da die Hafer-CER in das SC eingebracht werden müssen, ist dies besonders interessant. Somit sind Gelformulierungen vielversprechend zum gezielten Einbringen der SC-Lipide in die oberen Hautschichten und Verringern der Eindringtiefe. Dennoch werden weitere Optimierungen der Formulierungen benötigt, um das Eindringen der Hafer-CER in tiefere Hautschichten zu Verringern. Zusammenfassend hat diese Studie, die qualitative und quantitative Analyse der PhytoCER umfasst, einen ersten Einblick in die direkte Verabreichung von PhytoCER in das SC der Haut geliefert. Weiterhin haben sich die in dieser Arbeit verwendeten Vorschriften der Extraktion und Aufreinigung, sowie die LC-MS/MS- und AMD-HPTLC-Methoden als verlässlich herausgestellt und können zur Isolierung, strukturellen Charakterisierung und Quantifizierung von GLcCER anderer Pflanzen verwendet werden.

8. Outlook

The topical delivery of PhytoCERs is an interesting area of research. This is the first attempt of delivering PhytoCERs into the SC of the skin using nanocarriers. Therefore, it opens a room for research in the field in the future. The followings would be interesting for future investigations to document the dermal efficacy of topically administered PhytoCERs:

- Further *ex vivo* and *in vivo* studies are needed to provide supporting evidence for the skin health benefits of oat CERs. The roles of PhytoCERs in epidermal barrier function need to be investigated in animal models as well as human skin.
- The molecular arrangement of oat CERs and other PhytoCERs in the SC nanostructure is still to be investigated. *In vitro* studies can be carried out by using neutron and x-ray diffraction studies. This will give an insight into the influence of structural variations of PhytoCERs on the morphology of the lipid structure and the possibility of mimicking the structure and function of the natural skin barrier. The results can be compared with the native skin CERs.
- As GlcCERs containing d18:2 and t18:1 SBs are prone to allylic-rearrangements and chemical degradations under strong acidic conditions, enzymatic hydrolysis of these GlcCERs should be investigated.
- As PhytoCERs exist mainly in glycosylated form, the possibility of delivering CER precursors like GlcCERs into the viable layers of EP as a way to correct the reduced CER level in the SC could also be investigated as an alternative strategy.

9. Appendices

Appendix A: Isolation, Structural Characterization and Quantification of GlcCERs

I. Screening of Plants

Table A1 shows the list of plants collected from Ethiopia and screened for their for GlcCER contents.

Table A1: Plants screened for their GlcCER contents and TLC-based preliminary screening results.

Botanical Name	Common/Local Name	Family	Source	GlcCERs*
<i>Avena abyssinica</i>	Oat	Poaceae	LM, Holleta Area	++
<i>Lathyrus sativus</i>	Grass pea/Guaya	Fabaceae/Leguminosae	Debrezeit ARC, EIAR	++
<i>Brassica carinata</i>	Ethiopian Mustard	Cruciferae/Brassicaceae	Holleta ARC, EIAR	++
<i>Phaseolus vulgaris</i>	Haricot beans	Fabaceae/Leguminosae	Melkassa ARC, EIAR	++
<i>Acacia decurrens</i>		Fabaceae/Leguminosae	EFRC	++
<i>Acacia saligna</i>		Fabaceae/Leguminosae	EFRC	++
<i>Acacia senegal</i>		Fabaceae/Leguminosae	EFRC	+
<i>Acacia seyal</i>	White whistling thorn	Fabaceae/Leguminosae	EFRC	++
<i>Acacia tortilis</i>		Fabaceae/Leguminosae	EFRC	++
<i>Leuceana leucocephala</i>	Leucaena	Fabaceae/Leguminosae	EFRC	++
<i>Sesbnia aculeata</i>	Dhaincha	Fabaceae/Leguminosae	EFRC	++
<i>Faidherbia albida</i>	Ana tree/Grar	Fabaceae/Leguminosae	EFRC	+
<i>Parkinsonia aculeata</i>	Palo verde/Filfile	Fabaceae/Leguminosae	EFRC	+
<i>Millettia ferruginea</i>	Birbira	Fabaceae/Leguminosae	EFRC	+/-
<i>Linum usitatissimum</i>	Flaxseed/Linseed	Linaceae	LM, Addis Ababa	-
<i>Sorghum bicolor</i>	Sorghum/Zengaga	Poaceae	LM, Asella	+/-
<i>Eleusine coracana</i>	Finger-millet/Dagusa	Poaceae	LM, Asella	-
<i>Sesamum indicum</i>	Sesame	Pedaliaceae	LM, Asella	+
<i>Moringa stenoptala</i>	Moringa (kernel)	Moringaceae	LM, Asella	+/-
<i>Cucurbita maxima</i>	Pumpkin	Cucurbitaceae	LM, Asella	-

LM: local markets in Ethiopia; ARC: Agricultural Research Center; EIAR: Ethiopian Institute of Agricultural Research; EFRC: Ethiopian Forestry Research Center. *++ Visible band on the TLC plate, + not strong band, +/- unclear, - no visible band at the applied concentrations. All the plants were collected from Ethiopia. The seeds were used for extraction except Moringa (kernel was used).

II. Extraction and Purification

A scheme showing the extraction and purification of plant GlcCERs is depicted in Fig. A1. Successive purification of total lipid extracts with liquid-liquid extraction ($\text{CHCl}_3/\text{MeOH}/\text{H}_2\text{O}$ (1:1:1)) and silica gel column chromatography (gradient elution from 100% CHCl_3 to $\text{CHCl}_3/\text{MeOH}$ (8:2)) resulted in GELFs.

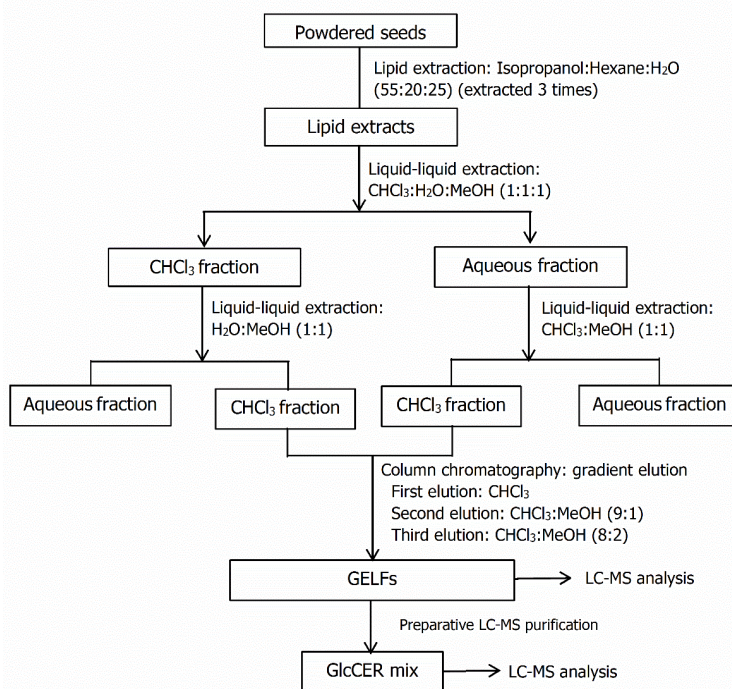


Figure A1: Scheme for extraction and purification of plant GlcCERs.

The TLC chromatograms of GELF of grass pea, Ethiopian mustard and haricot bean are shown in Fig. A2. Both qualitative and quantitative analyses of plant GlcCERs have been made from the GELFs of the extracts.

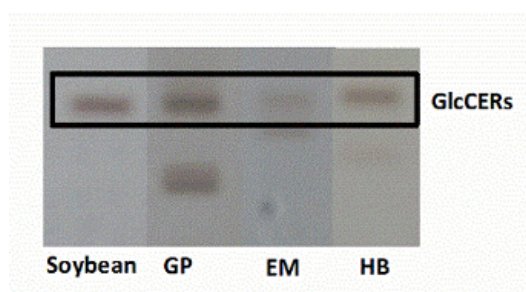


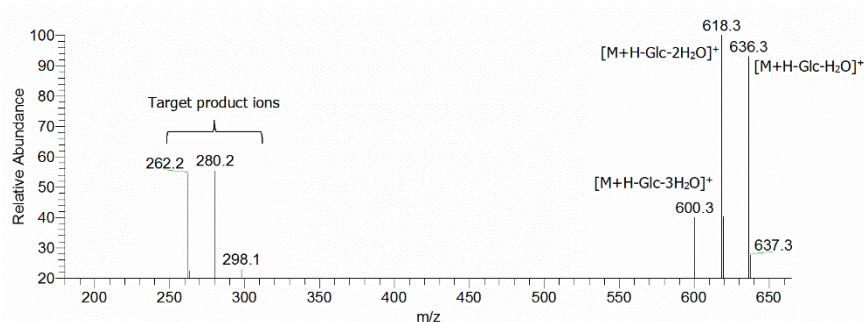
Figure A2: TLC chromatograms of GELFs of grass pea (GP), Ethiopian mustard (EM) and haricot bean (HB). Soybean GlcCERs was used as a reference standard.

III. Structural Characterization of Plant GlcCERs

GlcCERs can readily form protonated ions ($[M+H]^+$) in a positive-ion mode. These ions are very labile and readily lose Glc (those with C4-hydroxylated SBs) or water (those with C4-desaturated SBs) molecule to become $[M+H-162]^+$ or $[M+H-18]^+$ ion in the ion source, respectively. These ions were subjected to MS/MS analysis for further fragmentations resulting in the fragment ions corresponding to characteristic of the SBs. Representative tandem mass spectra of grass pea, Ethiopian mustard and haricot bean GlcCERs are depicted in Fig. A3. GlcCERs with trihydroxy bases exhibited the three possible product ions resulting from single, double and triple dehydration of the SBs. On the other hand, as GlcCERs containing d18:2^{A4,8} base are readily dehydrated/deglucosylated even at lower relative collision energy, the abundant ion detected during MS/MS analysis was $[M+H-Glc-2H_2O]^+$.

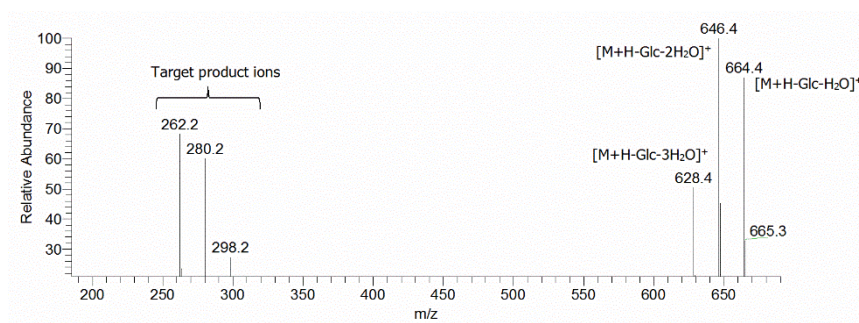
a) Grass pea-derived GlcCERs

- Representative GlcCER species: *Glc-t18:1/h22:0* (The ion subjected to MS/MS to detect the target product ion was $[M+H-Glc]^+$ m/z 654).



b) Ethiopian mustard-derived GlcCERs

- Representative GlcCER species: *Glc-t18:1/h24:0* (The ion subjected to MS/MS to detect the target product ion was $[M+H-Glc]^+$ m/z 682).



c) Haricot bean-derived GlcCERs

- Representative GlcCER species: Glc-d18:2/h16:0 (The ion subjected to MS/MS to detect the target product ion was $[M+H-H_2O]^+$ m/z 696).

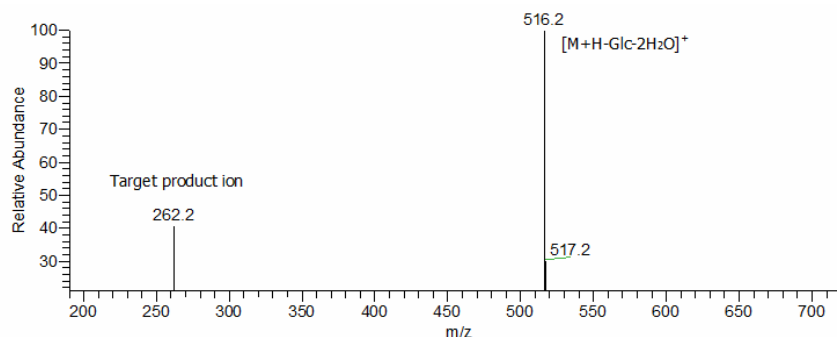


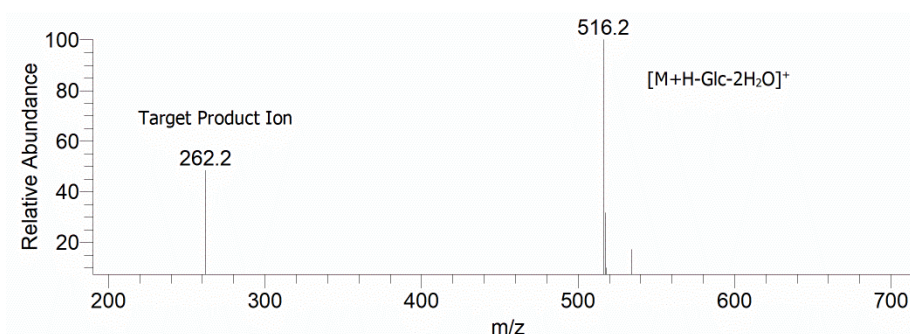
Figure A3: Representative tandem mass spectra of GlcCER fragments acquired under full scan mode (m/z 200 - 900) at a relative collision energy of 80%. (a): Representative grass pea GlcCER species with trihydroxy SB, Glc-t18:1/h22:0. The ion subjected to MS/MS to detect the target product ion was $[M+H-Glc]^+$ m/z 654. (b): Representative Ethiopian mustard GlcCER species with trihydroxy SB, Glc-t18:1/h24:0. The ion subjected to MS/MS to detect the target product ion was $[M+H-Glc]^+$ m/z 682. (c): Representative haricot bean GlcCERs species with di-unsaturated SB, Glc-d18:2/h16:0. The ion subjected to MS/MS to detect the target product ion was $[M+H-H_2O]^+$ m/z 696).

Oat-derived GlcCERs

The tandem mass spectra of oat GlcCERs at different scan modes are shown in Fig. A4.

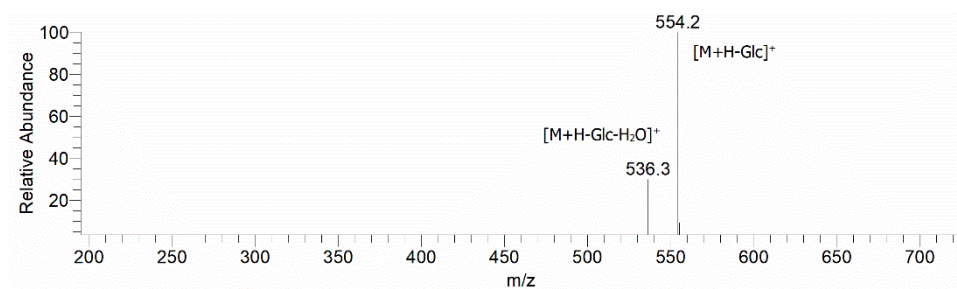
a) Glc-d18:2/h16:0

When $[M+H-H_2O]^+$ m/z 696 ion was subjected to MS/MS under full scan mode (m/z 200 - 725)

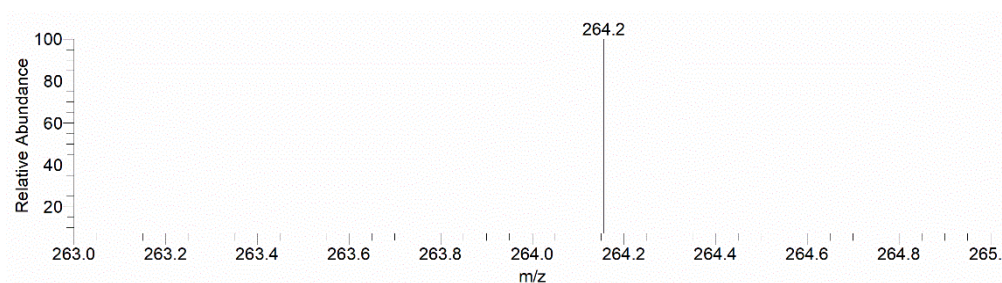


b) *Glc-d18:1/h16:0* (*m/z* 716)

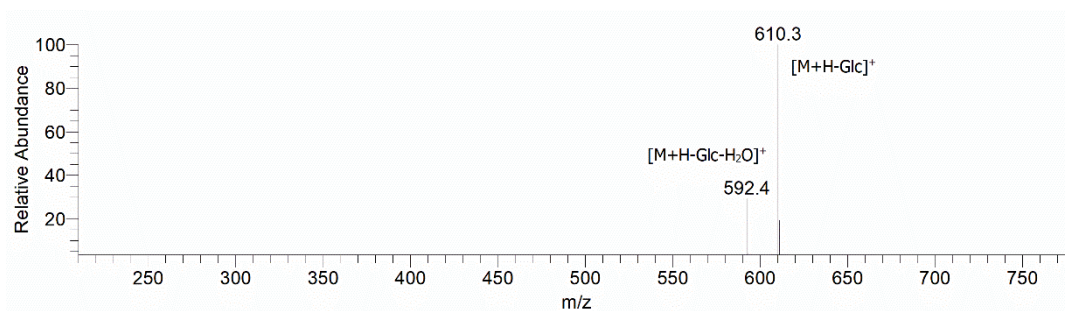
When $[M+H]^+$ ion was subjected to MS/MS under full scan mode (*m/z* 200 - 725)



When $[M+H]^+$ ion was subjected to MS/MS to detect the target product ion (*m/z* 264.3) under SRM scan mode

c) *Glc-d18:1/h20:0* (*m/z* 772)

When $[M+H]^+$ ion was subjected to MS/MS under full scan mode (*m/z* 200 - 800)



When $[M+H]^+$ ion was subjected to MS/MS to detect the target product ion (m/z 264.3) under SRM scan mode

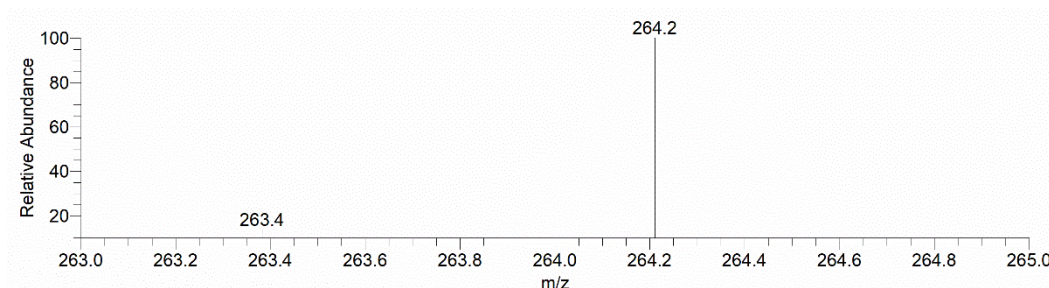


Figure A4: Representative tandem mass spectra of oat GlcCER fragments acquired at a relative collision energy of 80%. (a): oat GlcCER with di-unsaturated SB, Glc-d18:2/h16:0. The ion subjected to MS/MS to detect the target product ion was $[M+H-H_2O]^+$ m/z 696). (b) and (c) are the two predominant oat GlcCERs with C-4 saturated/C-8 unsaturated SBs. For these oat GlcCERs, SRM scan mode was used for the detection of selected target product ions.

Comparison of oat and haricot bean GlcCERs with standard soybean GlcCER

Among the plants investigated, two of them (oat and haricot bean) have GlcCER which is structurally similar to the standard soybean GlcCER (Glc-d18:2/h16:0) (Fig. A5). The base peaks at m/z 696 $[M+H-18]^+$ (A) and the mass spectra of the peak components (B) as well as the MS/MS fragmentation pattern (C) of the GlcCER species obtained from the three plants are shown in Fig. A6. The oat and haricot bean GlcCERs exhibited identical fragmentation patterns to the standard soybean GlcCER.

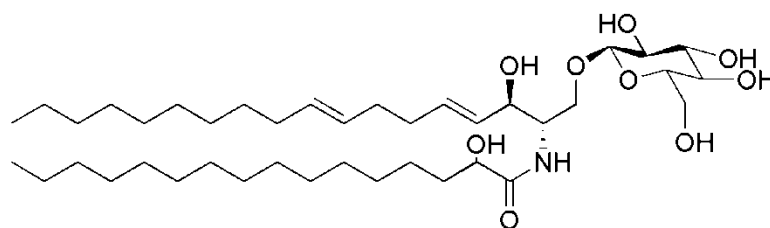


Figure A5: Representative structure of predominant soybean GlcCER (>98%)

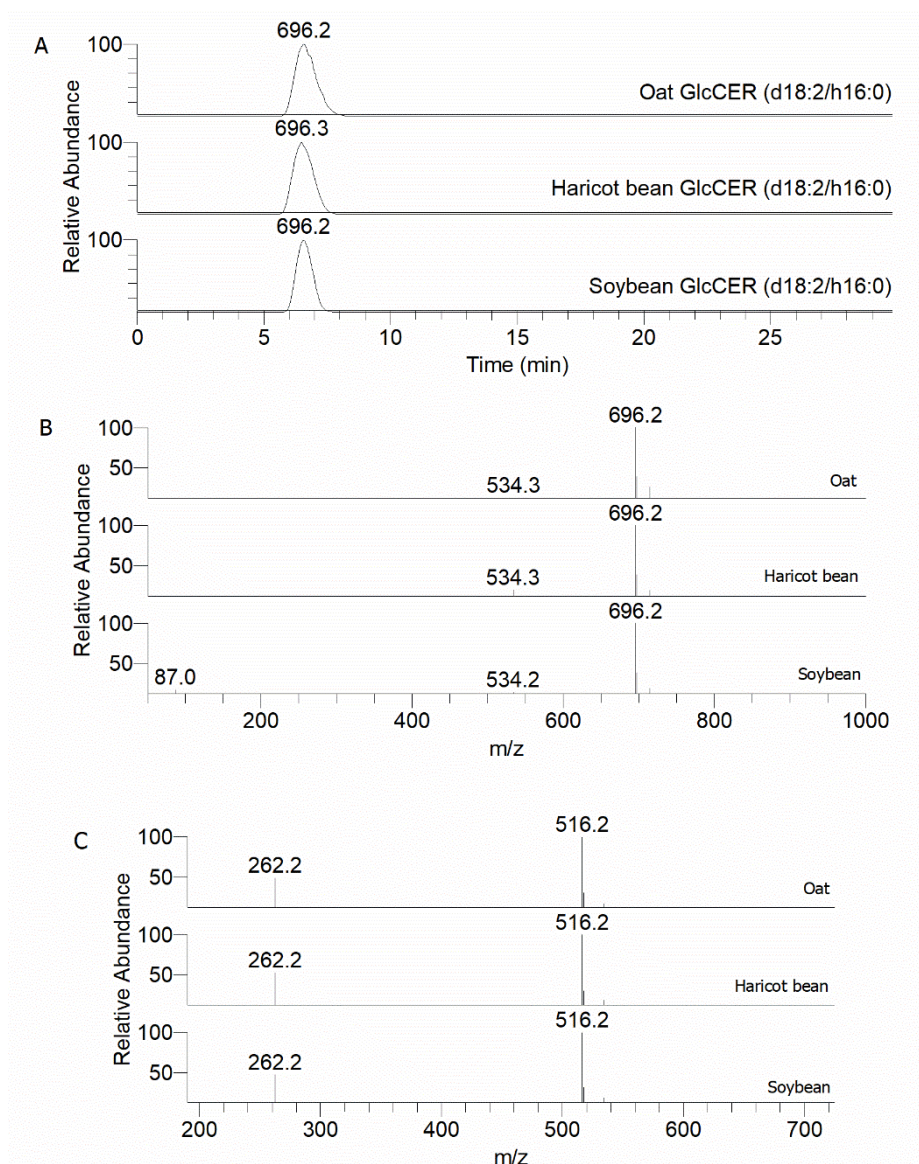


Figure A6: The base peaks at m/z 696 $[M+H-18]^+$ (A) and corresponding mass spectra (B) as well as the MS/MS fragmentation pattern at CID of 80% (C) of a GlcCER species (Glc-d18:2/h16:0) obtained from oat, haricot bean and the standard soybean GlcCER. The ion subjected to MS/MS was $[M+H-H_2O]^+$ m/z 696 as the parent ion was readily dehydrated in the ion source.

IV. Quantification of Plant GlcCERs by AMD-HPTLC

Calibration curve

The AMD-HPTLC method which was used for the quantification of plant GlcCERs was validated using soybean GlcCER reference standard. A representative calibration curve obtained from seven different concentrations of soybean GlcCER is shown Fig. A7.

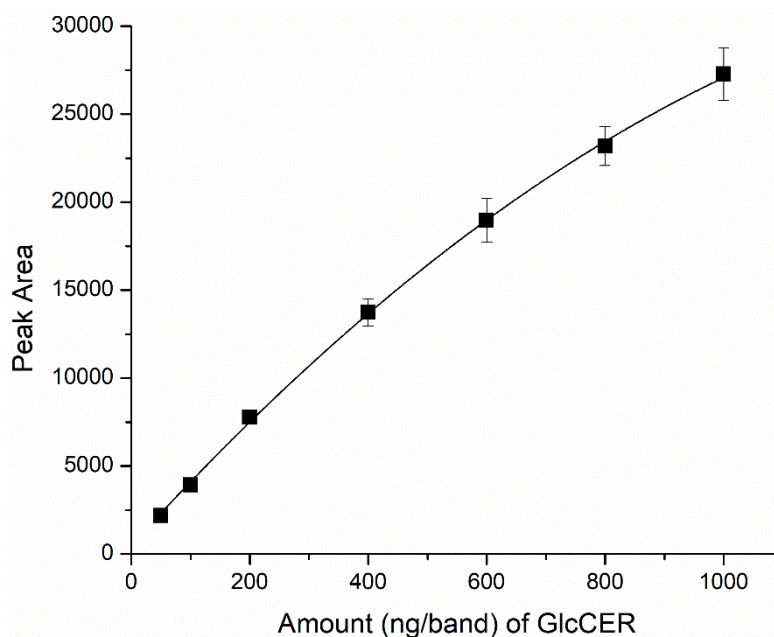


Figure A7: Calibration curve obtained from seven different concentrations (50 - 1000 ng/band) of soybean GlcCER reference standard applied to HPTLC plate (n = 5). The polynomial regression equation was $Y = -0.011X^2 + 37.24X + 453.13$ with a correlation coefficient (R^2) of 0.9996.

Quantification of GlcCERs in Acacia species

As GlcCERs occur widely in Fabaceae family, the GlcCER contents of five acacia species were quantified by AMD-HPTLC. The results are presented in Table A2.

Table A2: Amounts of total lipid extracts, CHCl₃ fractions, GELFs and GlcCERs in Acacia species.

Plants	Total lipid extract (g/kg)	CHCl ₃ fraction (g/kg)	GELF (mg/kg)	GlcCERs (mg/kg)
<i>Acacia decurrens</i>	126.3	16.0	299.6	94.5 (0.6)
<i>Acacia saligna</i>	146.4	33.2	116.1	84.8 (1.8)
<i>Acacia senegal</i>	61.4	11.4	126.8	54.7 (1.0)
<i>Acacia seyal</i>	116.9	31.7	1265.6	128.3 (4.8)
<i>Acacia tortilis</i>	134.3	16.6	332.6	70.2 (1.6)

The values in parentheses are the SD of the instrument readings (SD).

Appendix B: Production and Characterization of Oat CERs

I. Cleavage of Glucosidic Linkage (Deglucosylation)

A scheme showing the method for the cleavage of the sugar moiety of oat GlcCERs and the subsequent purification procedure is shown in Fig. B1. The oat CERs were purified by column chromatography using $\text{CHCl}_3/\text{MeOH}$ gradient elution. Alternatively, ethylacetate/MeOH gradient elution can also be used for the purification of oat CERs: first elution with ethylacetate (100%) followed by a second elution ethylacetate/MeOH (9:1).

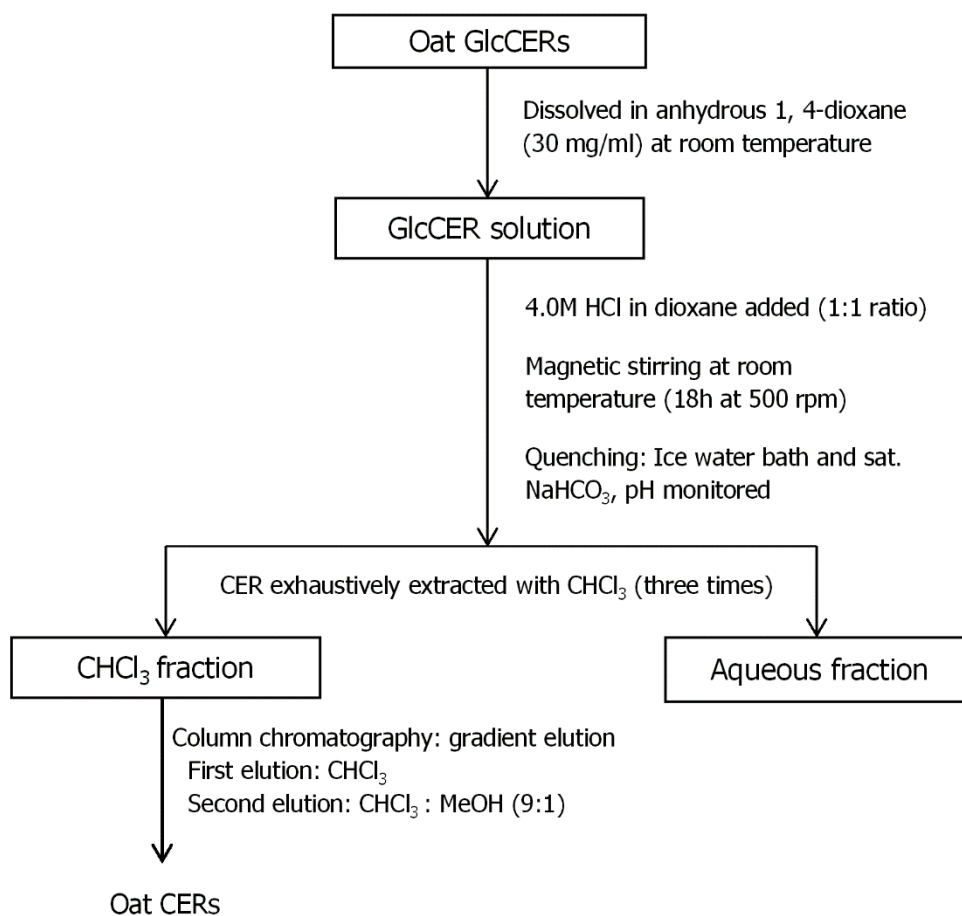


Figure B1: Scheme for the preparation and purification of oat CERs.

II. Strong acid-induced chemical alterations in the SBs of CERs/GlcCERs

Strong acidic conditions (mainly anhydrous acidic methanolysis and aqueous acidic hydrolysis) can result in stereo-chemical alterations such as isomerization (stereo-inversion, conversion of the natural *erythro*-isomer into the *threo* isomer in aqueous solution), allylic

rearrangements (formation of 3-O-methyl and 5-O-methyl ethers caused by the reaction of allylic alcohol group with solvents such as methanol in methanolic acids and formation of 5-hydroxy isomers and dienic compounds in aqueous systems) [290-295]. The possible chemical alterations and allylic-rearrangements are shown in Fig. B2.

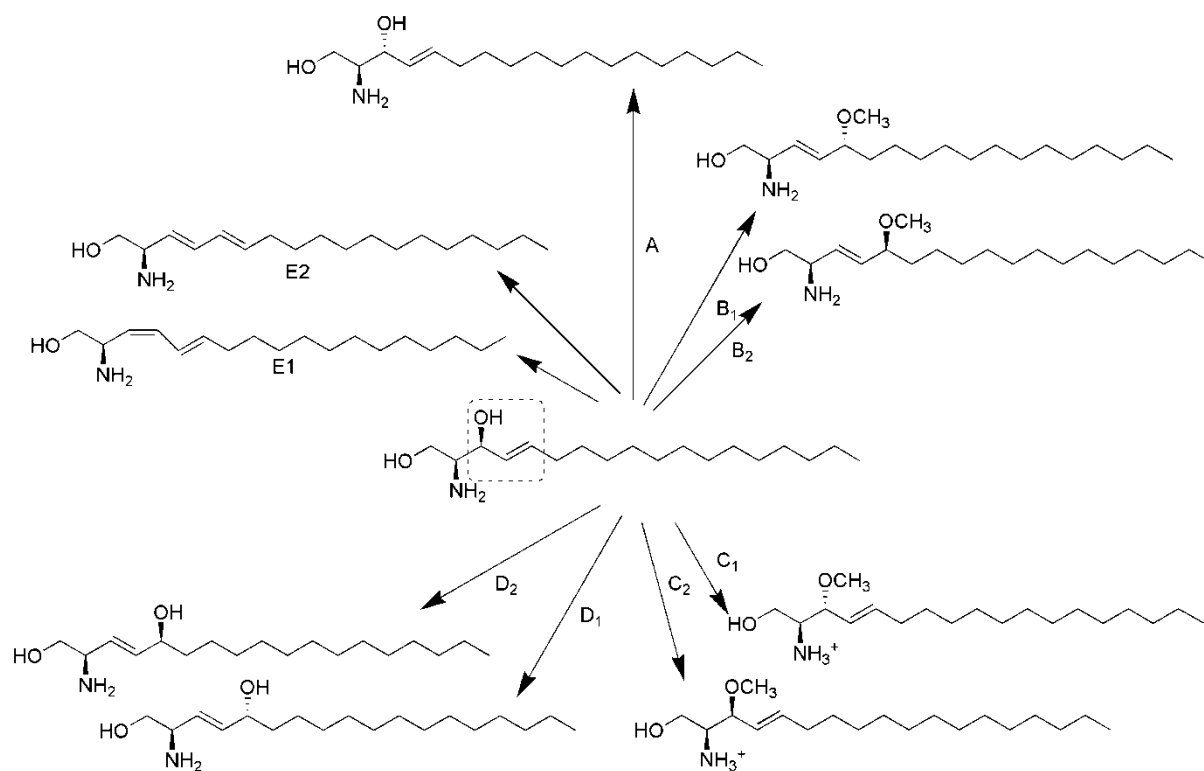


Figure B2: Scheme illustrating possible chemical alterations and allylic-rearrangements in the SBs of CERs and GlcCERs in methanolic and aqueous systems. A: stereo-inversion; B₁/B₂: 5-O-methyl ethers (5-methoxy-3-deoxy-sphing-3-ene); C₁/C₂: 3-O-methyl ethers (3-O-methylsphingosine); D₁/D₂: 5-hydroxy isomers and E₁/E₂: dienic compounds (up on dehydration) [294, 318]. Those derivatives with conjugated double bonds were suggested to be derived from the 5-hydroxy isomers.

III. Structural Characterization of Oat CERs

ESI-HRMS Spectra

The ESI-HRMS spectra of the two predominant oat CERs (d18:1/h16:0 and d18:1/h20:0) are depicted in Fig. B3 and Fig. B4.

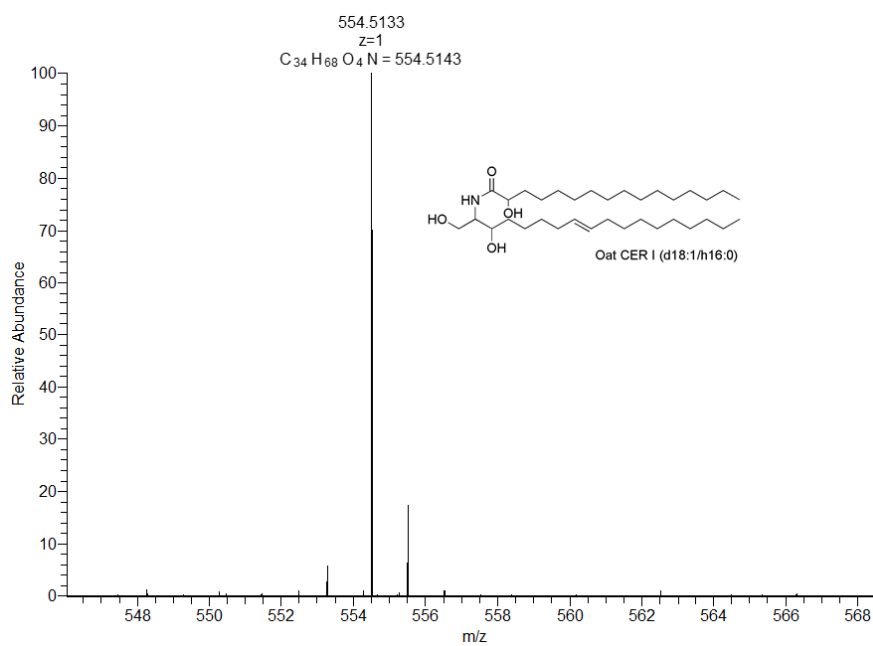


Figure B3: HR-MS spectrum of oat CER I obtained under positive mode

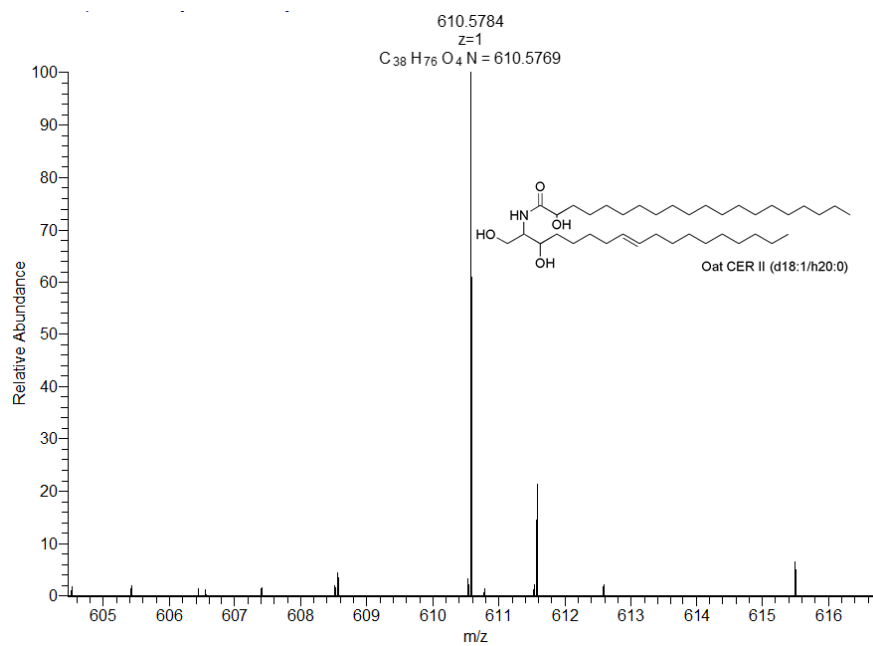


Figure B4: HR-MS spectrum of oat CER II obtained under positive mode

¹H NMR Spectrum

The ¹H NMR spectrum of oat CER I (d18:1/h16:0) is shown in Fig. B5.

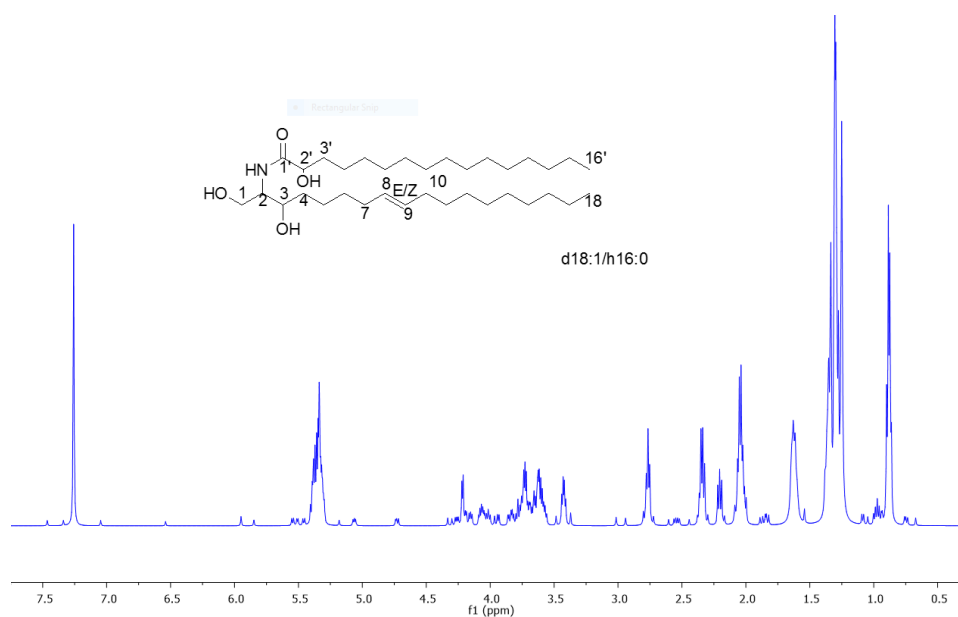


Figure 5B: ¹H NMR spectrum of oat CER (d18:1/h16:0).

¹³C NMR Spectrum

The ¹³C NMR spectrum of oat CER I (d18:1/h16:0) is shown in Fig. B6.

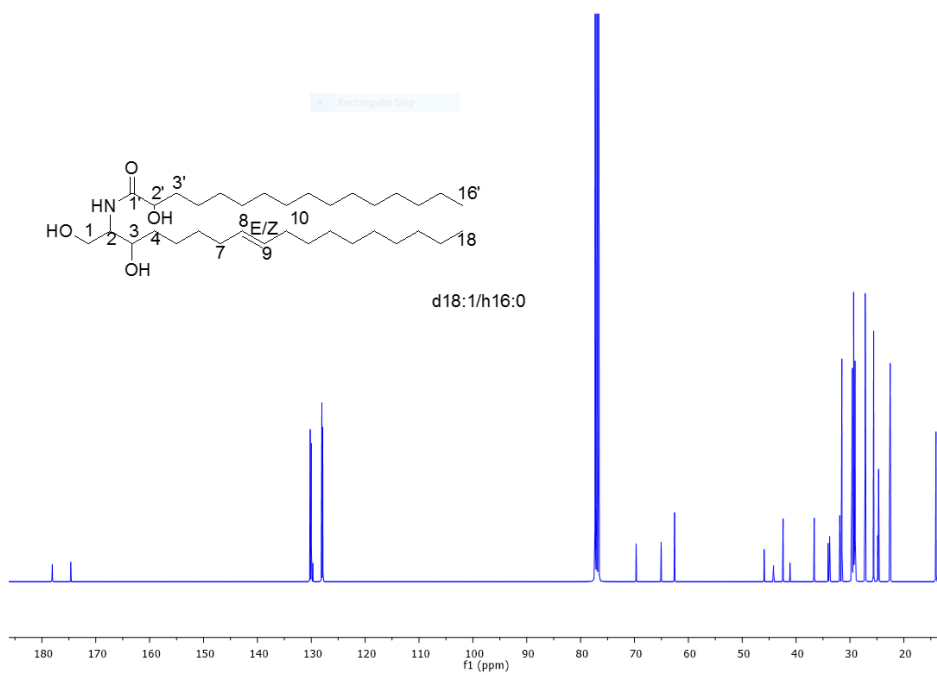


Figure B6: ¹³C NMR spectrum of oat CER (d18:1/h16:0).

^1H COSY spectrum

The ^1H COSY spectrum of oat CER I (d18:1/h16:0) is shown in Fig. B7.

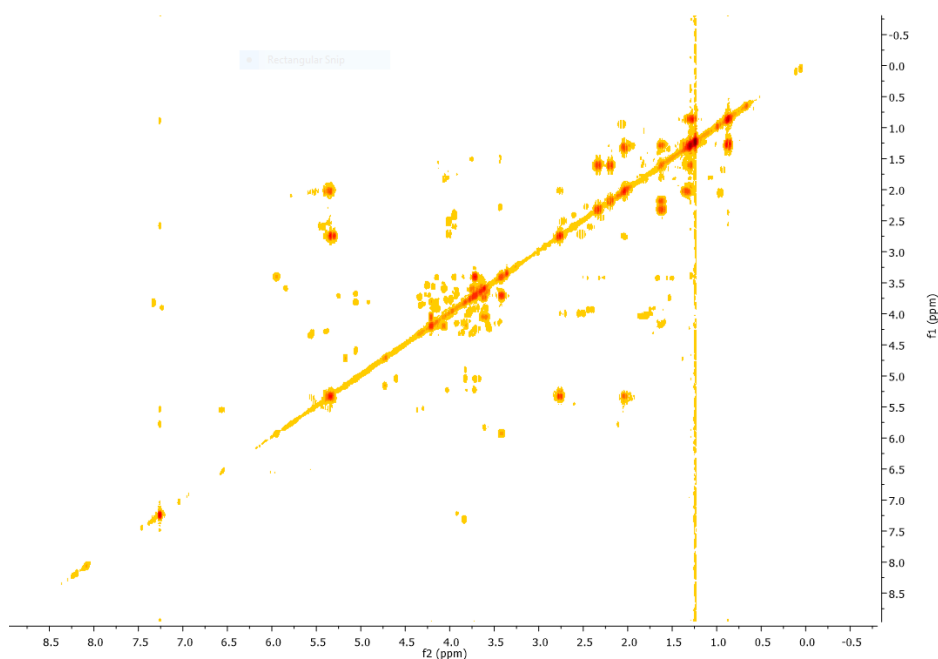


Figure B7: ^1H COSY spectrum of oat CER (d18:1/h16:0).

HMBC spectrum

The HMBC spectrum of oat CER I (d18:1/h16:0) is shown in Fig. B8.

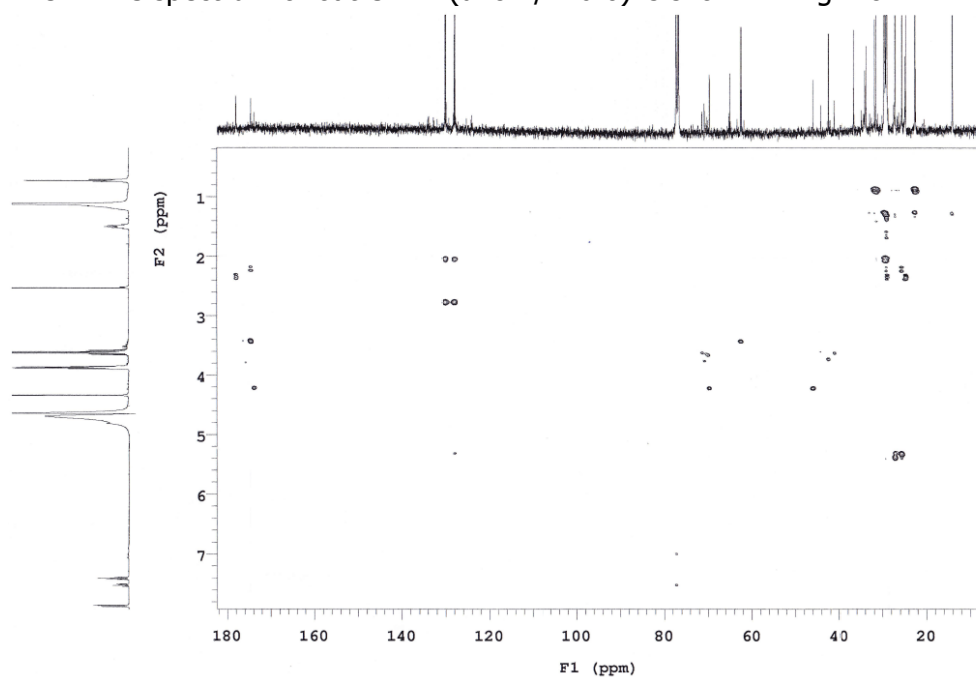


Figure B8: HMBC spectrum of oat CER (d18:1/h16:0).

Purity of Oat CERs

The HPLC-ELSD chromatogram of oat CER I (d18:1/h16:0) is depicted in Fig. B9.

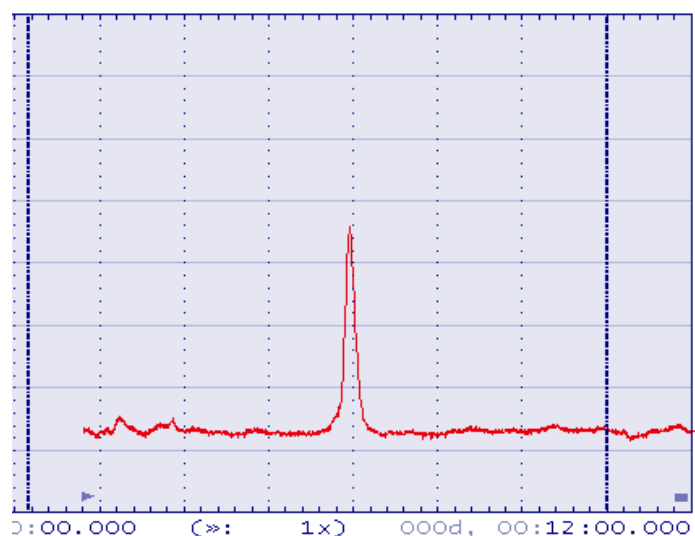


Figure B9: HPLC-ELSD chromatogram of oat CER (d18:1/h16:0)

IV. Sugar Analysis

Benedict's test for reducing sugars was used to confirm the existence of glucose cleaved from oat GlcCERs in the aqueous phase after the extraction of oat CERs with CHCl_3 . The brick red cuprous oxide precipitate confirmed the cleavage of the sugar moiety from the GlcCERs (Fig. B10).

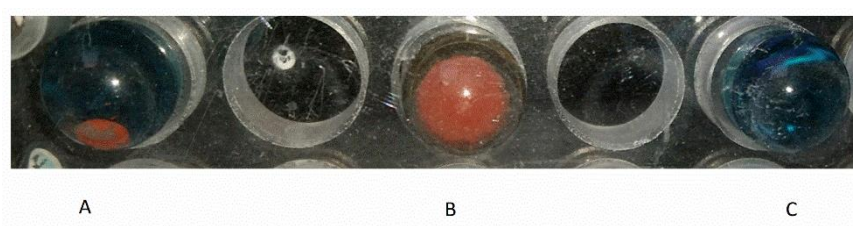


Figure B10: The bottom view of the brick red precipitate in test tubes during Benedict's testing for reducing sugars: (A) is the aqueous phase remaining after liquid-liquid extraction of oat CERs with CHCl_3 ; (B) is positive control (glucose solution) and (C) is negative control (distilled water).

Appendix C: Formulation of Oat CERs

SEM Images of Cassava SAs

The SEM images of acetylated cassava starch with three different DSs are given in Fig. C1.

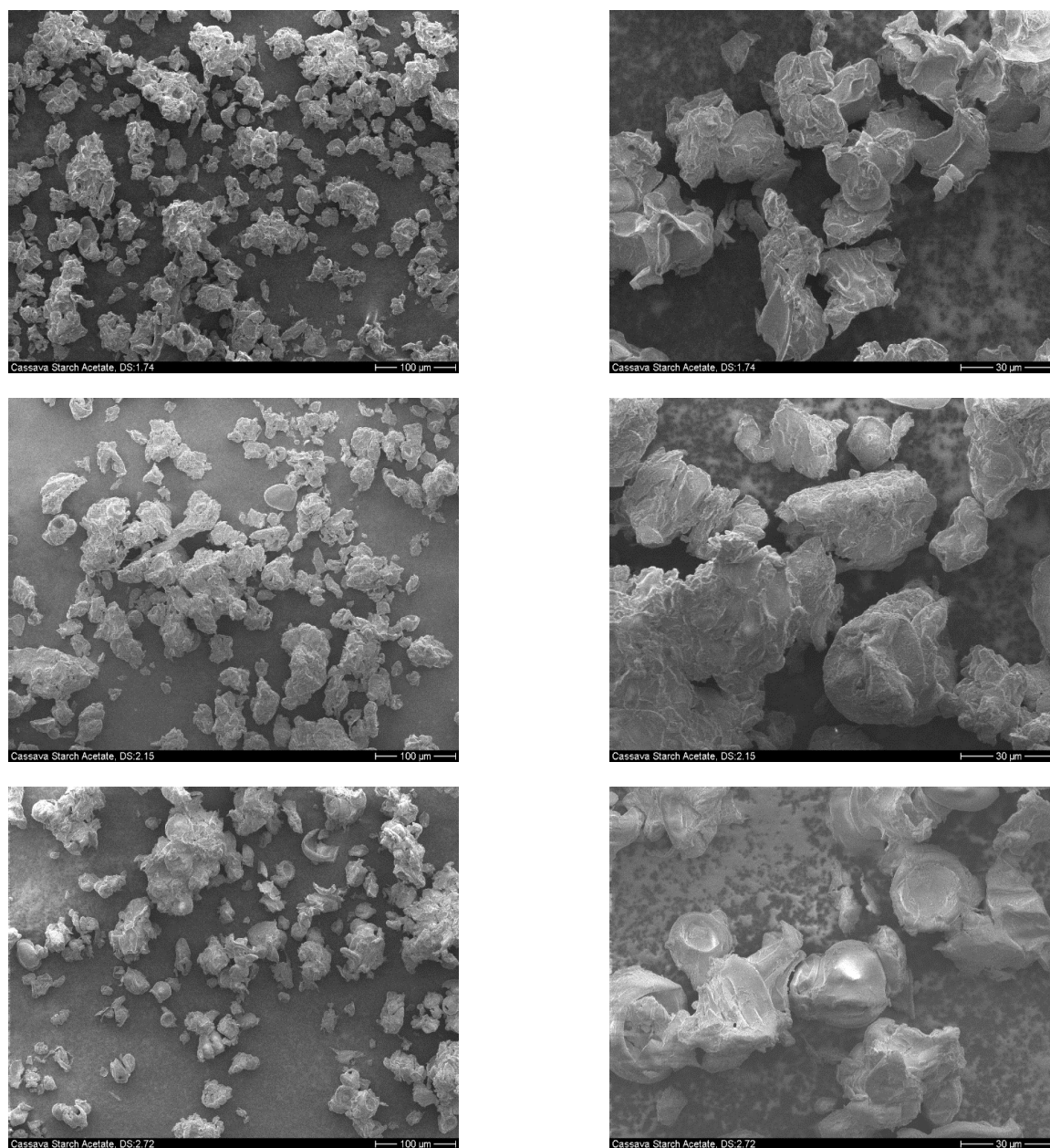


Figure C1: SEM images of acetylated cassava starch with different DS (1.74, 2.15 and 2.72).

List of Publications**Research Articles**

Tessema EN., Gebre-Mariam, T., Wohlrab, J., Neubert, R. H. H., Delivery of Oat CERs into the SC of the Skin using Nanocarriers: Formulation, Characterization and *in vitro* and *ex-vivo* Penetration Studies, *JID*, *ready for submission*.

Tessema EN., Gebre-Mariam, T. Frolov, A., Wohlrab, J., Neubert, R. H. H., Development and Validation of LC/APCI-MS Method for Quantification of Oat Ceramides in Skin Permeation Studies, *Anal Bioanal Chem*, *revised and being re-submitted*.

Tessema EN., Gebre-Mariam, T., Lange, S., Dobner, B., Neubert, R. H. H., Potential Application of Oat-derived Ceramides in Improving Skin Barrier Function: Part 1. Isolation and Structural Characterization. *J Chrom B*. 1065 - 1066 (2017) 87 - 95.

Tessema EN., Gebre-Mariam, T., Schmelzer, C. E.H., Neubert, R. H. H., Structural Characterization of Glucosylceramides from Ethiopian Plants by LC-APCI-MS/MS, *J Pharm Biomed Anal*. 141 (2017) 241 - 249.

Tessema EN., Gebre-Mariam, T., Neubert, R. H. H., Wohlrab, J., Potential Applications of Phyto-derived Ceramides in Improving Epidermal Barrier Function, *Skin Pharmacol Physiol*. 30(3) (2017) 115 - 138.

Poster presentation

Efrem N. Tessema, Tsige Gebre-Mariam, Reinhard H.H. Neubert, Potential Application of Oat Ceramides in Improving Skin Barrier Function. GRC, Barrier Function of Mammalian Skin 08/13/2017 - 08/18/2017, Waterville Valley Resort in Waterville Valley, NH, USA.

Acknowledgements

First I would like to express my deepest gratitude and appreciation to my supervisor Prof. Dr. Dr. h.c. Reinhard Neubert for his continuous support and scientific guidance throughout my stay. I appreciate your willingness to accept my request to join your working group and all the things you have done to me.

I am deeply grateful to my supervisor, Prof. Tsige Gebre-Mariam, for his guidance and constructive feedback for my PhD project starting from writing the proposal to submission of the thesis and thereafter. I will always be grateful to you for your scientific as well as personal advice, support, encouragement and positive influence in my life, in general.

I also thank Prof. Dr. Johannes Wohlrab for advising me on some key scientific aspects of my work.

I am thankful to Dr. Andrej Frolov, Leibniz Institute of Plant Biochemistry, for allowing me use the LC-MS instrument and for his guidance. I also acknowledge Dr. Klaus Schröter, Institute of Physics, and Dr. Karsten Busse, Institute of Chemistry, MLU Halle-Wittenberg, Halle (Saale) for measuring the viscosity and droplet size of the formulations, respectively. Frank Syrowatka, Interdisciplinary Center for Material Science, is acknowledged for taking the SEM images of the starch samples.

I would like to acknowledge Mathias Reisberg for his unreserved support at the beginning of my PhD work.

I would like to offer my special thanks to Manuela Woigk, Anke Nies, Anja Ehrlich, Claudia Bruhne and Andrea Stennett for their excellent technical assistance.

Getahun Paulos is acknowledged for collection of cassava tubers as well as isolation and acetylation of cassava starch.

The Ethiopian Institute of Agricultural Research and Ethiopian Forestry Research Center are acknowledged for supplying the seeds of the plants. Special thanks to Gelila Asamenew and Fikremariam Haile.

I greatly acknowledge the financial support provided by the German Academic Exchange Service (DAAD).

I am also thankful to Dr. Christian Schmelzer for his scientific advice and for being there for me the time I needed his expertise. I also acknowledge Prof. Bodo Dobner, Stefan Lange and Dr. Yahya Mrestani who were more than willing to help me.

I thank Moritz Schüller and Paul Robert Neumann for translating the English version of the 'Summary' into German version.

I am indebted to Dr. Henok Asfaw not only for making my stay in Halle lively and enjoyable but also for his key scientific contributions to my work. I also thank my friend and colleague, Dr. Tizita Haimanot, for having time together and for her supports along the way. My friends Tadiwos Feyissa, Bethelhem Messele and Dr. Adem Yusuf are greatly acknowledged for being there for me all the time and sharing my thoughts and feelings.

I would like to extend my appreciations to all the members of the former 'AG Neubert' and 'AG Dailey' for making my stay enjoyable. Special thanks to Hina Hussain, Khaled Alkassem and Angela Cristina Mora Huertas.

Finally, I am very grateful to my families and friends for their emotional and moral supports and understanding. Special thanks to my lovely sister Aster Nigussu and my fiancée Kalkidan Solomon for sharing my feelings and for their help and encouragement.

Curriculum Vitae**Personal Details:**

Name	Efrem Nigussu Tessema
Date of Birth	16.10.1983
Place of Birth	Arsi Asasa, Ethiopia
Nationality	Ethiopian
Marital Status	Single

Education:

10/2014 - now	PhD student at Department of Pharmaceutical Technology and Biopharmacy, Institute of Pharmacy, Martin Luther University Halle-Wittenberg, Germany
09/2008 - 07/2011	MSc in Pharmaceutics, School of Pharmacy, Addis Ababa University, Addis Ababa, Ethiopia
09/2003 - 08/2007	Bachelor in Pharmacy, School of Pharmacy, Addis Ababa University, Addis Ababa, Ethiopia

Work Experience:

11/2009 - 05/2014	Lecturer at Department of Pharmaceutics, School of Pharmacy, Addis Ababa University, Addis Ababa, Ethiopia
10/2008 - 10/2009	Assistant Lecture at Department of Pharmaceutics, School of Pharmacy, Addis Ababa University, Addis Ababa, Ethiopia
09/2007 - 09/2008	Graduate Assistant at Department of Pharmaceutics, School of Pharmacy, Addis Ababa University, Addis Ababa, Ethiopia
09/2012 - 05/2014	Secretary of Academic Commission (AC) of School of Pharmacy, Addis Ababa University
09/2013 - 05/2014	Member of Department Academic Commission (DAC), Department of Pharmaceutics and Social Pharmacy, School of Pharmacy, Addis Ababa University

References

1. Proksch, E., J.M. Brandner, and J.M. Jensen, *The skin: an indispensable barrier*. Exp Dermatol, 2008. **17**(12): p. 1063-72.
2. van Smeden, J., et al., *The important role of stratum corneum lipids for the cutaneous barrier function*. Biochim Biophys Acta, Mol Cell Biol Lipids, 2014. **1841**(3): p. 295-313.
3. Holleran, W.M., Y. Takagi, and Y. Uchida, *Epidermal sphingolipids: metabolism, function, and roles in skin disorders*. FEBS Lett, 2006. **580**(23): p. 5456-66.
4. Kuempel, D., et al., *In vitro reconstitution of stratum corneum lipid lamellae*. Biochim Biophys Acta, 1998. **1372**(1): p. 135-40.
5. Bouwstra, J.A. and P.L. Honeywell-Nguyen, *Skin structure and mode of action of vesicles*. Adv Drug Deliv Rev, 2002. **54 Suppl 1**: p. S41-55.
6. Menon, G.K., G.W. Cleary, and M.E. Lane, *The structure and function of the stratum corneum*. Int J Pharm, 2012. **435**(1): p. 3-9.
7. Bouwstra, J.A. and M. Ponec, *The skin barrier in healthy and diseased state*. Biochim Biophys Acta, 2006. **1758**(12): p. 2080-95.
8. Man, M.M., et al., *Optimization of physiological lipid mixtures for barrier repair*. J Invest Dermatol, 1996. **106**(5): p. 1096-101.
9. Mizutani, Y., et al., *Ceramide biosynthesis in keratinocyte and its role in skin function*. Biochimie, 2009. **91**(6): p. 784-90.
10. Ponec, M., et al., *New acylceramide in native and reconstructed epidermis*. J Invest Dermatol, 2003. **120**(4): p. 581-8.
11. Masukawa, Y., et al., *Characterization of overall ceramide species in human stratum corneum*. J Lipid Res, 2008. **49**(7): p. 1466-76.
12. Masukawa, Y., et al., *Comprehensive quantification of ceramide species in human stratum corneum*. J Lipid Res, 2009. **50**(8): p. 1708-19.
13. Karlsson, K.A., *Sphingolipid long chain bases*. Lipids, 1970. **5**(11): p. 878-91.
14. Kessner, D., et al., *Arrangement of ceramide [EOS] in a stratum corneum lipid model matrix: new aspects revealed by neutron diffraction studies*. Eur Biophys J, 2008. **37**(6): p. 989-99.
15. Schroter, A., et al., *Basic Nanostructure of Stratum Corneum Lipid Matrices Based on Ceramides [EOS] and [AP]: A Neutron Diffraction Study*. Biophys J, 2009. **97**(4): p. 1104-1114.
16. Wartewig, S. and R.H.H. Neubert, *Properties of Ceramides and their impact on the stratum corneum structure: A review*. Skin Pharmacol Physiol, 2007. **20**(5): p. 220-229.
17. de Sousa Neto, D., G. Gooris, and J. Bouwstra, *Effect of the omega-acylceramides on the lipid organization of stratum corneum model membranes evaluated by X-ray diffraction and FTIR studies (Part I)*. Chem Phys Lipids, 2011. **164**(3): p. 184-95.

18. Behne, M., et al., *Omega-hydroxyceramides are required for corneocyte lipid envelope (CLE) formation and normal epidermal permeability barrier function*. J Invest Dermatol, 2000. **114**(1): p. 185-92.
19. Uchida, Y. and W.M. Holleran, *Omega-O-acylceramide, a lipid essential for mammalian survival*. J Dermatol Sci, 2008. **51**(2): p. 77-87.
20. t'Kindt, R., et al., *Profiling and characterizing skin ceramides using reversed-phase liquid chromatography-quadrupole time-of-flight mass spectrometry*. Anal Chem, 2012. **84**(1): p. 403-11.
21. Robson, K.J., et al., *6-Hydroxy-4-sphingenine in human epidermal ceramides*. J Lipid Res, 1994. **35**(11): p. 2060-8.
22. Motta, S., et al., *Ceramide Composition of the Psoriatic Scale*. Biochim Biophys Acta, 1993. **1182**(2): p. 147-151.
23. Farwanah, H., et al., *Profiling of human stratum corneum ceramides by means of normal phase LC/APCI-MS*. Anal Bioanal Chem, 2005. **383**(4): p. 632-7.
24. Farwanah, H., et al., *Ceramide profiles of the uninvolved skin in atopic dermatitis and psoriasis are comparable to those of healthy skin*. Arch Dermatol Res, 2005. **296**(11): p. 514-521.
25. Sahle, F.F., et al., *Skin Diseases Associated with the Depletion of Stratum Corneum Lipids and Stratum Corneum Lipid Substitution Therapy*. Skin Pharmacol Physiol, 2015. **28**(1): p. 42-55.
26. Uchida, Y., W.M. Holleran, and P.M. Elias, *On the effects of topical synthetic pseudoceramides: Comparison of possible keratinocyte toxicities provoked by the pseudoceramides, PC104 and BIO391, and natural ceramides*. J Dermatol Sci, 2008. **51**(1): p. 37-43.
27. Carneiro, R., et al., *Topical emulsions containing ceramides: Effects on the skin barrier function and anti-inflammatory properties*. Eur J Lipid Sci Technol, 2011. **113**(8): p. 961-966.
28. Moore, D.J. and M.E. Rerek, *Insights into the molecular organization of lipids in the skin barrier from infrared spectroscopy studies of stratum corneum lipid models*. Acta Derm Venereol, 2000: p. 16-22.
29. Hamanaka, S., et al., *Human epidermal glucosylceramides are major precursors of stratum corneum ceramides*. J Invest Dermatol, 2002. **119**(2): p. 416-23.
30. Vielhaber, G., et al., *Localization of ceramide and glucosylceramide in human epidermis by immunogold electron microscopy*. J Invest Dermatol, 2001. **117**(5): p. 1126-36.
31. Hamanaka, S., et al., *Glucosylceramide accumulates preferentially in lamellar bodies in differentiated keratinocytes*. Br J Dermatol, 2005. **152**(3): p. 426-34.
32. Alessandrini, F., et al., *Alterations of glucosylceramide-beta-glucosidase levels in the skin of patients with psoriasis vulgaris*. J Invest Dermatol, 2004. **123**(6): p. 1030-6.
33. Uchida, Y., et al., *Epidermal sphingomyelins are precursors for selected stratum corneum ceramides*. J Lipid Res, 2000. **41**(12): p. 2071-82.
34. Holleran, W.M., et al., *Consequences of beta-glucocerebrosidase deficiency in epidermis. Ultrastructure and permeability barrier alterations in Gaucher disease*. J Clin Invest, 1994. **93**(4): p. 1756-64.

35. Grayson, S. and P.M. Elias, *Isolation and lipid biochemical characterization of stratum corneum membrane complexes: implications for the cutaneous permeability barrier*. J Invest Dermatol, 1982. **78**(2): p. 128-35.
36. Breathnach, A.S., et al., *Freeze-fracture replication of cells of stratum corneum of human epidermis*. J Anat, 1973. **114**(Pt 1): p. 65-81.
37. Breathnach, A.S., *Aspects of epidermal ultrastructure*. J Invest Dermatol, 1975. **65**(1): p. 2-15.
38. Madison, K.C., et al., *Presence of intact intercellular lipid lamellae in the upper layers of the stratum corneum*. J Invest Dermatol, 1987. **88**(6): p. 714-8.
39. Hou, S.Y., et al., *Membrane structures in normal and essential fatty acid-deficient stratum corneum: characterization by ruthenium tetroxide staining and x-ray diffraction*. J Invest Dermatol, 1991. **96**(2): p. 215-23.
40. Bouwstra, J.A., et al., *Structural investigations of human stratum corneum by small-angle X-ray scattering*. J Invest Dermatol, 1991. **97**(6): p. 1005-12.
41. Bouwstra, J.A., et al., *Role of ceramide 1 in the molecular organization of the stratum corneum lipids*. J Lipid Res, 1998. **39**(1): p. 186-96.
42. McIntosh, T.J., M.E. Stewart, and D.T. Downing, *X-ray diffraction analysis of isolated skin lipids: reconstitution of intercellular lipid domains*. Biochemistry, 1996. **35**(12): p. 3649-53.
43. de Jager, M.W., et al., *Lipid mixtures prepared with well-defined synthetic ceramides closely mimic the unique stratum corneum lipid phase behavior*. J Lipid Res, 2005. **46**(12): p. 2649-56.
44. Kiselev, M.A., et al., *New insights into the structure and hydration of a stratum corneum lipid model membrane by neutron diffraction*. Eur Biophys J with Biophysics Letters, 2005. **34**(8): p. 1030-1040.
45. Engelbrecht, T.N., et al., *The impact of ceramides NP and AP on the nanostructure of stratum corneum lipid bilayer. Part I: neutron diffraction and H-2 NMR studies on multilamellar models based on ceramides with symmetric alkyl chain length distribution*. Soft Matter, 2012. **8**(24): p. 6599-6607.
46. Kessner, D., et al., *Properties of ceramides and their impact on the stratum corneum structure. Part 2: stratum corneum lipid model systems*. Skin Pharmacol Physiol, 2008. **21**(2): p. 58-74.
47. Imokawa, G., et al., *Decreased Level of Ceramides in Stratum-Corneum of Atopic-Dermatitis - an Etiologic Factor in Atopic Dry Skin*. J Invest Dermatol, 1991. **96**(4): p. 523-526.
48. Di Nardo, A., et al., *Ceramide and cholesterol composition of the skin of patients with atopic dermatitis*. Acta Derm Venereol, 1998. **78**(1): p. 27-30.
49. Bleck, O., et al., *Two ceramide subfractions detectable in Cer(AS) position by HPTLC in skin surface lipids of non-lesional skin of atopic eczema*. J Invest Dermatol, 1999. **113**(6): p. 894-900.
50. Macheleidt, O., H.W. Kaiser, and K. Sandhoff, *Deficiency of epidermal protein-bound omega-hydroxyceramides in atopic dermatitis*. J Invest Dermatol, 2002. **119**(1): p. 166-173.
51. Hara, J., et al., *High-expression of sphingomyelin deacylase is an important determinant of ceramide deficiency leading to barrier disruption in atopic dermatitis*. J Invest Dermatol, 2000. **115**(3): p. 406-413.

52. Imokawa, G., *A possible mechanism underlying the ceramide deficiency in atopic dermatitis: expression of a deacylase enzyme that cleaves the N-acyl linkage of sphingomyelin and glucosylceramide.* J Dermatol Sci, 2009. **55**(1): p. 1-9.
53. Ishibashi, M., et al., *Abnormal expression of the novel epidermal enzyme, glucosylceramide deacylase, and the accumulation of its enzymatic reaction product, glucosylsphingosine, in the skin of patients with atopic dermatitis.* Lab Investig, 2003. **83**(3): p. 397-408.
54. Ohnishi, Y., et al., *Ceramidase activity in bacterial skin flora as a possible cause of ceramide deficiency in atopic dermatitis.* Clin Diagn Lab Immunol, 1999. **6**(1): p. 101-104.
55. Jin, K., et al., *Analysis of Beta-Glucocerebrosidase and Ceramidase Activities in Atopic and Aged Dry Skin.* Acta Derm Venereol, 1994. **74**(5): p. 337-340.
56. Kusuda, S., et al., *Localization of sphingomyelinase in lesional skin of atopic dermatitis patients.* J Invest Dermatol, 1998. **111**(5): p. 733-738.
57. Motta, S., et al., *Abnormality of Water Barrier Function in Psoriasis - Role of Ceramide Fractions.* Arch Dermatol, 1994. **130**(4): p. 452-456.
58. Berardesca, E., et al., *In vivo hydration and water-retention capacity of stratum corneum in clinically uninvolved skin in atopic and psoriatic patients.* Acta Derm Venereol, 1990. **70**(5): p. 400-4.
59. Serup, J. and C. Blichmann, *Epidermal Hydration of Psoriasis Plaques and the Relation to Scaling - Measurement of Electrical Conductance and Trans-Epidermal Water-Loss.* Acta Derm Venereol, 1987. **67**(4): p. 357-359.
60. Alessandrini, F., et al., *The level of prosaposin is decreased in the skin of patients with psoriasis vulgaris.* J Invest Dermatol, 2001. **116**(3): p. 394-400.
61. Pata, M.O., Y.A. Hannun, and C.K.Y. Ng, *Plant sphingolipids: decoding the enigma of the Sphinx.* New Phytol, 2010. **185**(3): p. 611-630.
62. Spassieva, S. and J. Hille, *Plant sphingolipids today - Are they still enigmatic?* Plant Biology, 2003. **5**(2): p. 125-136.
63. Lynch, D.V. and T.M. Dunn, *An introduction to plant sphingolipids and a review of recent advances in understanding their metabolism and function.* New Phytol, 2004. **161**(3): p. 677-702.
64. Warnecke, D. and E. Heinz, *Recently discovered functions of glucosylceramides in plants and fungi.* Cell Mol Life Sci, 2003. **60**(5): p. 919-941.
65. Fujino, Y., M. Ohnishi, and S. Ito, *Molecular-Species of Ceramide and Mono-Glycosylceramide, Di-Glycosylceramide, Tri-Glycosylceramide, and Tetraglycosylceramide in Bran and Endosperm of Rice Grains.* Agric Biol Chem, 1985. **49**(9): p. 2753-2762.
66. Ohnishi, M., S. Ito, and Y. Fujino, *Sphingolipid Classes and Their Molecular-Species in Wheat-Flour.* Agric Biol Chem, 1985. **49**(12): p. 3609-3611.
67. Bromley, P.E., et al., *Complex sphingolipid synthesis in plants: characterization of inositolphosphorylceramide synthase activity in bean microsomes.* Arch Biochem Biophys, 2003. **417**(2): p. 219-226.

68. Sullards, M.C., et al., *Structure determination of soybean and wheat glucosylceramides by tandem mass spectrometry*. J Mass Spectrom, 2000. **35**(3): p. 347-53.
69. Markham, J.E., et al., *Plant sphingolipids: function follows form*. Curr Opin Plant Biol, 2013. **16**(3): p. 350-7.
70. Sperling, P., et al., *Functional identification of a delta8-sphingolipid desaturase from *Borago officinalis**. Arch Biochem Biophys, 2001. **388**(2): p. 293-8.
71. Sugawara, T., et al., *Identification of glucosylceramides containing sphingatrienine in maize and rice using ion trap mass spectrometry*. Lipids, 2010. **45**(5): p. 451-5.
72. Sugawara, T., et al., *Analysis of glucosylceramides from various sources by liquid chromatography-ion trap mass spectrometry*. J Oleo Sci, 2010. **59**(7): p. 387-94.
73. Sperling, P. and E. Heinz, *Plant sphingolipids: structural diversity, biosynthesis, first genes and functions*. Biochim Biophys Acta, Mol Cell Biol Lipids, 2003. **1632**(1-2): p. 1-15.
74. Imai, H., et al., *Sphingoid base composition of cerebrosides from plant leaves*. Biosci Biotechnol Biochem, 1997. **61**(2): p. 351-353.
75. Ohnishi, M., S. Ito, and Y. Fujino, *Characterization of Sphingolipids in Spinach Leaves*. Biochim Biophys Acta, 1983. **752**(3): p. 416-422.
76. Fujino, Y. and M. Ohnishi, *Sphingolipids in Wheat-Grain*. J Cereal Sci, 1983. **1**(2): p. 159-168.
77. Imai, H., Y. Morimoto, and K. Tamura, *Sphingoid base composition of monoglucosylceramide in Brassicaceae*. J Plant Physiol, 2000. **157**(4): p. 453-456.
78. Imai, H., et al., *Structure and Distribution of Cerebroside Containing Unsaturated Hydroxy Fatty-Acids in Plant-Leaves*. Biosci Biotechnol Biochem, 1995. **59**(7): p. 1309-1313.
79. Imai, H., et al., *Determining double-bond positions in monoenoic 2-hydroxy fatty acids of glucosylceramides by gas chromatography-mass spectrometry*. Lipids, 2000. **35**(2): p. 233-236.
80. Uemura, M. and P.L. Steponkus, *A Contrast of the Plasma-Membrane Lipid-Composition of Oat and Rye Leaves in Relation to Freezing Tolerance*. Plant Physiology, 1994. **104**(2): p. 479-496.
81. Wartewig, S. and R.H. Neubert, *Properties of ceramides and their impact on the stratum corneum structure: a review. Part 1: ceramides*. Skin Pharmacol Physiol, 2007. **20**(5): p. 220-9.
82. Ohnishi, M. and Y. Fujino, *Sphingolipids in Immature and Mature Soybeans*. Lipids, 1982. **17**(11): p. 803-810.
83. Cahoon, E.B. and D.V. Lynch, *Analysis of Glucocerebrosides of Rye (*Secale-Cereale L Cv Puma*) Leaf and Plasma-Membrane*. Plant Physiology, 1991. **95**(1): p. 58-68.
84. Fujino, Y. and M. Ohnishi, *Species of Sphingolipids in Rice Grain*. Proceedings of the Japan Academy Series B-Physical and Biological Sciences, 1982. **58**(2): p. 36-39.
85. Aida, K., et al., *Prevention of Aberrant Crypt Foci Formation by Dietary Maize and Yeast Cerebrosides in 1,2-Dimethylhydrazine-treated Mice*. J Oleo Sci, 2005. **54**(1): p. 45-49.
86. Bartke, N., A. Fischbeck, and H.U. Humpf, *Analysis of sphingolipids in potatoes (*Solanum tuberosum L.*) and sweet potatoes (*Ipomoea batatas (L.) Lam.*) by reversed phase high-performance liquid chromatography electrospray ionization tandem mass spectrometry (HPLC-ESI-MS/MS)*. Mol Nutr Food Res, 2006. **50**(12): p. 1201-11.

87. Gutierrez, E., T. Wang, and W.R. Fehr, *Quantification of sphingolipids in soybeans*. J Am Oil Chem Soc, 2004. **81**(8): p. 737-742.
88. Shirakura, Y., et al., *4,8-Sphingadienine and 4-hydroxy-8-sphingenine activate ceramide production in the skin*. Lipids Health Dis, 2012. **11**: p. 108.
89. Usuki, S., et al., *Chemoenzymatically prepared konjac ceramide inhibits NGF-induced neurite outgrowth by a semaphorin 3A-like action*. Biochem Biophys Rep, 2016. **5**: p. 160-167.
90. Kojima, M., M. Ohnishi, and S. Ito, *Composition and Molecular-Species of Ceramide and Cerebroside in Scarlet Runner Beans (Phaseolus-Coccineus L) and Kidney Beans (Phaseolus-Vulgaris L)*. J Agric Food Chem, 1991. **39**(10): p. 1709-1714.
91. Goto, H., et al., *Determination of sphingoid bases from hydrolyzed glucosylceramide in rice and wheat by online post-column high-performance liquid chromatography with O-phthalaldehyde derivatization*. J Oleo Sci, 2012. **61**(12): p. 681-8.
92. Hori, M., et al., *Double-Blind Study on Effects of Glucosyl Ceramide in Beet Extract on Skin Elasticity and Fibronectin Production in Human Dermal Fibroblasts*. ANTI-AGING MEDICINE, 2010. **7**(11): p. 129-142.
93. Guillou, S., et al., *The moisturizing effect of a wheat extract food supplement on women's skin: a randomized, double-blind placebo-controlled trial*. Int J Cosmet Sci, 2011. **33**(2): p. 138-143.
94. Uchiyama, T., et al., *Oral intake of glucosylceramide improves relatively higher level of transepidermal water loss in mice and healthy human subjects*. J Health Sci, 2008. **54**(5): p. 559-566.
95. Yeom, M., et al., *Oral administration of glucosylceramide ameliorates inflammatory dry-skin condition in chronic oxazolone-induced irritant contact dermatitis in the mouse ear*. J Dermatol Sci, 2012. **67**(2): p. 101-110.
96. Tsuji, K., et al., *Dietary glucosylceramide improves skin barrier function in hairless mice*. J Dermatol Sci, 2006. **44**(2): p. 101-107.
97. Kawano, K. and K. Umemura, *Oral Intake of Beet Extract Provides Protection Against Skin Barrier Impairment in Hairless Mice*. Phytother Res, 2013. **27**(5): p. 775-783.
98. Kimata, H., *Improvement of atopic dermatitis and reduction of skin allergic responses by oral intake of konjac ceramide*. Pediatr Dermatol, 2006. **23**(4): p. 386-389.
99. Miyanishi, K., et al., *Reduction of transepidermal water loss by oral intake of glucosylceramides in patients with atopic eczema*. Allergy, 2005. **60**(11): p. 1454-1455.
100. Loden, M. and E. Barany, *Skin-identical lipids versus petrolatum in the treatment of tape-stripped and detergent-perturbed human skin*. Acta Derm Venereol, 2000. **80**(6): p. 412-415.
101. Fujii, M., et al., *Atopic dermatitis-like pruritic skin inflammation caused by feeding a special diet to HR-1 hairless mice*. Exp Dermatol, 2005. **14**(6): p. 460-8.
102. Makiura, M., et al., *Atopic dermatitis-like symptoms in HR-1 hairless mice fed a diet low in magnesium and zinc*. J Int Med Res, 2004. **32**(4): p. 392-399.
103. Ishikawa, J., et al., *Dietary glucosylceramide is absorbed into the lymph and increases levels of epidermal sphingolipids*. J Dermatol Sci, 2009. **56**(3): p. 216-218.

104. Ueda, O., M. Hasegawa, and S. Kitamura, *Distribution in skin of ceramide after oral administration to rats*. Drug Metab Pharmacokinet, 2009. **24**(2): p. 180-4.
105. Ueda, O., T. Uchiyama, and M. Nakashima, *Distribution and Metabolism of Sphingosine in Skin after Oral Administration to Mice*. Drug Metab Pharmacokinet, 2010. **25**(5): p. 456-465.
106. Hasegawa, T., et al., *Dietary Glucosylceramide Enhances Cornified Envelope Formation via Transglutaminase Expression and Involucrin Production*. Lipids, 2011. **46**(6): p. 529-535.
107. Ideta, R., et al., *Orally administered glucosylceramide improves the skin barrier function by upregulating genes associated with the tight junction and cornified envelope formation*. Biosci Biotechnol Biochem, 2011. **75**(8): p. 1516-23.
108. Kawada, C., et al., *Dietary glucosylceramide enhances tight junction function in skin epidermis via induction of claudin-1*. Biosci Biotechnol Biochem, 2013. **77**(4): p. 867-9.
109. Murakami, I., et al., *Phytoceramide and sphingoid bases derived from brewer's yeast *Saccharomyces pastorianus* activate peroxisome proliferator-activated receptors*. Lipids Health Dis, 2011. **10**.
110. Duan, J.J., et al., *Dietary sphingolipids improve skin barrier functions via the upregulation of ceramide synthases in the epidermis*. Exp Dermatol, 2012. **21**(6): p. 448-452.
111. Weber, T.M., et al., *Treatment of xerosis with a topical formulation containing glyceryl glucoside, natural moisturizing factors, and ceramide*. J Clin Aesthet Dermatol, 2012. **5**(8): p. 29-39.
112. Hon, K.L., et al., *Pseudoceramide for childhood eczema: does it work?* Hong Kong Med J, 2011. **17**(2): p. 132-6.
113. Lee, Y.B., et al., *Beneficial effects of pseudoceramide-containing physiologic lipid mixture as a vehicle for topical steroids*. Eur J Dermatol, 2011. **21**(5): p. 710-6.
114. Kim, H.J., et al., *Pseudoceramide-containing physiological lipid mixture reduces adverse effects of topical steroids*. Allergy Asthma Immunol Res, 2011. **3**(2): p. 96-102.
115. Grimalt, R., et al., *The steroid-sparing effect of an emollient therapy in infants with atopic dermatitis: a randomized controlled study*. Dermatology, 2007. **214**(1): p. 61-7.
116. Loden, M., et al., *Treatment with a barrier-strengthening moisturizer prevents relapse of hand-eczema. An open, randomized, prospective, parallel group study*. Acta Derm Venereol, 2010. **90**(6): p. 602-6.
117. Simpson, E.L., *Atopic dermatitis: a review of topical treatment options*. Curr Med Res Opin, 2010. **26**(3): p. 633-40.
118. Frankel, A., et al., *Bilateral comparison study of pimecrolimus cream 1% and a ceramide-hyaluronic acid emollient foam in the treatment of patients with atopic dermatitis*. J Drugs Dermatol, 2011. **10**(6): p. 666-72.
119. Chamlin, S.L., et al., *Ceramide-dominant barrier repair lipids alleviate childhood atopic dermatitis: changes in barrier function provide a sensitive indicator of disease activity*. J Am Acad Dermatol, 2002. **47**(2): p. 198-208.
120. Hon, K.L. and A.K. Leung, *Use of ceramides and related products for childhood-onset eczema*. Recent Pat Inflamm Allergy Drug Discov, 2013. **7**(1): p. 12-9.

121. Kwun, K.H., et al., *Production of ceramide with Saccharomyces cerevisiae*. Appl Biochem Biotechnol, 2006. **133**(3): p. 203-10.
122. Loden, M., *The skin barrier and use of moisturizers in atopic dermatitis*. Clin Dermatol, 2003. **21**(2): p. 145-57.
123. Sahle, F.F., J. Wohlrab, and R.H. Neubert, *Controlled penetration of ceramides into and across the stratum corneum using various types of microemulsions and formulation associated toxicity studies*. Eur J Pharm Biopharm, 2014. **86**(2): p. 244-50.
124. Neubert, R.H.H., et al., *Controlled Penetration of a Novel Dimeric Ceramide into and across the Stratum Corneum Using Microemulsions and Various Types of Semisolid Formulations*. Skin Pharmacol Physiol, 2016. **29**(3): p. 130-134.
125. Heuschkel, S., A. Goebel, and R.H. Neubert, *Microemulsions--modern colloidal carrier for dermal and transdermal drug delivery*. J Pharm Sci, 2008. **97**(2): p. 603-31.
126. Sahle, F.F., et al., *Polyglycerol fatty acid ester surfactant-based microemulsions for targeted delivery of ceramide AP into the stratum corneum: formulation, characterisation, in vitro release and penetration investigation*. Eur J Pharm Biopharm, 2012. **82**(1): p. 139-50.
127. Sahle, F.F., et al., *Lecithin-based microemulsions for targeted delivery of ceramide AP into the stratum corneum: formulation, characterizations, and in vitro release and penetration studies*. Pharm Res, 2013. **30**(2): p. 538-51.
128. de Jager, M.W., et al., *Modelling the stratum corneum lipid organisation with synthetic lipid mixtures: the importance of synthetic ceramide composition*. Biochim Biophys Acta-Biomembranes, 2004. **1664**(2): p. 132-140.
129. Tokudome, Y., et al., *Effect of topically applied sphingomyelin-based liposomes on the ceramide level in a three-dimensional cultured human skin model*. J Liposome Res, 2010. **20**(1): p. 49-54.
130. Tokudome, Y., et al., *Increase in Ceramide Level after Application of Various Sizes of Sphingomyelin Liposomes to a Cultured Human Skin Model*. Skin Pharmacol Physiol, 2011. **24**(4): p. 218-223.
131. Shimoda, H., et al., *Changes in ceramides and glucosylceramides in mouse skin and human epidermal equivalents by rice-derived glucosylceramide*. J Med Food, 2012. **15**(12): p. 1064-72.
132. Tokudome, Y., M. Endo, and F. Hashimoto, *Application of glucosylceramide-based liposomes increased the ceramide content in a three-dimensional cultured skin epidermis*. Skin Pharmacol Physiol, 2014. **27**(1): p. 18-24.
133. Asai, S. and H. Miyachi, *[Evaluation of skin-moisturizing effects of oral or percutaneous use of plant ceramides]*. Rinsho Byori, 2007. **55**(3): p. 209-15.
134. Shimada, E., et al., *Inhibitory effect of topical maize glucosylceramide on skin photoaging in UVA-irradiated hairless mice*. J Oleo Sci, 2011. **60**(6): p. 321-5.
135. Napolitano, A., et al., *Qualitative on-line profiling of ceramides and cerebroside by high performance liquid chromatography coupled with electrospray ionization ion trap tandem mass spectrometry: the case of Dracontium lorentense*. J Pharm Biomed Anal, 2011. **55**(1): p. 23-30.

136. Markham, J.E., et al., *Separation and identification of major plant sphingolipid classes from leaves*. J Biol Chem, 2006. **281**(32): p. 22684-94.
137. Farwanah, H., T. Kolter, and K. Sandhoff, *Mass spectrometric analysis of neutral sphingolipids: methods, applications, and limitations*. Biochim Biophys Acta, 2011. **1811**(11): p. 854-60.
138. Markham, J.E. and J.G. Jaworski, *Rapid measurement of sphingolipids from Arabidopsis thaliana by reversed-phase high-performance liquid chromatography coupled to electrospray ionization tandem mass spectrometry*. Rapid Commun Mass Spectrom, 2007. **21**(7): p. 1304-14.
139. Sullards, M.C., et al., *Analysis of mammalian sphingolipids by liquid chromatography tandem mass spectrometry (LC-MS/MS) and tissue imaging mass spectrometry (TIMS)*. Biochim Biophys Acta, 2011. **1811**(11): p. 838-53.
140. Canela, N., et al., *Analytical methods in sphingolipidomics: Quantitative and profiling approaches in food analysis*. J Chromatogr A, 2016. **1428**: p. 16-38.
141. Merrill, A.H., et al., *Sphingolipidomics: High-throughput, structure-specific, and quantitative analysis of sphingolipids by liquid chromatography tandem mass spectrometry*. Methods, 2005. **36**(2): p. 207-224.
142. Haynes, C.A., et al., *Sphingolipidomics: Methods for the comprehensive analysis of sphingolipids*. J Chromatogr B Analyt Technol Biomed Life Sci, 2009. **877**(26): p. 2696-2708.
143. Haynes, C.A., et al., *Sphingolipidomics: methods for the comprehensive analysis of sphingolipids*. J Chromatogr B Analyt Technol Biomed Life Sci, 2009. **877**(26): p. 2696-708.
144. Samuelsson, B. and K. Samuelsson, *Gas-liquid chromatographic separation of ceramides as di-O-trimethylsilyl ether derivatives*. Biochim Biophys Acta, 1968. **164**(2): p. 421-3.
145. Imai, H., H. Hattori, and M. Watanabe, *An improved method for analysis of glucosylceramide species having cis-8 and trans-8 isomers of sphingoid bases by LC-MS/MS*. Lipids, 2012. **47**(12): p. 1221-9.
146. Pettus, B.J., et al., *Observation of different ceramide species from crude cellular extracts by normal-phase high-performance liquid chromatography coupled to atmospheric pressure chemical ionization mass spectrometry*. Rapid Commun Mass Spectrom, 2003. **17**(11): p. 1203-1211.
147. Farwanah, H., et al., *Normal-phase liquid chromatographic separation of stratum corneum ceramides with detection by evaporative light scattering and atmospheric pressure chemical ionization mass spectrometry*. Anal Chim Acta, 2003. **492**(1-2): p. 233-239.
148. Farwanah, H., et al., *Normal phase liquid chromatography coupled to quadrupole time of flight atmospheric pressure chemical ionization mass spectrometry for separation, detection and mass spectrometric profiling of neutral sphingolipids and cholesterol*. J Chromatogr B Analyt Technol Biomed Life Sci, 2009. **877**(27): p. 2976-2982.
149. van Smeden, J., et al., *LC/MS analysis of stratum corneum lipids: ceramide profiling and discovery*. J Lipid Res, 2011. **52**(6): p. 1211-1221.
150. Pettus, B.J., et al., *Quantitative measurement of different ceramide species from crude cellular extracts by normal-phase high-performance liquid chromatography coupled to atmospheric pressure ionization mass spectrometry*. Rapid Commun Mass Spectrom, 2004. **18**(5): p. 577-583.

151. Suzuki, Y., et al., *Convenient structural analysis of glycosphingolipids using MALDI-QIT-TOF mass spectrometry with increased laser power and cooling gas flow*. J Biochem, 2006. **139**(4): p. 771-777.
152. Fujiwaki, T., et al., *Quantitative evaluation of sphingolipids using delayed extraction matrix-assisted laser desorption ionization time-of-flight mass spectrometry with sphingosylphosphorylcholine as an internal standard. Practical application to cardiac valves from a patient with Fabry disease*. J Chromatogr B Analyt Technol Biomed Life Sci, 2006. **832**(1): p. 97-102.
153. Farwanah, H. and T. Kolter, *Lipidomics of glycosphingolipids*. Metabolites, 2012. **2**(1): p. 134-64.
154. Hsu, F.F. and J. Turk, *Structural determination of glycosphingolipids as lithiated adducts by electrospray ionization mass spectrometry using low-energy collisional-activated dissociation on a triple stage quadrupole instrument*. J Am Soc Mass Spectrom, 2001. **12**(1): p. 61-79.
155. Merrill, A.H., *Sphingolipid and Glycosphingolipid Metabolic Pathways in the Era of Sphingolipidomics*. Chemical Reviews, 2011. **111**(10): p. 6387-6422.
156. Blackler, A.R., et al., *Quantitative comparison of proteomic data quality between a 2D and 3D quadrupole ion trap*. Anal Chem, 2006. **78**(4): p. 1337-44.
157. Metelmann, W., J. Muthing, and J. Peter-Katalinic, *Nano-electrospray ionization quadrupole time-of-flight tandem mass spectrometric analysis of a ganglioside mixture from human granulocytes*. Rapid Commun Mass Spectrom, 2000. **14**(7): p. 543-50.
158. Metelmann, W., J. Peter-Katalinić, and J. Muthing, *Gangliosides from human granulocytes: a nano-ESI QTOF mass spectrometry fucosylation study of low abundance species in complex mixtures*. J Am Soc Mass Spectrom, 2001. **12**(8): p. 964-973.
159. Ejsing, C.S., et al., *Collision-induced dissociation pathways of yeast sphingolipids and their molecular profiling in total lipid extracts: a study by quadrupole TOF and linear ion trap-orbitrap mass spectrometry*. J Mass Spectrom, 2006. **41**(3): p. 372-89.
160. Ivleva, V.B., et al., *Coupling thin-layer chromatography with vibrational cooling matrix-assisted laser desorption/ionization Fourier transform mass spectrometry for the analysis of ganglioside mixtures*. Anal Chem, 2004. **76**(21): p. 6484-91.
161. Lawrence, M.J. and G.D. Rees, *Microemulsion-based media as novel drug delivery systems*. Adv Drug Deliv Rev, 2000. **45**(1): p. 89-121.
162. Kreilgaard, M., *Influence of microemulsions on cutaneous drug delivery*. Adv Drug Deliv Rev, 2002. **54**: p. S77-S98.
163. Date, A.A. and M.S. Nagarsenker, *Parenteral microemulsions: An overview*. Int J Pharm, 2008. **355**(1-2): p. 19-30.
164. Lopes, L.B., *Overcoming the cutaneous barrier with microemulsions*. Pharmaceutics, 2014. **6**(1): p. 52-77.
165. Nguyen, T.T.L., et al., *Biocompatible lecithin-based microemulsions with rhamnolipid and sophorolipid biosurfactants: Formulation and potential applications*. J Colloid Interface Sci, 2010. **348**(2): p. 498-504.

166. Santos, P., et al., *Application of microemulsions in dermal and transdermal drug delivery*. Skin Pharmacol Physiol, 2008. **21**(5): p. 246-259.
167. Dreher, F., et al., *Human skin irritation studies of a lecithin microemulsion gel and of lecithin liposomes*. Skin Pharmacol, 1996. **9**(2): p. 124-129.
168. Paolino, D., et al., *Lecithin microemulsions for the topical administration of ketoprofen: percutaneous adsorption through human skin and in vivo human skin tolerability*. Int J Pharm, 2002. **244**(1-2): p. 21-31.
169. Chaiyana, W., et al., *Characterization of potent anticholinesterase plant oil based microemulsion (vol 401, pg 32, 2010)*. Int J Pharm, 2011. **414**(1-2): p. 333-334.
170. Hathout, R.M., et al., *Microemulsion formulations for the transdermal delivery of testosterone*. Eur J Pharm Sci, 2010. **40**(3): p. 188-196.
171. Liu, C.-H., F.-Y. Chang, and D.-K. Hung, *Terpene microemulsions for transdermal curcumin delivery: Effects of terpenes and cosurfactants*. Colloids Surf B Biointerfaces, 2011. **82**(1): p. 63-70.
172. El Maghraby, G.M., *Self-microemulsifying and microemulsion systems for transdermal delivery of indomethacin: Effect of phase transition*. Colloids Surf B Biointerfaces, 2010. **75**(2): p. 595-600.
173. Ho, H.O., C.C. Hsiao, and M.T. Sheu, *Preparation of microemulsions using polyglycerol fatty acid esters as surfactant for the delivery of protein drugs*. J Pharm Sci, 1996. **85**(2): p. 138-143.
174. Teichmann, A., et al., *Comparison of stratum corneum penetration and localization of a lipophilic model drug applied in an o/w microemulsion and an amphiphilic cream*. Eur J Pharm Biopharm, 2007. **67**(3): p. 699-706.
175. Shukla, A., et al., *Investigation of pharmaceutical oil/water microemulsions by small-angle scattering*. Pharm Res, 2002. **19**(6): p. 881-886.
176. Goebel, A.S.B., et al., *Dermal targeting using colloidal carrier systems with linoleic acid*. Eur J Pharm Biopharm, 2010. **75**(2): p. 162-172.
177. Sathishkumar, M., et al., *Role of bicontinuous microemulsion in the rapid enzymatic hydrolysis of (R,S)-ketoprofen ethyl ester in a micro-reactor*. Bioresour Technol, 2010. **101**(20): p. 7834-7840.
178. Narang, A.S., D. Delmarre, and D. Gao, *Stable drug encapsulation in micelles and microemulsions*. Int J Pharm, 2007. **345**(1-2): p. 9-25.
179. Trotta, M., et al., *Influence of ion pairing on topical delivery of retinoic acid from microemulsions*. J Control Release, 2003. **86**(2-3): p. 315-321.
180. Peira, E., P. Scolari, and M.R. Gasco, *Transdermal permeation of apomorphine through hairless mouse skin from microemulsions*. Int J Pharm, 2001. **226**(1-2): p. 47-51.
181. Yuan, Y., et al., *Investigation of microemulsion system for transdermal delivery of meloxicam*. Int J Pharm, 2006. **321**(1-2): p. 117-123.
182. Yuan, J.S., et al., *Effect of surfactant concentration on transdermal lidocaine delivery with linker microemulsions*. Int J Pharm, 2010. **392**(1-2): p. 274-284.
183. Lin, C.-C., et al., *Stability and characterisation of phospholipid-based curcumin-encapsulated microemulsions*. Food Chem, 2009. **116**(4): p. 923-928.

184. Djekic, L. and M. Primorac, *The influence of cosurfactants and oils on the formation of pharmaceutical microemulsions based on PEG-8 caprylic/capric glycerides*. Int J Pharm, 2008. **352**(1–2): p. 231-239.
185. Changez, M., et al., *Effect of the composition of lecithin/n-propanol/isopropyl myristate/water microemulsions on barrier properties of mice skin for transdermal permeation of tetracaine hydrochloride: In vitro*. Colloids Surf B Biointerfaces, 2006. **50**(1): p. 18-25.
186. Warisnoicharoen, W., A.B. Lansley, and M.J. Lawrence, *Nonionic oil-in-water microemulsions: the effect of oil type on phase behaviour*. Int J Pharm, 2000. **198**(1): p. 7-27.
187. Shevachman, M., et al., *Enhanced percutaneous permeability of diclofenac using a new U-Type dilutable microemulsion*. Drug Dev Ind Pharm, 2008. **34**(4): p. 403-412.
188. Neubert, R.H.H., et al., *Microemulsions as colloidal vehicle systems for dermal drug delivery. Part V: Microemulsions without and with glycolipid as penetration enhancer*. J Pharm Sci, 2005. **94**(4): p. 821-827.
189. Kantarci, G., et al., *In vitro permeation of diclofenac sodium from novel microemulsion formulations through rabbit skin*. Drug Dev Res, 2005. **65**(1): p. 17-25.
190. Sintov, A.C., H.V. Levy, and S. Botner, *Systemic delivery of insulin via the nasal route using a new microemulsion system: In vitro and in vivo studies*. J Control Release, 2010. **148**(2): p. 168-176.
191. Sharma, G., et al., *Microemulsions for oral delivery of insulin: Design, development and evaluation in streptozotocin induced diabetic rats*. Eur J Pharm Biopharm, 2010. **76**(2): p. 159-169.
192. Chen, H., et al., *Hydrogel-thickened microemulsion for topical administration of drug molecule at an extremely low concentration*. Int J Pharm, 2007. **341**(1–2): p. 78-84.
193. Papadimitriou, V., et al., *Microemulsions based on virgin olive oil: A model biomimetic system for studying native oxidative enzymatic activities*. Colloids Surf A Physicochem Eng Asp, 2011. **382**(1–3): p. 232-237.
194. Shukla, A., A. Krause, and R.H.H. Neubert, *Microemulsions as colloidal vehicle systems for dermal drug delivery. Part IV: investigation of microemulsion systems based on a eutectic mixture of lidocaine and prilocaine as the colloidal phase by dynamic light scattering*. J Pharm Pharmacol, 2003. **55**(6): p. 741-748.
195. Margulis-Goshen, K., et al., *Formation of organic nanoparticles from volatile microemulsions*. J Colloid Interface Sci, 2010. **342**(2): p. 283-292.
196. Zech, O., et al., *Ethylammonium nitrate in high temperature stable microemulsions*. J Colloid Interface Sci, 2010. **347**(2): p. 227-232.
197. Regev, O., et al., *A study of the microstructure of a four-component nonionic microemulsion by cryo-TEM, NMR, SAXS, and SANS*. Langmuir, 1996. **12**(3): p. 668-674.
198. Fanun, M., *Properties of microemulsions with mixed nonionic surfactants and citrus oil*. Colloids Surf A Physicochem Eng Asp, 2010. **369**(1–3): p. 246-252.
199. Cheng, M.-B., et al., *Characterization of water-in-oil microemulsion for oral delivery of earthworm fibrinolytic enzyme*. J Control Release, 2008. **129**(1): p. 41-48.

200. Wellert, S., et al., *Structure of biodiesel based bicontinuous microemulsions for environmentally compatible decontamination: A small angle neutron scattering and freeze fracture electron microscopy study*. J Colloid Interface Sci, 2008. **325**(1): p. 250-258.
201. Rojas, O., et al., *A new type of microemulsion consisting of two halogen-free ionic liquids and one oil component*. Colloids Surf A Physicochem Eng Asp, 2010. **369**(1-3): p. 82-87.
202. Boonme, P., et al., *Characterization of microemulsion structures in the pseudoternary phase diagram of isopropyl palmitate/water/Brij 97:1-butanol*. AAPS PharmSciTech, 2006. **7**(2): p. E99-E104.
203. Yuan, J.S., et al., *Linker-based lecithin microemulsions for transdermal delivery of lidocaine*. Int J Pharm, 2008. **349**(1-2): p. 130-143.
204. Banga, A.K., S. Bose, and T.K. Ghosh, *Iontophoresis and electroporation: comparisons and contrasts*. Int J Pharm, 1999. **179**(1): p. 1-19.
205. Cichewicz, A., et al., *Cutaneous delivery of alpha-tocopherol and lipoic acid using microemulsions: influence of composition and charge*. J Pharm Pharmacol, 2013. **65**(6): p. 817-826.
206. Pakpayat, N., et al., *Formulation of ascorbic acid microemulsions with alkyl polyglycosides*. Eur J Pharm Biopharm, 2009. **72**(2): p. 444-452.
207. Arevalo, M.I., et al., *Rapid skin anesthesia using a new topical amethocaine formulation: A preclinical study*. Anesth Analg, 2004. **98**(5): p. 1407-1412.
208. Escribano, E., et al., *Rapid human skin permeation and topical anaesthetic activity of a new amethocaine microemulsion*. Skin Pharmacol Physiol, 2005. **18**(6): p. 294-300.
209. Getie, M., J. Wohlrab, and R.H.H. Neubert, *Dermal delivery of desmopressin acetate using colloidal carrier systems*. J Pharm Pharmacol, 2005. **57**(4): p. 423-427.
210. Huang, C.T., et al., *Effect of microemulsions on transdermal delivery of citalopram: optimization studies using mixture design and response surface methodology*. Int J Nanomedicine, 2013. **8**: p. 2295-2304.
211. Zhao, J.H., et al., *Microemulsion-based novel transdermal delivery system of tetramethylpyrazine: preparation and evaluation in vitro and in vivo*. Int J Nanomedicine, 2011. **6**: p. 1611-1619.
212. Elshafeey, A.H., A.O. Kamel, and M.M. Fathallah, *Utility of Nanosized Microemulsion for Transdermal Delivery of Tolterodine Tartrate: Ex-Vivo Permeation and In-Vivo Pharmacokinetic Studies*. Pharm Res, 2009. **26**(11): p. 2446-2453.
213. Hathout, R.M. and M. Nasr, *Transdermal delivery of betahistine hydrochloride using microemulsions: Physical characterization, biophysical assessment, confocal imaging and permeation studies*. Colloids Surf B Biointerfaces, 2013. **110**: p. 254-260.
214. Bhatia, G., Y. Zhou, and A.K. Banga, *Adapalene Microemulsion for Transfollicular Drug Delivery*. J Pharm Sci, 2013. **102**(8): p. 2622-2631.
215. Mora-Huertas, C.E., H. Fessi, and A. Elaissari, *Polymer-based nanocapsules for drug delivery*. Int J Pharm, 2010. **385**(1-2): p. 113-42.
216. Pinto Reis, C., et al., *Nanoencapsulation I. Methods for preparation of drug-loaded polymeric nanoparticles*. Nanomedicine: Nanotechnology, Biology and Medicine, 2006. **2**(1): p. 8-21.

217. Yoo, H.S., et al., *Biodegradable nanoparticles containing doxorubicin-PLGA conjugate for sustained release*. *Pharm Res*, 1999. **16**(7): p. 1114-8.
218. Nobs, L., et al., *Poly(lactic acid) nanoparticles labeled with biologically active Neutravidin for active targeting*. *Eur J Pharm Biopharm*, 2004. **58**(3): p. 483-90.
219. Chawla, J.S. and M.M. Amiji, *Biodegradable poly(epsilon -caprolactone) nanoparticles for tumor-targeted delivery of tamoxifen*. *Int J Pharm*, 2002. **249**(1-2): p. 127-38.
220. Bravo-Osuna, I., et al., *Elaboration and characterization of thiolated chitosan-coated acrylic nanoparticles*. *Int J Pharm*, 2006. **316**(1-2): p. 170-5.
221. Balzus, B., et al., *Formulation and ex vivo evaluation of polymeric nanoparticles for controlled delivery of corticosteroids to the skin and the corneal epithelium*. *Eur J Pharm Biopharm*, 2017. **115**: p. 122-130.
222. Mandal, S., et al., *Cellulose Acetate Phthalate and Antiretroviral Nanoparticle Fabrications for HIV Pre-Exposure Prophylaxis*. *Polymers*, 2017. **9**(9): p. 423.
223. Shi, A.-m., et al., *Preparation of starch-based nanoparticles through high-pressure homogenization and miniemulsion cross-linking: Influence of various process parameters on particle size and stability*. *Carbohydr Polym*, 2011. **83**(4): p. 1604-1610.
224. Santander-Ortega, M.J., et al., *Nanoparticles made from novel starch derivatives for transdermal drug delivery*. *J Control Release*, 2010. **141**(1): p. 85-92.
225. Elzoghby, A.O., *Gelatin-based nanoparticles as drug and gene delivery systems: Reviewing three decades of research*. *J Control Release*, 2013. **172**(3): p. 1075-1091.
226. Crucho, C.I.C. and M.T. Barros, *Polymeric nanoparticles: A study on the preparation variables and characterization methods*. *Mater Sci Eng C Mater Biol Appl*, 2017. **80**: p. 771-784.
227. Mora-Huertas, C.E., H. Fessi, and A. Elaissari, *Influence of process and formulation parameters on the formation of submicron particles by solvent displacement and emulsification-diffusion methods: Critical comparison*. *Adv Colloid Interface Sci*, 2011. **163**(2): p. 90-122.
228. Paulos, G., et al., *Fabrication of acetylated dioscorea starch nanoparticles: Optimization of formulation and process variables*. *J Drug Deliv Sci*, 2016. **31**: p. 83-92.
229. Chorny, M., et al., *Lipophilic drug loaded nanospheres prepared by nanoprecipitation: effect of formulation variables on size, drug recovery and release kinetics*. *J Control Release*, 2002. **83**(3): p. 389-400.
230. Asadi, H., et al., *Preparation of biodegradable nanoparticles of tri-block PLA-PEG-PLA copolymer and determination of factors controlling the particle size using artificial neural network*. *J Microencapsul*, 2011. **28**(5): p. 406-16.
231. McClements, J. and D.J. McClements, *Standardization of Nanoparticle Characterization: Methods for Testing Properties, Stability, and Functionality of Edible Nanoparticles*. *Crit Rev Food Sci Nutr*, 2016. **56**(8): p. 1334-62.
232. Jin, S.E., J.W. Bae, and S. Hong, *Multiscale observation of biological interactions of nanocarriers: from nano to macro*. *Microsc Res Tech*, 2010. **73**(9): p. 813-23.

233. Guinebretiere, S., et al., *Nanocapsules of biodegradable polymers: preparation and characterization by direct high resolution electron microscopy*. Mater Sci Eng C Biomim Supramol Syst, 2002. **21**(1-2): p. 137-142.
234. Dumont, E., et al., *From near-infrared and Raman to surface-enhanced Raman spectroscopy: progress, limitations and perspectives in bioanalysis*. Bioanalysis, 2016. **8**(10): p. 1077-103.
235. Corrigan, O.I. and X. Li, *Quantifying drug release from PLGA nanoparticulates*. Eur J Pharm Sci, 2009. **37**(3): p. 477-485.
236. Sajilata, M.G., R.S. Singhal, and P.R. Kulkarni, *Resistant starch - A review*. Compr Rev Food Sci Food Saf, 2006. **5**(1): p. 1-17.
237. Copeland, L., et al., *Form and functionality of starch*. Food Hydrocoll, 2009. **23**(6): p. 1527-1534.
238. Tharanathan, R.N., *Starch-value addition by modification*. Crit Rev Food Sci Nutr, 2005. **45**(5): p. 371-384.
239. Singh, J., L. Kaur, and O.J. McCarthy, *Factors influencing the physico-chemical, morphological, thermal and rheological properties of some chemically modified starches for food applications - A review*. Food Hydrocoll, 2007. **21**(1): p. 1-22.
240. Tran, T., K. Piyachomkwan, and K. Sriroth, *Gelatinization and thermal properties of modified cassava starches*. Starch-Starke, 2007. **59**(1): p. 46-55.
241. Fang, J.M., et al., *The chemical modification of a range of starches under aqueous reaction conditions*. Carbohydr Polym, 2004. **55**(3): p. 283-289.
242. Odeku, O.A. and K.M. Picker-Freyer, *Evaluation of the material and tablet formation properties of modified forms of Dioscorea starches*. Drug Dev Ind Pharm, 2009. **35**(11): p. 1389-1406.
243. Bello-Perez, L.A., et al., *Acetylation and characterization of banana (*Musa paradisiaca*) starch*. Acta Cient Venez, 2000. **51**(3): p. 143-9.
244. Gonzalez, Z. and E. Perez, *Effect of acetylation on some properties of rice starch*. Starch-Starke, 2002. **54**(3-4): p. 148-154.
245. Mormann, W. and M. Al-Higari, *Acylation of starch with vinyl acetate in water*. Starch-Starke, 2004. **56**(3-4): p. 118-121.
246. Xu, Y.X., V. Miladinov, and M.A. Hanna, *Synthesis and characterization of starch acetates with high substitution*. Cereal Chem, 2004. **81**(6): p. 735-740.
247. Raatikainen, P., et al., *Acetylation enhances the tableting properties of starch*. Drug Dev Ind Pharm, 2002. **28**(2): p. 165-175.
248. Tarvainen, M., et al., *Starch acetate - A novel film-forming polymer for pharmaceutical coatings*. J Pharm Sci, 2002. **91**(1): p. 282-289.
249. Tarvainen, M., et al., *Aqueous starch acetate dispersion as a novel coating material for controlled release products*. J Control Release, 2004. **96**(1): p. 179-191.
250. Nutan, M.T.H., et al., *Optimization and characterization of controlled release multi-particulate beads coated with starch acetate*. Int J Pharm, 2005. **294**(1-2): p. 89-101.

251. Nutan, M.T.H., S.R. Vaithiyalingam, and M.A. Khan, *Controlled release multiparticulate beads coated with starch acetate: Material characterization, and identification of critical formulation and process variables*. Pharm Dev Technol, 2007. **12**(3): p. 307-320.
252. Xiao, S., et al., *Preparation of folate-conjugated starch nanoparticles and its application to tumor-targeted drug delivery vector*. Chin Sci Bull, 2006. **51**(14): p. 1693-1697.
253. Yu, D.M., et al., *Dialdehyde starch nanoparticles: Preparation and application in drug carrier*. Chin Sci Bull, 2007. **52**(21): p. 2913-2918.
254. Jain, A.K., et al., *Effective insulin delivery using starch nanoparticles as a potential trans-nasal mucoadhesive carrier*. Eur J Pharm Biopharm, 2008. **69**(2): p. 426-435.
255. Minimol, P.F., W. Paul, and C.P. Sharma, *PEGylated starch acetate nanoparticles and its potential use for oral insulin delivery*. Carbohydr Polym, 2013. **95**(1): p. 1-8.
256. Simi, C.K. and T. Emilia Abraham, *Hydrophobic grafted and cross-linked starch nanoparticles for drug delivery*. Bioprocess Biosyst Eng, 2007. **30**(3): p. 173-80.
257. Neubert, R.H.H., *Potentials of new nanocarriers for dermal and transdermal drug delivery*. Eur J Pharm Biopharm, 2011. **77**(1): p. 1-2.
258. Alvarez-Roman, R., et al., *Enhancement of topical delivery from biodegradable nanoparticles*. Pharm Res, 2004. **21**(10): p. 1818-1825.
259. de Jalón, E.G., et al., *Topical application of acyclovir-loaded microparticles: quantification of the drug in porcine skin layers*. J Control Release, 2001. **75**(1): p. 191-197.
260. Alves, M.P., et al., *Human skin penetration and distribution of nimesulide from hydrophilic gels containing nanocarriers*. Int J Pharm, 2007. **341**(1-2): p. 215-220.
261. Guterres, S.S., M.P. Alves, and A.R. Pohlmann, *Polymeric nanoparticles, nanospheres and nanocapsules, for cutaneous applications*. Drug Target Insights, 2007. **2**: p. 147-57.
262. Jennings, V., M. Schäfer-Korting, and S. Gohla, *Vitamin A-loaded solid lipid nanoparticles for topical use: drug release properties*. J Control Release, 2000. **66**(2): p. 115-126.
263. Luengo, J., et al., *Influence of nanoencapsulation on human skin transport of flufenamic acid*. Skin Pharmacol Physiol, 2006. **19**(4): p. 190-7.
264. Rogers, J., et al., *Stratum corneum lipids: The effect of ageing and the seasons*. Arch Dermatol Res, 1996. **288**(12): p. 765-770.
265. Proksch, E., R. Folster-Holst, and J.M. Jensen, *Skin barrier function, epidermal proliferation and differentiation in eczema*. J Dermatol Sci, 2006. **43**(3): p. 159-69.
266. Jungersted, J.M., et al., *Stratum corneum lipids, skin barrier function and filaggrin mutations in patients with atopic eczema*. Allergy, 2010. **65**(7): p. 911-8.
267. Shahriari, M., et al., *Vitamin D and the skin*. Clinics in Dermatology, 2010. **28**(6): p. 663-668.
268. Reisberg, M., et al., *Production of Rare Phyto-Ceramides from Abundant Food Plant Residues*. J Agric Food Chem, 2017. **65**(8): p. 1507-1517.
269. EMEA, *Guideline on bioanalytical method validation*. 2011, European Medicines Agency.

270. Zheng, W., et al., *Ceramides and other bioactive sphingolipid backbones in health and disease: Lipidomic analysis, metabolism and roles in membrane structure, dynamics, signaling and autophagy*. Biochim Biophys Acta, 2006. **1758**(12): p. 1864-1884.
271. Uemura, M., R.A. Joseph, and P.L. Steponkus, *Cold-Acclimation of Arabidopsis-Thaliana - Effect on Plasma-Membrane Lipid-Composition and Freeze-Induced Lesions*. Plant Physiol, 1995. **109**(1): p. 15-30.
272. Carter, H.E. and J.L. Koob, *Sphingolipids in Bean Leaves (Phaseolus Vulgaris)*. J Lipid Res, 1969. **10**(4): p. 363-&.
273. Sugawara, T. and T. Miyazawa, *Separation and determination of glycolipids from edible plant sources by high-performance liquid chromatography and evaporative light-scattering detection*. Lipids, 1999. **34**(11): p. 1231-1237.
274. Zellmer, S. and J. Lasch, *Individual variation of human plantar stratum corneum lipids, determined by automated multiple development of high-performance thin-layer chromatography plates*. J Chromatogr B, 1997. **691**(2): p. 321-329.
275. Farwanah, H., et al., *Improved procedure for the separation of major stratum corneum lipids by means of automated multiple development thin-layer chromatography*. J Chromatogr B, 2002. **780**(2): p. 443-450.
276. Fowler, J.F., et al., *Colloidal oatmeal formulations as adjunct treatments in atopic dermatitis*. J Drugs Dermatol, 2012. **11**(7): p. 804-7.
277. Kurtz, E.S. and W. Wallo, *Colloidal oatmeal: history, chemistry and clinical properties*. J Drugs Dermatol, 2007. **6**(2): p. 167-70.
278. Cerio, R., et al., *Mechanism of action and clinical benefits of colloidal oatmeal for dermatologic practice*. J Drugs Dermatol, 2010. **9**(9): p. 1116-20.
279. Nebus, J., et al., *A daily oat-based skin care regimen for atopic skin*. J Am Acad Dermatol, 2009. **60**(3): p. Ab67-Ab67.
280. Lisante, T.A., et al., *A 1% Colloidal Oatmeal Cream Alone is Effective in Reducing Symptoms of Mild to Moderate Atopic Dermatitis: Results from Two Clinical Studies*. J Drugs Dermatol, 2017. **16**(7): p. 671-676.
281. Parikh-Das, A., et al., *A clinical trial to evaluate the efficacy of a OTC colloidal oatmeal skin protectant cream in the management of mild to moderate atopic dermatitis in infants and toddlers*. J Am Acad Dermatol, 2017. **76**(6): p. Ab10-Ab10.
282. Nunez, C., et al., *A colloidal oatmeal OTC cream is as clinically effective as a prescription barrier repair cream for the management of mild to moderate atopic dermatitis in African American children*. J Am Acad Dermatol, 2013. **68**(4): p. Ab73-Ab73.
283. Kalaaji, A.N. and W. Wallo, *A randomized controlled clinical study to evaluate the effectiveness of an active moisturizing lotion with colloidal oatmeal skin protectant versus its vehicle for the relief of xerosis*. J Drugs Dermatol, 2014. **13**(10): p. 1265-8.
284. Sur, R., et al., *Avenanthramides, polyphenols from oats, exhibit anti-inflammatory and anti-itch activity*. Arch Dermatol Res, 2008. **300**(10): p. 569-574.

285. Banas, A., et al., *Lipids in grain tissues of oat (Avena sativa): differences in content, time of deposition, and fatty acid composition*. J Exp Bot, 2007. **58**(10): p. 2463-70.
286. Singh, R., S. De, and A. Belkheir, *Avena sativa (Oat), A Potential Nutraceutical and Therapeutic Agent: An Overview*. Crit Rev Food Sci Nutr, 2013. **53**(2): p. 126-144.
287. Norberg, P., et al., *Glucosylceramides of oat root plasma membranes - Physicochemical behaviour in natural and in model systems*. Biochim Biophys Acta-Lipids and Lipid Metabolism, 1996. **1299**(1): p. 80-86.
288. Tessema, E.N., et al., *Isolation and structural characterization of glucosylceramides from Ethiopian plants by LC/APCI-MS/MS*. J Pharm Biomed Anal, 2017. **141**: p. 241-249.
289. Norberg, P., J.E. Mansson, and C. Liljenberg, *Characterization of Glucosylceramide from Plasma-Membranes of Plant-Root Cells*. Biochim Biophys Acta, 1991. **1066**(2): p. 257-260.
290. Grob, C.A. and E.F. Jenny, *Die Synthese Von Dihydro-Sphingosin*. Helv Chim Acta, 1952. **35**(6): p. 2106-2111.
291. Carter, H.E., D. Shapiro, and J.B. Harrison, *Synthesis and Configuration of Dihydrosphingosine*. J Am Chem Soc, 1953. **75**(4): p. 1007-1008.
292. Fujino, Y. and T. Negishi, *Studies on the Conjugated Lipids .5. Configuration of the Galactoside Linkage in Cerebrosides*. Bull Agr Chem Soc Jpn, 1956. **20**(4): p. 183-187.
293. Carter, H.E., O. Nalbandov, and P.A. Tavormina, *Biochemistry of the Sphingolipides .6. The O-Methyl Ethers of Sphingosine*. J Biol Chem, 1951. **192**(1): p. 197-207.
294. Karlsson, K.A., *On the chemistry and occurrence of sphingolipid long-chain bases*. Chem Phys Lipids, 1970. **5**(1): p. 6-43.
295. Sambasivarao, K. and R.H. McCluer, *Thin-Layer Chromatographic Separation of Sphingosine and Related Bases*. J Lipid Res, 1963. **4**: p. 106-8.
296. Gatt, S., *Enzymic Hydrolysis of Sphingolipids - Hydrolysis of Ceramide Glucoside by an Enzyme from Ox Brain*. Biochem J, 1966. **101**(3): p. 687-691.
297. Gatt, S. and M.M. Rapport, *Enzymic Hydrolysis of Sphingolipids - Hydrolysis of Ceramide Lactoside by an Enzyme from Rat Brain*. Biochem J, 1966. **101**(3): p. 680-686.
298. Barnholz, Y., A. Roitman, and S. Gatt, *Enzymatic Hydrolysis of Sphingolipids .2. Hydrolysis of Sphingomyelin by an Enzyme from Rat Brain*. J Biol Chem, 1966. **241**(16): p. 3731-3737.
299. Tessema, E.N., et al., *Potential Applications of Phyto-Derived Ceramides in Improving Epidermal Barrier Function*. Skin Pharmacol Physiol, 2017. **30**(3): p. 115-138.
300. Boiten, W., et al., *Quantitative analysis of ceramides using a novel lipidomics approach with three dimensional response modelling*. Biochim Biophys Acta-Molecular and Cell Biology of Lipids, 2016. **1861**(11): p. 1652-1661.
301. Raith, K. and R.H.H. Neubert, *Liquid chromatography-electrospray mass spectrometry and tandem mass spectrometry of ceramides*. Anal Chim Acta, 2000. **403**(1-2): p. 295-303.
302. Vietzke, J.P., M. Strassner, and U. Hintze, *Separation and identification of ceramides in the human stratum corneum by high-performance liquid chromatography coupled with electrospray ionization*

- mass spectrometry and electrospray multiple-stage mass spectrometry profiling*. Chromatographia, 1999. **50**(1-2): p. 15-20.
303. Bonte, F., et al., *Analysis of All Stratum-Corneum Lipids by Automated Multiple Development High-Performance Thin-Layer Chromatography*. J Chromatogr B Biomed Sci Appl, 1995. **664**(2): p. 311-316.
304. Sahle, F.F., et al., *Development and validation of LC/ESI-MS method for the detection and quantification of exogenous ceramide NP in stratum corneum and other layers of the skin*. J Pharm Biomed Anal, 2012. **60**: p. 7-13.
305. Neubert, R.H.H., et al., *Development and Validation of Analytical Methods for the Detection and Quantification of a Novel Dimeric Ceramide in Stratum Corneum and Other Layers of the Skin*. Chromatographia, 2016. **79**(23): p. 1615-1624.
306. Tessema, E.N., et al., *Potential application of oat-derived ceramides in improving skin barrier function: Part 1. Isolation and structural characterization*. J Chromatogr B Analyt Technol Biomed Life Sci, 2017. **1065-1066**: p. 87-95.
307. W.D.o.N., Resources, *Analytical Detection Limit Guidance & Laboratory Guide for Determining Method Detection Limits*. 1996, Wisconsin Department of Natural Resources Laboratory Certification Program.
308. Zhang, Q., et al., *Topically applied ceramide accumulates in skin glyphs*. Clin Cosmet Investig Dermatol, 2015. **8**: p. 329-37.
309. Lawrence, M.J. and G.D. Rees, *Microemulsion-based media as novel drug delivery systems*. Adv Drug Deliv Rev, 2012. **64**: p. 175-193.
310. Najafi, S.H.M., M. Baghaie, and A. Ashori, *Preparation and characterization of acetylated starch nanoparticles as drug carrier: Ciprofloxacin as a model*. Int J Biol Macromol, 2016. **87**: p. 48-54.
311. Han, F., C.M. Gao, and M.Z. Liu, *Fabrication and Characterization of Size-Controlled Starch-Based Nanoparticles as Hydrophobic Drug Carriers*. J Nanosci Nanotechnol, 2013. **13**(10): p. 6996-7007.
312. Paulos G, E.A., Bultosa G, Gebre-Mariam T, *Isolation and physicochemical characterization of cassava starches obtained from different regions of Ethiopia*. Ethiopian Pharmaceutical Journal 2010. **27**(1).
313. Neubert, R., et al., *A Multilayer Membrane System for Modeling Drug Penetration into Skin*. Int J Pharm, 1991. **75**(1): p. 89-94.
314. Bello-Pérez, L.A., et al., *Effect of low and high acetylation degree in the morphological, physicochemical and structural characteristics of barley starch*. LWT - Food Science and Technology, 2010. **43**(9): p. 1434-1440.
315. Souto, E.B., et al., *Evaluation of the physical stability of SLN and NLC before and after incorporation into hydrogel formulations*. Eur J Pharm Biopharm, 2004. **58**(1): p. 83-90.
316. Alves, P.M., A.R. Pohlmann, and S.S. Guterres, *Semisolid topical formulations containing nimesulide-loaded nanocapsules, nanospheres or nanoemulsion: development and rheological characterization*. Pharmazie, 2005. **60**(12): p. 900-4.

317. Joshi, M. and V. Patravale, *Formulation and evaluation of Nanostructured Lipid Carrier (NLC)-based gel of Valdecoxib*. Drug Dev Ind Pharm, 2006. **32**(8): p. 911-8.
318. Taketomi, T. and N. Kawamura, *Degradation of Sphingosine Bases during Acid-Hydrolysis of Sphingomyelin, Cerebroside or Psychosine*. J Biochem, 1972. **72**(1): p. 189-193.

Declaration of academic integrity

With this statement I declare that I have independently completed the above PhD thesis entitled Delivery of Phyto-Ceramides into the *Stratum Corneum* of the Skin using Nanocarriers: Structural Characterization, Formulation and Skin Permeation Studies. The thoughts taken directly or indirectly from external sources are properly marked as such. This thesis was not previously submitted to another academic institution and has also not yet been published.

Halle (Saale), _____

Efrem Nigussu Tessema